Dissertation zur Erlangung des Doktorgrades
der Fakultät für Chemie und Pharmazie
der Ludwig-Maximilians-Universität München

Genome-wide Analysis of TREX Recruitment

and

Analysis of Rpb1 Ubiquitylation upon Transcriptional Impairment

Cornelia Burkert-Kautzsch

aus

Kulmbach, Deutschland

2013

Summary

Transcription and mRNA export are tightly regulated processes, which are highly interconnected. Different adaptor proteins have been described, which recruit the mRNA export receptor Mex67-Mtr2 to the mRNA; however, their specificities remained to be elucidated. Additionally, it was not known how the conserved TREX complex, which couples transcription to mRNA export, interacts with the transcription machinery.

In a joint project, fellow Ph.D. student Dominik Meinel and I conducted chromatin immunoprecipitation experiments and subsequent hybridization to high-density tiling arrays, which provided a comprehensive genome-wide analysis of the mRNA export machinery in *Saccharomyces cerevisiae*. We found that the TREX complex and other mRNA adaptor proteins are globally recruited to transcribed genes, and that TREX recruitment to genes increases from 5' to 3' in a length-dependent manner. Mr. Meinel showed that this is mediated by an interaction with the S2,S5-diphosphorylated CTD of Rpb1. Since we noticed that a C-terminal TAP tag on TREX subunit Tho2 impairs this normal length-dependent recruitment of the complex, I excluded similar effects for two other subunits. I furthermore found that expression of a C-terminal TAP tag on TREX subunit Yra1 impairs normal Yra1 recruitment in deletion mutants of the TREX subcomplex THO. This is also reflected by genetic interactions of the *YRA1-TAP* allele with *HPR1* and *THO2* deletions. I performed recruitment analyses of several TREX subunits in different deletion mutants of THO to find out which subunit mediates TREX recruitment. Further experiments are necessary to answer this question conclusively, but the data point towards a role of Tho2 and / or Mft1 in TREX recruitment as well as to a function of the THO complex in stabilization of Yra1 occupancy. Taken together, this project provides further insight into how the CTD of Rpb1 couples transcription with mRNA export by recruitment of the TREX complex.

The second part of this thesis addresses an important mechanism of ensuring continued transcription, namely the removal of persistently stalled RNA Polymerase II complexes. In cases of stalling due to DNA damage the biggest subunit of RNAPII, Rpb1, is known to be polyubiquitylated with K48-linked ubiquitin chains (the canonical signal for proteasomal degradation). The resulting degradation is used as drastic "last resort" mechanism as an alternative to transcription-coupled repair. However, it was not clear whether this process is identical in cases of DNA damage-independent stalling.

Previous work of former Ph.D. student Eleni Karakasili had already elucidated the molecular mechanism of Rpb1 polyubiquitylation in *S. cerevisiae* mutants that lack transcription elongation factors and exhibit increased RNAPII stalling. She found it to be overall similar to the DNA damage-dependent pathway but, unexpectedly, identified a more pronounced increase in K63-linked polyubiquitylation and no dependence on Elc1, an E3 ubiquitin ligase important for the DNA-damage-dependent degradation.

I continued this work and confirmed that Rpb1 is specifically polyubiquitylated and that an increased turnover of the Rpb1 protein is the reason for the lower protein levels we observe in transcription elongation mutants. Furthermore, I found some evidence that K63-linked polyubiquitylation might play a role in Rpb1 degradation. There is a genetic interaction between a K63R-mutated ubiquitin allele (precluding the formation of K63-linked chains) and transcription impairment by deletion of *DST1*. While I found no evidence that K63-linked chains directly influence Rpb1 degradation upon transcription elongation impairment, there is a certain decrease in total Rpb1 polyubiquitylation when only K63R ubiquitin is available. The exact mechanism by which the K63-linked polyubiquitin chains act in that context will need to be elucidated. All in all, this study provides first evidence that the cell might distinguish between RNAPII complexes stalled due to different reasons.

Publications

Parts of the present thesis will be submitted for publication in revised version or have been published already:

Karakasili E*, <u>Burkert-Kautzsch C</u>*, Kieser A, Strässer K (2013). Degradation of DNA damage-independently stalled RNA polymerase II is independent of the E3 ligase Elc1. *Nucl Acids Res   *these authors contributed equally*

Meinel DM, <u>Burkert-Kautzsch C</u>, Kieser A, O'Duibhir E, Siebert M, Mayer A, Cramer P, Söding J, Holstege FC, Sträßer K (2013). Recruitment of TREX to the Transcription Machinery by Its Direct Binding to the Phospho-CTD of RNA Polymerase II. *PLoS Genet,* 9(11):e1003914.

In addition I contributed to the following publication:

Röther S*, <u>Burkert C</u>*, Brünger KM*, Mayer A*, Kieser A, Strässer K (2010). Nucleocytoplasmic shuttling of the La motif-containing protein Sro9 might link its nuclear and cytoplasmic functions. *RNA,* 16(7):1393-401.   *these authors contributed equally*

Table of Contents

Table of Contents *continued*

Table of Contents *continued*

Table of Contents *continued*

1. General Introduction

1.1. Transcription in eukaryotes

1.1.1. DNA-dependent RNA polymerases

In eukaryotes, several different DNA-dependent RNA polymerases (RNAP) transcribe different types of genes. While RNAPI synthesizes ribosomal RNAs (rRNAs) (Drygin 2010), RNAPII transcribes all protein-coding genes into mRNAs and synthesizes some of the short non-coding RNAs, such as the spliceosomal small nuclear RNAs (snRNAs), small nucleolar RNAs (snoRNAs), and microRNAs (miRNAs) as well as cryptic unstable transcripts (CUTs) and stable unannotated transcripts (SUTs) (Egloff 2008, Beretta 2009). RNAPIII transcribes tRNA genes but also synthesizes various other short non protein-coding RNAs such as the 5S rRNA, U6 snRNA, and 7SL RNA (White 2011). Plants additionally possess a fourth and fifth RNA polymerase, which play a role in siRNA-mediated gene silencing (Haag 2011).

RNA polymerases I, II, and III are multi-subunit complexes of 14, 12, and 17 subunits, respectively, with a conserved ten subunit core. Five subunits of this core, which provide structural stability, are common between them and the other five core subunits, important for the catalytic activity and start site selection, are structural and functional homologs. While the core enzyme with its active center is similar in all three polymerases the additional subunits account for structural differences on the surface with concomitant distinctions in function (Cramer 2008).

Interestingly, recent genome-wide studies have revealed a certain amount of crosstalk between the different RNAP transcription machineries. RNAPII is also associated with RNAPIII (Raha 2010), and the RNAPII transcription factors TFIIS and Paf1 complex, for example, have been shown to also function in RNAPIII (Ghavi-Helm 2008) and RNAPI (Zhang 2009) transcription, respectively.

1.1.2. RNA Polymerase II structure and function

RNA Polymerase II (RNAPII) consists of twelve subunits (Rpb1 - Rpb12). It comprises the ten subunit core plus the Rpb4/7 heterodimer, which can dissociate from the core enzyme and fulfills various functions, not only in transcription but also in DNA repair, mRNA decay and, interestingly, even in translation (Sampath 2005, Harel-Sharvit 2010). Numerous studies have elucidated the structure of RNAP II under different conditions, either alone or bound to a DNA template, with our without associated transcription factors (Cramer 2008).

These structural studies revealed that Rpb1 and Rpb2 are positioned on opposite sides of an active center cleft. The Rpb1 side of the cleft forms a mobile clamp which is connected to the remaining polymerase by a flexible switch region, while Rpb2 forms a wall blocking the end of the cleft (Cramer 2008; Figure 1).
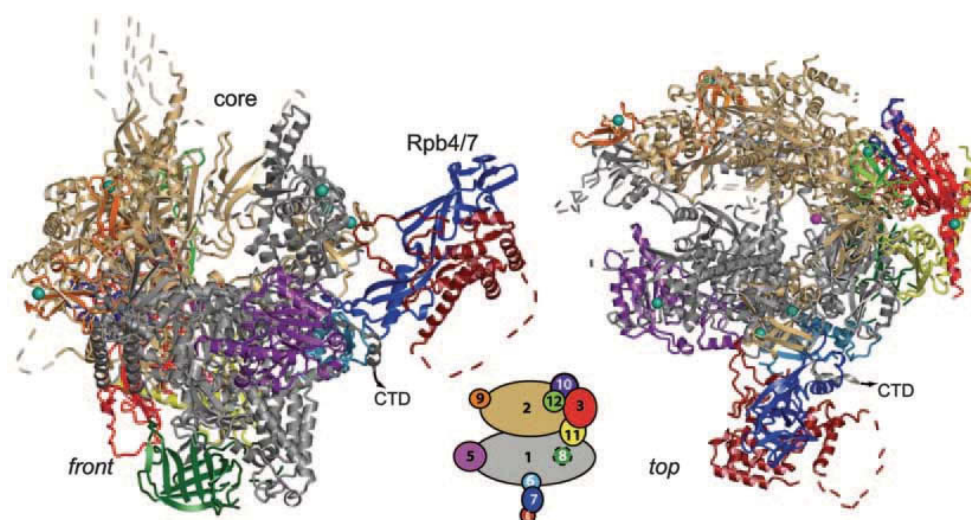
Figure 1: Front and top views of the 12-subunit RNAPII complex (taken from Armache et al. 2005). The schematic depiction in the middle shows the color code for the single subunits (1 - 12), zinc ions are depicted as cyan spheres and the magnesium ion in the active site as a pink sphere.

Several conserved structures such as the bridge helix and the trigger loop have been identified that are important for RNAPII function and enable it to efficiently initiate RNA synthesis and catalyze subsequent rounds of nucleotide addition. This nucleotide addition cycle involves selection of the appropriate ribonucleotide according to the DNA template, phosphodiester bond formation to attach the new nucleotide to the 3' end of the RNA, pyrophosphate release and translocation along DNA and RNA (Martinez-Rucobo 2013). The double-stranded DNA is accommodated within the cleft of the polymerase holoenzyme, where the strands are separated and form the so-called transcription bubble. The growing RNA chain is synthesized according to the template-strand sequence, leaves via the mRNA exit tunnel and emerges from the holoenzyme close to the flexible C-terminal domain of Rpb1, thus allowing for a coupling of transcription with RNA processing events (see further below).

1.1.3. Transcription takes place on a chromatin template

In eukaryotes, the DNA is compacted into chromatin, which is made up of nucleosomes as basic units which are connected via linker DNA. In a nucleosome, 147 bp of DNA are wrapped around a histone octamer, consisting of two copies each of the basic histone proteins H2A, H2B, H3 and H4 (Richmond 2003). Thus, transcription does not take place on naked

DNA, but the transcription machinery has to overcome these nucleosomal barriers. While promoter and terminator regions tend to be depleted of nucleosomes, often due to sequences which are not easily bent and thus disfavor nucleosome formation, downstream nucleosomes within the transcribed region present obstacles for RNAPII progression (Struhl 2013). Chromatin remodelers, nucleosome assembly factors (histone chaperones) and other transcription factors have evolved to help RNAPII transcribe through chromatin by rearranging nucleosomes during transcription (Petesch 2012, Kulaeva 2013).

Furthermore, histones play an important role in transcriptional regulation as they are subject to extensive posttranslational modifications, which regulate binding of factors to chromatin (Rando 2012). Histone marks denote active or repressed states of chromatin. Recruitment of the factors establishing these marks is regulated by the phosphorylation status of Rpb1's C-terminal domain (see further below). The histone methylation pattern then influences the recruitment of other histone modifying enzymes and chromatin remodeling complexes and thus subsequent rounds of transcription (Buratowski 2009).

1.1.4. The transcription cycle of RNAPII

Transcription by RNAPII can be divided into the successive stages of initiation (with preinitiation complex formation, transition to open complex formation, and initiation of transcription), productive elongation and finally termination and polymerase recycling (Shandilya 2012). The different stages of transcription are closely linked to corresponding processing steps of the nascent RNA transcript (see section 2.1.).

1.1.4.1. The C-terminal domain (CTD) of Rpb1 plays an important role during the transcription cycle

Among the three RNA polymerases only RNAPII possesses an unstructured C-terminal domain (CTD) on its largest subunit Rpb1 (Figure 2). This special domain consists of heptapeptide repeats with the conserved sequence YSPTSPS (with 26 repeats present in yeast and 52 in humans), which are differentially phosphorylated during the transcription cycle, with two consecutive heptads forming a functional unit (Stiller and Cook 2004).
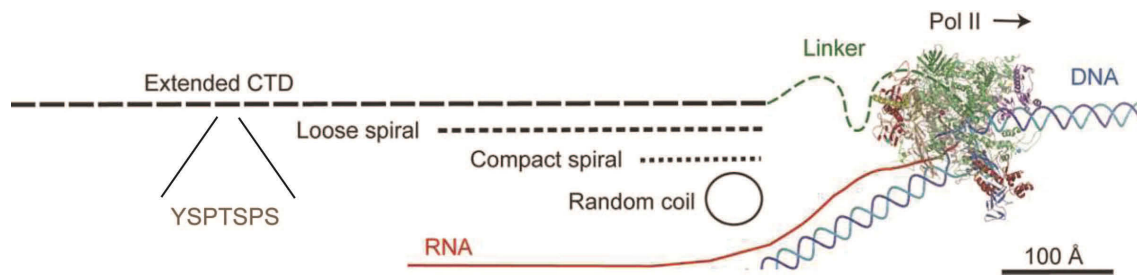
Figure 2: Depiction of the elongating RNAPII and relative size of the CTD in four putative states (figure modified from Meinhart et al. 2005). The 12-subunit elongation complex (Kettenberger et al. 2004, Armache et al. 2005) is shown as ribbon diagram with the DNA template in blue and the RNA in red. The CTD is connected to RNAPII's biggest subunit via a flexible linker region. The depiction shows the size of the CTD relative to RNAPII in four possible states - fully extended, as loose or compact β-spiral, or as random coil - and illustrates that the CTD can serve as a binding platform for interacting factors.

These CTD modifications, which are established by the actions of CTD kinases and phosphatases (Bataille 2012, Hsin 2012), facilitate the appropriate recruitment and release of a changing set of transcription and mRNP remodeling factors needed at each stage of the transcription cycle via their corresponding binding preferences (Figure 3).

Phosphorylation of S2 and S5 are the CTD modifications that have been known for the longest time. The observation that S5 phosphorylation is high during early elongation and drops later on while the reverse is true for S2 phosphorylation led to the proposal of a "CTD code" (Buratowski 2003). By now it is known that all three serine residues, the tyrosine, and the threonine residue can be phosphorylated, and that glycosylation of the serines and the threonine as well as proline isomerization can further modify the CTD repeats (Zhang 2012).
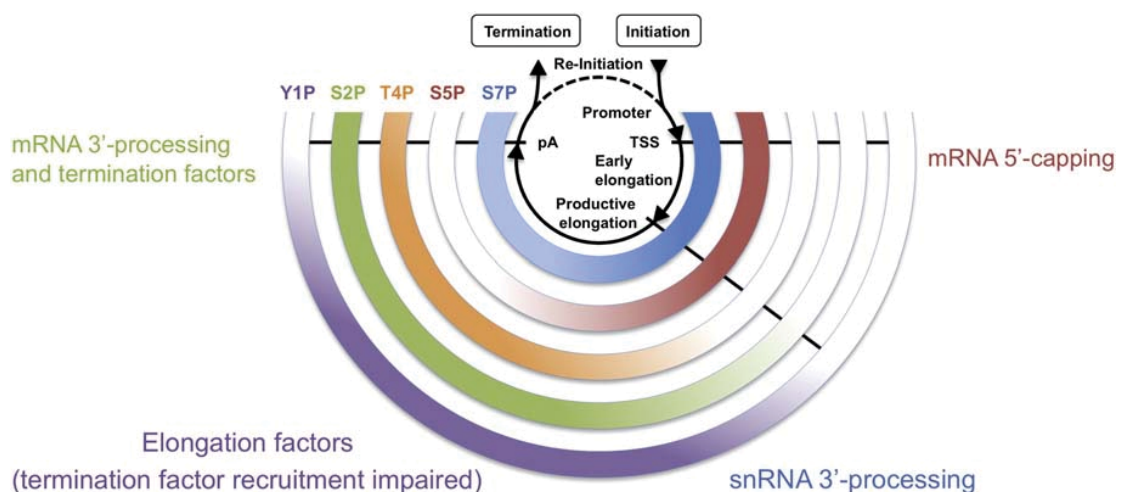
Figure 3: CTD modifications change during the transcription cycle and coordinate the cotranscriptional recruitment of transcription and mRNA processing factors (figure taken from Heidemann et al. 2013). Different phosphomarks on the CTD and their relative changes during the transcription cycle are reflected by color intensity, and transcript processing steps that are coordinated via differential CTD phosphorylation are indicated.

S5 phosphorylation decreases rapidly during early elongation but persists at a lower level while S2 phosphorylation increases continuously and then drops just after the poly(A) site. S5 phosphorylation, for example, recruits the capping enzyme (Cho 1997, McCracken 1997) and promotes the recruitment of S2 kinase Bur1 (Qiu 2009), while transcription elongation, splicing and 3' processing factors preferentially bind to the S2 or S2/S5 phosphorylated CTD (Heidemann 2012, Hsin 2012). In addition, S5 and S2 phosphorylation also influences histone methylation by promoting recruitment of the histone methyltransferases Set1 and Set2, respectively (Hampsey 2003).

Y1, T4 and S7 phosphorylation has been discovered more recently, and their functions are beginning to be elucidated. S7 phosphorylation appears early at the transcription start site and remains high towards the 3' end of protein-coding and non-coding genes (Tietjen 2010, Mayer 2010) and plays a well-characterized role in the transcription of snRNAs (Egloff 2007, Egloff 2012). Y1 phosphorylation resembles S2 phosphorylation but drops earlier, before RNAPII reaches the poly(A) site. This phosphomark stimulates binding of the transcription elongation factor Spt6 and prevents recruitment of termination factors (Mayer 2012). Lastly, T4 phosphorylation plays a gene-specific role in recruiting 3' end processing factors to histone mRNA in chicken cells (Hsin 2011) and its availability for phosphorylation has been shown to be necessary for transcription elongation and viability in mammalian cells, while T4A yeast mutants are viable (Hintermair, 2012). Possible further functions of this modification remain to be elucidated.

Thus, the Rpb1 CTD is an immensely important binding platform which, by its differential modification, orchestrates recruitment of the appropriate factors at each stage of transcription and also connects these different stages, making transcription and mRNA processing more efficient.

1.1.4.2. Transcription initiation

Transcription initiation begins with the assembly of the so-called preinitiation complex (PIC) at the promoter. The minimal set of factors needed for PIC formation comprises the general transcription factors (GTFs) TFIIB, TFIID (including TATA box binding protein TBP), TFIIE, TFIIF, TFIIH and the hypophosphorylated RNAPII. Specific interactions of GTFs with sequence elements of the promoter (*e.g.,* the TATA box or Downstream Promoter Element, DPE) mediate transcriptional start site selection (Nechaev 2011). The mediator complex, which binds to hypophosphorylated RNAPII, stimulates basal transcription but also relays regulatory signals from activators or repressors by acting as a bridge between upstream regulatory factors bound to the DNA and RNAPII (Conaway 2011).

The next step towards initiation of transcription is the ATP-dependent open complex formation. It requires TFIIE and TFIIF, and leads to the translocation of DNA into the RNAPII cleft and separation of the double-stranded DNA with positioning of the template strand close to the active site of Rpb1 (Grünberg 2012). Synthesis of the nascent RNA starts and leads to the formation of an RNA-DNA hybrid with the first 8 nucleotides of nascent RNA. As the RNA becomes longer it enters the RNA exit channel of RNAPII and emerges from within the enzyme at a length of around 17 nucleotides (Luse 2013).

The transition to productive elongation involves several changes: the transcription bubble, which in the very beginning continuously grows longer as initial transcription progresses, collapses and closes in the upstream region, leaving only a length of about 10 nucleotides unpaired at a time. Initiation factors are released - only TFIIF can associate with RNAPII throughout transcription (Luse 2013). Once incorporated in the PIC, mediator stimulates Kin28 (the kinase subunit of TFIIH) to phosphorylate S5 of the CTD, thereby triggering its own release (Buratowski 2009).

While in Drosophila and mammalian cells RNAPII is known to pause in promoter-proximal regions, especially at inducible genes such as heat-shock genes, there is currently no such evidence for promoter-proximal pausing in exponentially growing *S. cerevisiae* (Mayer 2010, Nechaev 2011, Adelman 2012).

1.1.4.3. Transcription elongation

The transition from initiation to productive elongation occurs when the nascent transcript is approximately 20 nucleotides long. At this point, GTFs have left and the transcript is stably capped (see below). RNAPII is now capable of transcription and proof-reading on its own. Upon transition to productive elongation the transcription initiation factors are replaced by transcription elongation factors, which include Paf1 complex, Spt16, Spt4/5, Spt6, Spn1 and Elf1 (Zhang 2012). During elongation, a large portion of S5 phosphomarks is removed near the +1 nucleosome by the phosphatase Rtr1 (Mosley 2009), but S5 phosphorylation persists at a lower level (see section 1.1.4.1.). Transcription elongation is characterized by increasing S2 phosphorylation. This is initially mediated by Bur1, which is recruited by S5 phosphorylation, and primes the CTD for recruitment of the CTDK1 complex, the main S2 kinase. Increasing S2 phosphorylation by CTDK1 then mediates new interactions for processes occurring cotranscriptionally (see below), such as the recruitment of splicing, mRNA export and 3' processing factors (Zhang 2012).

Besides *bona fide* transcription elongation factors, the TREX complex (discussed in more detail in the specific introduction to Part One) is necessary for efficient transcription elongation,

especially through long, GC-rich or repeat-containing genes (Chavez 1997, Chavez 2000, Chavez 2001, Rondon 2003, Voynov 2006).

1.1.4.4. Transcription termination

Transcription termination is very important to ensure proper expression of the genome, especially since recent genome-wide studies have discovered an unexpected pervasiveness of RNAPII transcription (Kuehner 2011).

When RNAPII has completely transcribed a gene it encounters termination signals, and pause sites have been described to aid in transcriptional termination in mammalian cells by slowing down RNAPII and providing additional time (Enriquez-Harris 1991, Gromak 2006). Termination is preceded by and interconnected with cleavage and polyadenylation of the transcript (discussed in section 2.1.3. of Part One). RNAPII stops synthesizing RNA, the RNA-DNA hybrid is destabilized and RNAPII detaches from the template DNA and releases the transcript.

The termination process has been described by two different models, the "anti-terminator model" and the "torpedo model". The true situation is probably best described by a mixture of both (Luo 2006). The "anti-terminator" or allosteric model postulates that passage of the poly(A) signal and/or binding of termination factors to the transcription elongation complex induces conformational changes in the transcription complex, thus destabilizing RNAPII on the template. The "torpedo model", on the other hand, stresses the role of the $5' \rightarrow 3'$ exonuclease Rat1, which rapidly degrades the RNA remaining after endonucleolytic cleavage from its unprotected 5' end and eventually catches up with the still transcribing polymerase. This model postulates that the exonuclease by its collision with RNPII destabilizes the complex on the DNA template and "pushes" the polymerase off (Richard 2009).

Protein-coding genes are terminated in a poly(A)-dependent manner, which involves the presence of a poly(A) signal and the recruitment of cleavage and polyadenylation factor (CPF), cleavage factors (CF) IA and IB and the exosome (Zhang 2012). These termination factors direct endonucleolytic cleavage, polyadenylation of the upstream pre-mRNA and degradation of the downstream transcript by the $5' \rightarrow 3'$ exonuclease Rat1 (Lykke-Andersen 2007, Mischo 2013). Again, the CTD orchestrates binding of termination factors: recruitment of CF IA subunit Pcf11 is enhanced by S2 phosphorylation of the CTD (Gu 2013), while Y1 phosphorylation, which is present during elongation and drops shortly before the poly(A) signal, prevents premature recruitment of termination factors Pcf11, Rtt103, and Nrd1 (Mayer 2012).

Non-coding transcripts of RNAPII (sn/snoRNAs and also CUTs), on the other hand, are terminated dependent on the Nrd1-Nab3-Sen1 complex (Mischo 2013). Interestingly, the RNA helicase Sen1, which binds to S2P-CTD (Chinchilla 2012), also plays a role in poly(A)-dependent termination, especially of some short protein-coding genes (Kuehner 2011).

1.1.4.5. Gene looping and polymerase recycling

Not only is transcription coupled to co-transcriptional mRNA processing events, but transcription termination is also linked to re-initiation, and defective termination can inhibit subsequent rounds of transcription. It has been shown in human cells, for example, that a mutated polyadenylation signal of an integrated β-globin reporter gene negatively affected re-initiation from this gene's promoter (Mapendano 2010). In addition, depletion of 3' end processing factor PCF11 in these cells not only caused defective transcription termination, as expected, but also led to decreased levels of RNAPII and TFIIB at the promoter, lowering transcription initiation of the same gene (Mapendano 2010).

Genetic and physical interactions between termination and initiation factors as well as chromosome conformation capture (3C) assays point towards the existence of "gene loops" (Hampsey 2011). The gene looping model suggests that genes are not linear structures with beginning and end rather far apart, but that looping of the DNA brings terminator and promoter regions into close proximity and thus allows efficient transfer of RNAPII for re-initiation (Lykke-Andersen 2011). The interaction of initiation factor TFIIB with the termination machinery (Singh 2007) and CPF components Ssu72 and Pta1 (Ansari 2005) are required for this connection. Gene looping thus increases the efficiency of re-initiation and creates a kind of "transcriptional memory" (Hampsey 2011). It furthermore might provide a mechanism to enforce directionality in transcription by suppressing divergent transcription (Tan-Wong 2012).

For re-initiation the CTD first has to be dephosphorylated. This is a prerequisite for polymerase recycling; the CTD phosphatases Fcp1 and Ssu72 are needed to remove S2 and S5 / S7 phosphorylation marks, respectively, thus converting RNAPII into the hypophosphorylated form, which is now again competent for transcription initiation (Shandilya 2012).

2. Specific Introduction to Part One

2.1. mRNA processing

Transcript processing comprises capping at the 5' end, splicing - if intron(s) are present -, and cleavage and polyadenylation at the 3' end.

Nascent mRNAs are processed by many different factors, which are recruited cotranscriptionally. Thus, although the transcription cycle and mRNA processing are described in separate sections here for simplicity, mRNA processing and transcription (as well as mRNA export described in section 2.2.) are interconnected and tightly coordinated.

2.1.1. Capping

The addition of a 7-methyl-guanosine to the terminal RNA nucleotide is the first modification of the nascent transcript. As soon as the RNA emerges from RNAPII's mRNA exit tunnel the capping complex, which is recruited by the S5-phosphorylated CTD (Cho 1997, Schroeder 2000), starts to modify the 5' end of the mRNA. This requires the consecutive actions of triphosphatase, guanylyltransferase and methyltransferase activities (Hocine 2010). The cap structure is subsequently recognized and bound by the nuclear cap-binding complex (CBC), which is later on replaced by the cytoplasmic translation initiation factor eIF4E. On the one hand, this confers stability by protecting the RNA against 5' → 3' exonucleases, but also facilitates splicing and export. On the other hand, it promotes translation of the capped transcript by mediating recruitment to the small ribosomal subunit (Topisirovic 2011).

2.1.2. Splicing

Splicing is the process of removing non-coding intronic sequences from gene transcripts and is mediated by the spliceosome, a large ribonucleoprotein complex consisting of U1, U2, U4, U5, and U6 snRNAs and about 170 associated proteins, which assembles in a step-wise manner and undergoes many dynamic rearrangements during the splicing reaction (Stark 2006). Removal of an intron and ligation of the flanking exons is achieved by two successive transesterification reactions, which require specific sequences in the intron, namely the 5' splice site, the branchpoint sequence (BPS), and the 3' splice site (and in metazoans additionally a polypyrimidine tract), and which occur cotranscriptionally but can also occur posttranscriptionally (Montes 2012).

Serine-arginine-rich (SR) proteins play an important role in constitutive as well as alternative splicing in higher eukaryotes (Long 2009). In yeast, on the other hand, only the SR-like protein

Npl3 (but not the other two yeast proteins of this class, Gbp2 and Hrb1) interacts genetically with splicing factors and promotes splicing, especially of ribosomal protein gene transcripts (Kress 2008).

Although only about 5 % of the *S. cerevisiae* genome consists of intron-containing genes (Spingola 1999, Parenteau 2008), compared to about 95 % in humans (Lander 2001, Venter 2011), splicing is still important in yeast, as introns are overrepresented in the highly expressed (*e.g.* ribosomal protein) genes. Hence, intron-containing transcripts account for more than one fourth of total transcripts in yeast (Ares 1999).

It is noteworthy that several genes encoding proteins involved in gene expression and mRNA export also contain one or more introns. These are *SUS1* (encoding a subunit of both the SAGA coactivator complex and the NPC-associated export complex THSC / TREX-2; Cuenca-Bono 2011), *YRA1* (encoding an mRNA export adaptor and subunit of the transcription-export complex TREX; Portman 1997), *DBP2* (DEAD box RNA helicase involved in RNA quality control and mRNP assembly; Barta 1995), and *MTR2* (part of the heterodimeric mRNP export receptor Mex67-Mtr2; Parenteau 2008). Introns in these genes are necessary for full viability and / or efficient mRNA export. The intron of *YRA1*, for instance, which has a non-canonical branchpoint sequence, controls Yra1 expression levels: Expression of an intronless *YRA1* gene leads to overproduction of Yra1 and impairs growth and mRNA export (Rodriguez-Navarro 2002, Preker 2002). The unusual BPS and the length of the intron lead to inefficient splicing and premature export with subsequent cytoplasmic degradation if Yra1 protein levels are high (Preker 2006, Dong 2007).

This indicates that splicing of some regulators of gene expression is important for homeostasis of these proteins and serves to fine-tune gene expression. It suggests a model of kinetic coupling between splicing and export (Johnson 2012), whereby special "sensor transcripts" allow a feedback loop between more or less robust mRNA processing and more or less efficient transcription and export: If splicing cannot keep up with export, the export pathway should be slowed down, which could, for example, be achieved by inefficient production of Yra1 or Sus1 (Johnson 2012).

Furthermore, cotranscriptional splicing processes seem to directly influence the kinetics of transcription elongation. Two different groups have described recently that RNAPII pauses in terminal yeast exons to allow sufficient time for cotranscriptional splicing (Carillo Oesterreich 2010; Alexander 2010).

Thus, splicing is coupled to transcription, just like other mRNA processing steps, and recruitment of the splicing machinery is orchestrated by the CTD of Rpb1, which enhances splicing (Montes 2012). The splicing factor Prp40 has been reported to bind to the S2-

phosphorylated CTD and thus mediate splicing complex recruitment (Morris 2000). However, a more recent analysis showed that the WW domain of Prp40, which interacts with the CTD, is dispensable for early spliceosome recruitment and is instead only needed for later stages of spliceosome assembly (Görnemann 2011). A study in mammalian cells showed that the CTD recruits a complex of the splicing factors U2AF65 and Prp19 complex and assigned a "bridge" function to U2AF65, which is proposed to link the transcription machinery with later stages of spliceosome assembly by binding to both the CTD and to Prp19 (David 2011).

2.1.3. 3' end processing: cleavage and polyadenylation

Once a protein-coding gene is has been transcribed, specific sequence elements in the 3' untranslated region of the nascent transcript (the polyadenylation signal) trigger endonucleolytic cleavage of the RNA and the addition of a poly(A) tail at the newly produced 3' OH by a complex 3' end processing machinery (Chan 2011).

This machinery is predominantly well conserved from yeast to human and consists of several subcomplexes. In yeast, these are cleavage factor IA (Rna14, Rna15, Clp1, Pcf11), cleavage factor IB (Hrp1), and cleavage and polyadenylation factor (CPF; with two subcomplexes CF II and PF I, including the poly(A) polymerase Pap1). The mammalian machinery comprises cleavage and polyadenylation specificity factor, cleavage stimulation factor, cleavage factor I, and cleavage factor II as well as poly(A) polymerase, poly(A) binding protein, and symplekin (Millevoi 2010).

In yeast, the poly(A) signal consists of four sequence elements, which are rather degenerate: an AU-rich efficiency element, an A-rich positioning element and two U-rich elements directly flanking the cleavage / polyadenylation site (Mischo 2012). Genes can have several polyadenylation sites, and alternative polyadenylation, giving rise to different mRNA isoforms per gene, seems to be rather common in all eukaryotes (Tian 2012). The use of alternative polyadenylation sites can alter the stability or translation efficiency of the respective transcript, and it even creates the possibility of a global regulatory response to environmental conditions. For example, treatment of yeast cells with the DNA damaging UV mimetic drug 4-NQO was shown to induce genome-wide variation in poly(A) site distribution, which was accompanied by an impairment in cleavage and polyadenylation (Graber 2013). The mRNA export factor Yra1 also modulates cleavage site choice, as Yra1 depletion causes widespread changes in poly(A) site choice by enhancing premature recruitment of CF1A subunit Clp1 (Johnson 2011). Furthermore, cleavage factor Hrp1/Nab4 has also been described to modulate 3' end processing by influencing cleavage site choice (Kim Guisbert 2007). In human cells, Thoc5 (a

subunit of the human TREX complex) seems to control cleavage site choice by recruiting cleavage factor CFIm68 (Katahira 2013).

The SR-like RNA-binding protein Npl3, which plays various roles in splicing, mRNA export, and translation (Kress 2008, Lei 2001, Windgassen 2004), has been shown to antagonize transcription termination by competing with termination factors for RNA binding, suggesting an interplay of transcription and mRNA packaging with termination (Bucheli 2005). More evidence for such interplay comes from a study which found that mRNA export factors (THO, Sub2, Yra1, Sac3, Mex67) are needed for efficient release of the cleavage factor Rna15 (Qu 2009).

The poly(A) tail that is added to the cleaved transcript has a rather constant length of about 70 to 80 adenosines in yeast and about 250 in mammals. It allows the binding of poly(A) binding proteins, conferring protection from exonucleases and increasing stability of the mRNA, is important for mRNA export, and additionally serves to stimulate translation initiation in the cytoplasm (Eckmann 2011).

As soon as it is synthesized, the poly(A) tail is coated with poly(A) binding proteins. In humans (which possess one nuclear and several cytoplasmic poly(A) binding proteins), the nuclear poly(A) binding protein PABPN1 binds to the tail, stabilizes the complex with the poly(A) polymerase PAP, stimulates its processivity, and also limits tail length (Eckmann 2011). Yeast possesses only one PABP, Pab1, which is the ortholog of mammalian cytoplasmic PABPCs. The functional homolog of PABPN1 in the nucleus is Nab2, which does not share sequence homology with PABPN1 and controls poly(A) tail length (Eckmann 2011, Millevoi 2010). It probably does so in interplay with the exosome component Rrp6, which can displace Nab2 and thus promote mRNA decay (Schmid 2012).

2.2. Packaging and nuclear export of mature mRNA transcripts in *S. cerevisiae*

Successful completion of the mRNA processing steps described above and the concomitant association with export factors finally lead to the formation of mature messenger ribonucleoprotein (mRNP) particles, which can be exported to the cytoplasm for translation into proteins. Packaging and export factors are recruited and dismissed at appropriate stages (see below), and mRNA export has been aptly described as a "series of molecular wardrobe changes" (Kelly 2009).

2.2.1. Cotranscriptional mRNP biogenesis and recruitment of the mRNA export receptor Mex67-Mtr2

The export of mature mRNP particles is mediated by the conserved heterodimeric export receptor Mex67-Mtr2, which is recruited cotranscriptionally, binds to the mRNP, and interacts with different FG-repeat domains of nucleoporins lining the channel of the nuclear pore complex (NPC) for passage through the pore (Gwizdek 2006; Dieppois 2006, Segref 1997, Hurt 2000, Sträßer 2000b). Although the export receptor can bind directly with low affinity to RNA *in vitro*, it is recruited by adaptor proteins, which mediate binding of Mex67-Mtr2 to mRNAs *in vivo* (Kelly 2009).

The association and dissociation of mRNA export factors during mRNP maturation and export as well as nuclear export and import of the factors themselves are in several instances regulated by posttranslational modifications such as phosphorylation, arginine methylation, and ubiquitylation (*e.g.* Gilbert 2001, Yu 2004, Gilbert 2004, McBride 2005, Gwizdek 2005, Gwizdek 2006, Iglesias 2010). The process of mRNP biogenesis begins early during transcription and takes place cotranscriptionally, allowing crosstalk between different steps and enhancing efficiency and accuracy (Perales 2009).

The TREX complex (discussed in more detail in section 2.4. below) is a key complex coupling transcription elongation and mRNA export. TREX component Yra1 is the canonical adaptor protein recruiting Mex67-Mtr2 to the mRNP (Sträßer 2000a, Zenklusen 2001). In addition, Yra1 interacts directly with the 3' end processing factor Pcf11 (Johnson 2009) and was reported to bind directly to the S2-phosphorylated CTD of Rpb1 (MacKellar 2011). The current model of recruitment proposes that Yra1 is recruited to the site of transcription by interaction with the 3' end processing machinery (Johnson 2011), is then handed off to Sub2, which is recruited by the THO complex, and recruits Mex67 in exchange for Sub2 (Sträßer 2001, Sträßer 2002, Zenklusen 2002, Johnson 2009). This involves two sequential exchanges

of binding partners due to mutually exclusive interactions: Pcf11 and Sub2 contact the same regions of Yra1 (Johnson 2009), as do Sub2 and Mex67 (Sträßer 2001).

However, not all mRNAs that are bound by Mex67 are also bound by Yra1 (Hieronymus 2003), and the shuttling SR-like protein Npl3 and hnRNP Nab2 are additional proteins that are required for mRNA export in *S. cerevisiae* (Gilbert 2004, Green 2002, Iglesias 2010). One genome-wide analysis of RNA binding profiles of adaptor proteins showed Npl3 to be altogether preferentially associated over Nab2 with the more abundant mRNAs (Kim Guisbert 2005), whereas a more recent study found Nab2 to be associated with the majority of yeast transcripts and described Nab2 as a general mRNA export factor (Batisse 2009). Subsequently, it was suggested that Nab2 also binds directly to Mex67, and that this interaction is promoted and stabilized by Yra1. Nuclear ubiquitylation of Yra1 by the ubiquitin ligase Tom1 then mediates the dissociation of Yra1 from the Nab2-bound mRNP (Iglesias 2010).

Npl3 is also recruited cotranscriptionally but independently of the THO complex to transcribed genes (Lei 2001, Häcker 2004) and, in its unphosphorylated form, associates with RNAPII and stimulates transcription elongation (Dermody 2008). In addition, it recruits the export receptor Mex67 to the nascent transcript, promoting mRNA export (Lee 1996, Gilbert 2004). A cycle of cytoplasmic phosphorylation and nuclear dephosphorylation controls Npl3's association with the mRNP and its nucleocytoplasmic shuttling: The action of the nuclear phosphatase Glc7 is required for the association of Npl3 with mRNAs and with Mex67, leading to mRNP export, whereas cytoplasmic phosphorylation by kinase Sky1 promotes binding of Npl3 to its nuclear import receptor Mtr10 (Gilbert 2004, Gilbert 2001). A prolonged association of Npl3 with polysomes can negatively influence translation, and Mtr10, not Sky1, was subsequently shown to mediate the timely release of Npl3 from the polysomes (Windgassen 2004).

Hpr1, a member of TREX subcomplex THO which is ubiquitylated by the ubiquitin ligase Rsp5 (Gwizdek 2005), is also able to bind directly to the UBA-binding domain of Mex67 and could thus recruit Mex67 to the mRNA by a Yra1/Nab2- or Npl3-independent pathway (Gwizdek 2006, Hobeika 2007).

Lastly, *THO1* (encoding a conserved nuclear RNA binding protein), just like *SUB2*, was discovered as a multicopy suppressor of the mRNA export defect of the *hpr1Δ* mutation of the THO complex (Piruat 1998, Jimeno 2002). Tho1 furthermore interacts genetically with Nab2, also pointing to a function in mRNA export. Thus, overexpression of Tho1 or Sub2 might provide alternative mRNP biogenesis pathways when the function of the THO complex is impaired (Jimeno 2006).

In summary, recruitment of the export receptor Mex67 to the mRNA can be mediated by several proteins, however, it remains to be further elucidated whether these factors display any specificity for special classes of transcripts.

2.2.2. mRNP remodeling events and passage through the nuclear pore

Maturation of the mRNP involves the regulated recruitment and release of proteins. RNA helicases of the DEAD box family play an important role in remodeling events during mRNP assembly and export. They do not only unwind RNA structures but have also been implicated in protein displacement and can thus mediate the exchange of protein factors during mRNP maturation (Linder 2011, Putnam 2013).

Recently, the DEAD box helicase Dbp2 was shown to be recruited to actively transcribed genes (Cloutier 2012) and has been implicated in promoting the loading of Yra1, Mex67, Nab2, and likely other RNA binding proteins on the RNA by unwinding inhibitory secondary structures of the nascent transcript (Ma 2013). Association with Yra1 then inhibits Dbp2's duplex unwinding activity and might also trigger Dbp2's release from the mRNP (Ma 2013). Yra1 on the other hand is released from the Nab2-bound mRNP prior to nuclear export by Tom1-mediated ubiquitylation (Iglesias 2010).

The Mex67-Mtr2 export complex escorts the correctly assembled mRNP through the nuclear pore. Directionality of this process is achieved by a major remodeling step of the mRNP upon its arrival on the cytoplasmic side of the nuclear envelope. The DEAD box RNA helicase Dbp5 is the key player here and causes the release of Mex67 and Nab2 from the mRNP in the cytoplasm (Tran 2007, Folkmann 2011). Dpb5 binds to RNA cotranscriptionally, interacts functionally with the transcription machinery, accompanies the mRNP through the nuclear pore, and binds to Nup159 on the cytoplasmic side of the NPC (Cordin 2006). Only there, its ATPase activity is locally activated by the nuclear pore protein Gle1 bound to the small molecule inositol hexakisphosphate (IP_6), which leads to mRNP remodeling (Folkmann 2011, Linder 2011).

Besides Dbp5, Nab2, and Mex67, other proteins have been shown to be exported along with the mRNA and shuttle between nucleus and cytoplasm: the cap binding complex, cleavage and polyadenylation factor Hrp1, poly(A)-binding protein Pab1, and the SR-like proteins Npl3, Gbp2 and Hrb1 (Häcker 2004 and references therein). Of the last three, Gbp2 and Hrb1 depend on the THO complex for recruitment and subsequent export, while Npl3 is recruited independently of THO (Hurt 2004, Häcker 2004; see Figure 4 for a summary).
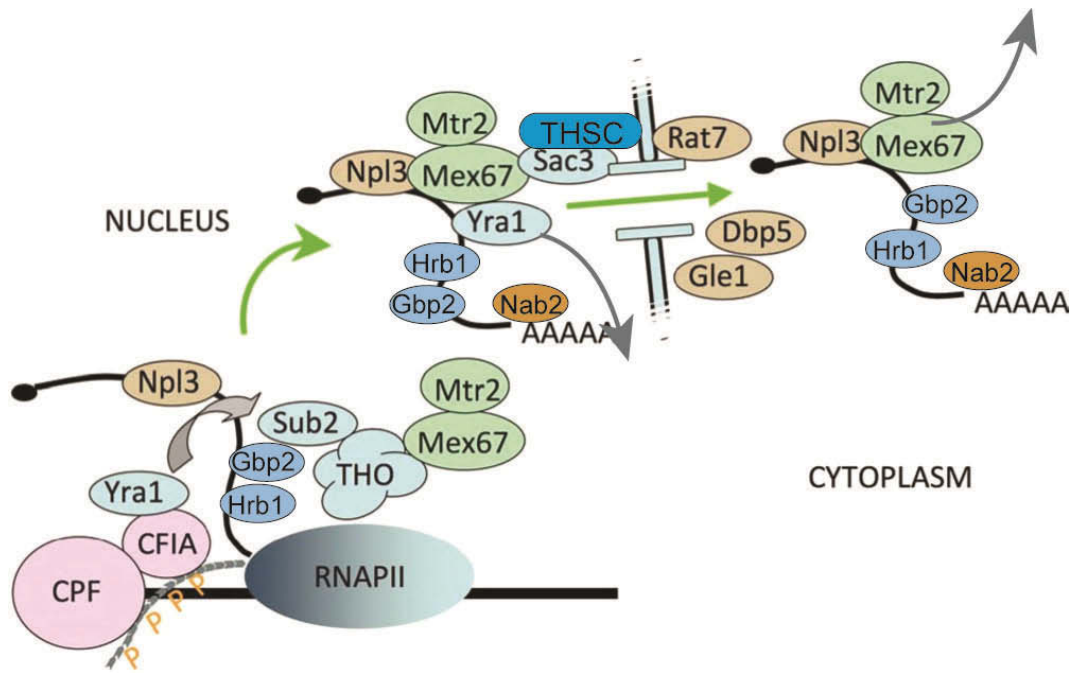
Figure 4: mRNA export requires successful maturation of the mRNP (modified from Qu 2009). Export factors are recruited, package the transcript, and dissociate again at different stages along the export pathway (see text for details).

Sub2 is another member of the DEAD-box helicase family and as part of the TREX complex plays an important role in mRNA export and the maintenance of genomic integrity (see 2.4.). A recent study analysed the domains of Sub2 and pinpointed Sub2's function in mRNA export to a previously uncharacterized N-terminal motif (NTM). Mutation or deletion of the NTM caused nuclear accumulation of poly(A) RNA but did not affect helicase activity *in vitro*, suggesting that the NTM is the region of Sub2 that mediates binding to other mRNA export factors (Saguez 2013).

Besides the TREX complex, which will be discussed in more detail below (section 2.4.), a second complex called THSC (TREX-2) is important for mRNA export. It consists of Sac3, Thp1, Sus1, Sem1, and Cdc31. THSC mutation confers most of the phenotypes also associated with THO/TREX mutations, but some differences suggest distinct roles in mRNP biogenesis for the two complexes, with THSC functioning further downstream from TREX (Rondon 2010). Unlike THO, the THSC complex is firmly associated with the nuclear pore complex via binding to nucleoporin Nup1 (Fischer 2002) and has been connected to "gene gating", the repositioning of activated genes to the nuclear periphery for facilitation of efficient mRNA export (Blobel 1985, Garcia-Oliver 2012).

2.3. Nuclear quality control mechanisms in mRNP formation and interconnections between transcription, mRNA processing, export and decay

As detailed above, many proteins need to be recruited and several processing steps have to be completed to yield a fully mature and export-competent mRNA packaged with the correct set of proteins (see also sections 2.2. & 2.4.). Cells have developed a number of quality control strategies to retain and degrade improperly processed transcripts, ensuring that only those mRNAs which will be able to be translated into functional proteins reach the cytoplasm (Schmid 2008).

Key effector proteins responsible for the degradation of improper RNA molecules in the nucleus are the 5' - 3' exonuclease Rat1 (XRN2 in human) with its cofactor Rai1 and the exosome, which possesses 3' - 5' exonucleolytic and endonucleolytic activity, with its nuclear cofactor TRAMP (Schmid 2013).

Rat1 not only functions in transcription termination but also serves as a control factor for mRNA capping. Together with the pyrophosphohydrolase Rai1 it rapidly degrades any transcripts without or with aberrant, e. g. non-methylated cap structures (Xiang 2009, Jimeno-Gonzalez 2010, Jiao 2010).

The cells furthermore ensure that transcripts of intron-containing genes are only exported after splicing has been completed. Unspliced transcripts seem to be actively degraded, since pre-mRNA levels increase in strains harboring mutations in the exosome, Rat1 or the Lsm2-8 complex involved with decapping (Schmid 2010). In addition, quality control takes place at the nuclear envelope where the NPC-associated protein Mlp1 is a key player in the retention of unspliced transcripts. It associates with the nucleoporin Nup60 on the nucleoplasmic side of the NPC (Feuerbach 2002) and retains unspliced transcripts in the nucleus (Galy 2004). Esc1, a non-NPC protein of the nuclear envelope, is further implicated in this nuclear retention machinery: It is required for normal localization of the Ulp1 SUMO protease as well as Nup60 and Mlp1 to the NPC (Lewis 2007). Similar to Mlp1, both Esc1 and the SUMO protease Ulp1 help to retain unspliced transcripts in the nucleus, leading to the speculation that localized protein desumoylation at the NPC might be an important regulatory event to prevent pre-mRNA export (Lewis 2007).

Not only exonucleases but also endonucleases seem to play a role in nuclear mRNA quality control. The endonuclease Swt1 interacts genetically with members of the THO/TREX and THSC (TREX2) complexes, the perinuclear surveillance machinery (Mlp1, Esc1, Nup60), and with Npl3 (Röther 2006, Skruzny 2009), and *SWT1* deletion leads to increased cytoplasmic

leakage of improperly spliced pre-mRNAs, which is further increased by concomitant deletion of *MLP1* or *NUP60* (Skruzny 2009).

In addition, both myosin-like proteins (Mlp1 and Mlp2) seem to fulfill a more general role in surveillance of mRNP export, *i. e.* also for intronless transcripts. In yeast strains expressing a mutant form of Yra1 certain transcripts are reduced and mRNA export is impaired. In this background, the deletion of Mlp1 or Mlp2 is able to rescue the growth defect associated with mutation of Yra1 (and also Nab2), probably due to an increased export of malformed mRNPs. Interestingly, this study also showed that in the mutant Yra1 background Mlp2 downregulates the expression of a subset of genes, pointing to the existence of a feedback loop which lowers transcription upon improper formation of mRNPs and impairment of mRNP export (Vinciguerra 2005).

Yeast strains lacking THO subunits or Sub2 provide insight into the effectiveness of 3' end surveillance mechanisms: These mutant strains exhibit defective polyadenylation (Saguez 2008), which leads to rapid degradation of the transcripts, in a manner dependent on the exosome component Rrp6 and also the TRAMP subunit Trf4 (Libri 2002, Rougemaille 2007, Saguez 2008). Another interesting phenotype of THO/Sub2 mutants is the retention of some improperly processed transcripts, which escape rapid degradation and instead accumulate as stalled mRNP intermediates (named "heavy chromatin"), that are detectable at the 3' end of several genes (Hilleren 2001, Libri 2002). This retention in foci at or near the transcription site is dependent on Rrp6 of the exosome but not TRAMP. The stalled mRNP intermediates contain nuclear pore components and polyadenylation factors in association with chromatin (Rougemaille 2007, Rougemaille 2008).

2.4. The TREX complex as key player coupling transcription and mRNA export

As described above, mRNA processing events take place cotranscriptionally and the responsible protein factors are recruited at different stages of transcription. The TREX complex is a key complex which couples transcription to mRNA export and fulfills diverse functions, ranging from transcription elongation to mRNA export and genomic integrity (see Fig. 5 for an overview).

This conserved complex consists of the THO subcomplex, the RNA helicase Sub2, the Mex67 adaptor protein Yra1, and the associated shuttling SR-rich proteins Gbp2 and Hrb1 (Sträßer 2002, Hurt 2004). THO was first purified from *S. cerevisiae* as a four-subunit complex

consisting of Tho2, Hpr1, Mft1, and Thp2 (Chavez 2000) and 12 years later described to also contain Tex1 as a core component (Pena 2012).

Yeast strains lacking THO subunits exhibit slow growth and transcription elongation impairment (Chavez 1997, Piruat 1998), and THO deletion negatively impacts RNAPII processivity (Mason 2005). THO is recruited to all protein-coding genes but is especially needed for the efficient transcription of long and GC-rich genes or genes containing internal repeats (Chavez 2001, Voynov 2006, Gomez-Gonzalez 2011).

TREX is required for mRNA export by recruiting the export receptor Mex67-Mtr2 via its subunit Yra1 (Sträßer 2000a, Zenklusen 2001; also see section 1.2.1. on mRNA export), and also functions in 3' end processing (Rougemaille 2008, Johnson 2011).

Besides its crucial functions connecting transcription and mRNA export, the TREX complex is also important for maintaining genomic integrity. Deletion of *HPR1* or *THO2* leads to defects in nucleotide excision repair (Gonzalez-Barrera 2002). Specifically, the transcription-coupled repair pathway is impaired in cells lacking THO, Sub2, or Yra1 (Gaillard 2007). Interestingly, THO and SUB2 mutants show elevated levels of transcription-associated recombination (TAR). Binding of THO to the nascent transcript, coating the RNA, is thought to prevent the formation of RNA-DNA hybrids called R loops between the nascent RNA and the upstream template strand of DNA. These structures are potentially dangerous because they slow down the polymerase, have been linked to impaired replication fork progression, increase susceptibility to DNA damage and overall increase genetic instability (Huertas 2003, Tous 2007, Wellinger 2006). The helicase activity of Sub2 might help to unwind R loops since the overexpression of Sub2 is able to suppress the hyperrecombination phenotype and transcriptional defects of *hpr1Δ* cells (Fan 2001, Jimeno 2002).
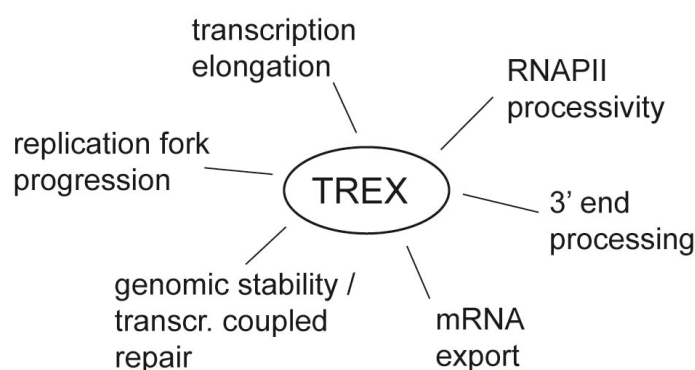
Figure 5: TREX functions in diverse processes in *S. cerevisiae*. See text for details.

In yeast, TREX is recruited to active chromatin in a transcription-dependent manner (Sträßer 2002, Zenklusen 2002), and recruitment of THO was published to be independent of RNA, whereas Yra1 and especially Sub2 occupancies depend also on RNA (Abruzzi 2004). In human cells, TREX is recruited in a splicing- and 5' cap-dependent manner by an interaction of Yra1 homolog Aly with the cap-binding protein CBP80 (Zhou 2000, Masuda 2005, Cheng 2006). Recent evidence suggests, however, that TREX also mediates the export of intronless transcripts in human cells via binding to a conserved sequence element termed CAR-E (Lei 2013).

Interestingly, a recent study in yeast provided a link between a splicing-associated complex and mRNA export. The Prp19 splicing complex was shown to stabilize TREX occupancy on transcribed genes since TREX occupancy was diminished at the 3' end of genes upon mutation of Prp19 complex subunit Syf1. However, the Prp19 complex is obviously not responsible for the initial cotranscriptional recruitment of TREX at the 5' end of genes (Chanarat 2011, Chanarat 2012). Thus, it remains to be determined how THO/TREX is initially recruited to the transcription machinery.

2.5. Aim of the study

Different adaptor proteins are known to function in recruiting the mRNA export receptor Mex67-Mtr2. However, their exact specificities remain to be determined. TREX recruitment to transcribed genes has long been known to occur cotranscriptionally in yeast but all the same the exact recruitment mechanism remained elusive.

In this project, my fellow PhD student Dominik Meinel and I used chromatin immunoprecipitation coupled to tiling array hybridization for a comprehensive survey of the mRNA export machinery in the yeast *S. cerevisiae*. We define and analyse the recruitment profiles of TREX and mRNA adaptor proteins and by additional experiments uncover the initial mechanism of THO recruitment to the transcription machinery.

3. Results

3.1. Genome-wide analysis of the mRNA export machinery in *S. cerevisiae*

The export of mRNAs relies on the coordinated action of various factors, which are recruited cotranscriptionally. The export receptor Mex67-Mtr2 needs adaptor proteins to mediate its interaction with the mRNA (see 1.2). We wanted to investigate whether different proteins with a known function in mRNA export (the THO complex, mRNA-binding proteins Sub2, Yra1, Gbp2, Hrb1, Nab2, and Npl3) are recruited differentially to transcribed genes. To this end, we performed chromatin immunoprecipitations with subsequent hybridization to high-density tiling arrays and calculated genome-wide occupancy profiles of these factors as well as of the RNAPII subunit Rpb3.

[Note: Approximately half of the ChIP-chip experiments were conducted by Dominik Meinel, Sträßer lab, who also performed the bioinformatic analyses for all data.]

3.1.1. Subunits of the transcription export complex TREX and other export adaptor proteins are globally recruited to RNAPII transcribed loci

To gain insight into recruitment profiles of TREX we grouped the top 50 % most highly transcribed genes into three different length classes and calculated meta profiles from normalized ChIP-chip occupancy data (similar to Mayer 2010; for details see legend to Fig. 8 and Methods section). This was done by mathematically scaling all genes within one length group to the same length and plotting average occupancies of the different factors across the gene from 250 bp upstream of the transcription start site to 250 bp downstream of the transcription termination site.

Meta profiles revealed a highly similar recruitment profile of the THO complex, Yra1, and Sub2, with low occupancy in the 5' region followed by increasing recruitment towards the 3' end of genes. Factors leave at the polyadenylation site and before the transcription termination site, in line with a function in mRNA export. Yra1 and Sub2 seem to leave slightly prior to the THO complex, which might be explained by their transferral to the nascent mRNA (Figure 6 A). In contrast, occupancy of the other TREX subunits Gbp2 and Hrb1 and the non-TREX export adaptors Nab2 and Npl3 increases only in the 5' region. Nab2 occupancy then reaches a plateau whereas Gbp2, Hrb1, and Npl3 occupancies even decrease slightly, before all factors drop off around the polyadenylation site together with the THO subunits (Figure 6 B).
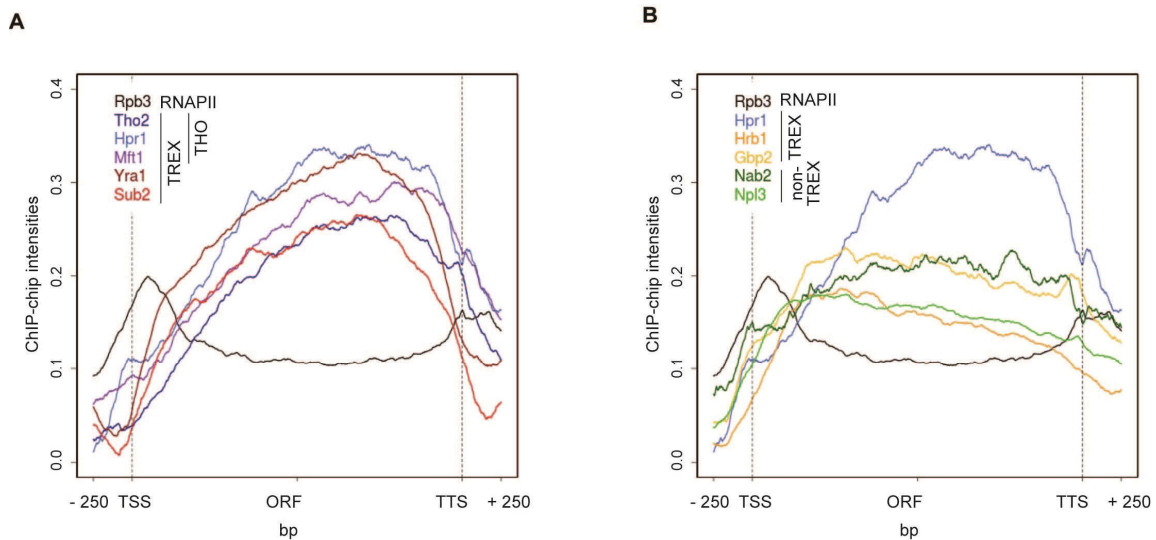
Figure 6: The TREX complex and other mRNA adaptor proteins are recruited to all protein-coding genes, but to varying amounts across the ORF. Meta profiles were calculated from ChIP-chip data of the top 50 % most highly transcribed genes (here exemplary profiles of the group of longer genes with 1,538-2,895 bp). All genes were scaled to the same length, and the average occupancies of the factors were plotted from 250 bp upstream of the transcription start site (TSS) to 250 bp downstream of the polyadenylation (pA) site. **(A)** Meta profiles of Rpb3 (RNAPII), and THO complex subunits Tho2, Hpr1 and Mft1 (Thp2 is not shown but looks similar) as well as TREX components Yra1 and Sub2. **(B)** Meta profiles of TREX subunits Hrb1 and Gbp2 as well as non-TREX export adaptors Nab2 and Npl3 are plotted together with the profile of Hpr1 for comparison. **[Note: ChIP-chip experiments were performed together with Dominik Meinel (Sträßer lab), who also did the bioinformatic analyses.]**

We found that all TREX subunits, Nab2, and Npl3 are recruited to all transcribed protein-coding genes and - to a lesser extent - also to sn/snoRNA genes, with Npl3 showing a slight preference for intron-containing genes and Yra1 for intron-less genes (Figure 7). This is in agreement with Npl3's known involvement in splicing (Kress 2008).
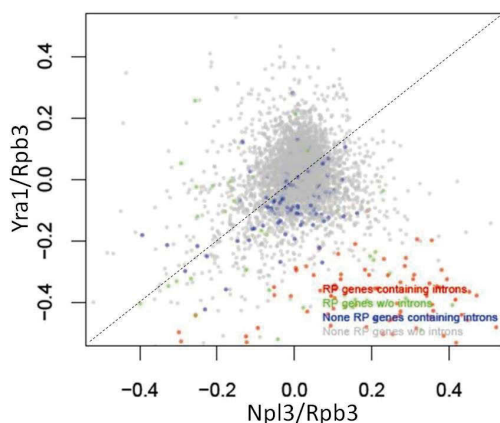
Figure 7: Mex67 adaptor protein Npl3 preferentially binds to intron-containing genes.
RNAPII-normalized peak occupancy values of Npl3 were plotted against the corresponding values of Yra1, with a discrimination between signals of bound probes representing intron-containing or intronless ribosomal protein genes (red / green) on the one hand and non-ribosomal protein genes (blue / grey) on the other hand.
[Analysis by Dominik Meinel (Sträßer lab)]

Other than that we were not able to discern any specific binding preferences among the different proteins. The global recruitment we observe is also consistent with recently published data on a genome-wide recruitment of Hpr1 and Sub2 to active ORFs (Gomez-Gonzalez 2011).

3.1.2. TREX occupancy increases with gene length

The meta profiles reveal that the core TREX complex (consisting of THO, Sub2, and Yra1) shows a genome-wide increase in occupancy from 5' to 3', as has been described for Hpr1, Sub2, and Yra1 on selected single genes (Abruzzi 2004) and more recently in another genome-wide study for Hpr1 and Sub2 (Gomez-Gonzalez 2011). This becomes especially apparent when the meta profiles for the three different length classes are graphically aligned at their transcription start sites and combined in one graph (Figure 8, A - E). In contrast to Yra1 and Sub2, the other mRNA binding proteins Gbp2, Hrb1, Nab2 and Npl3 do not increase in gene length (Figure 8, F - I).
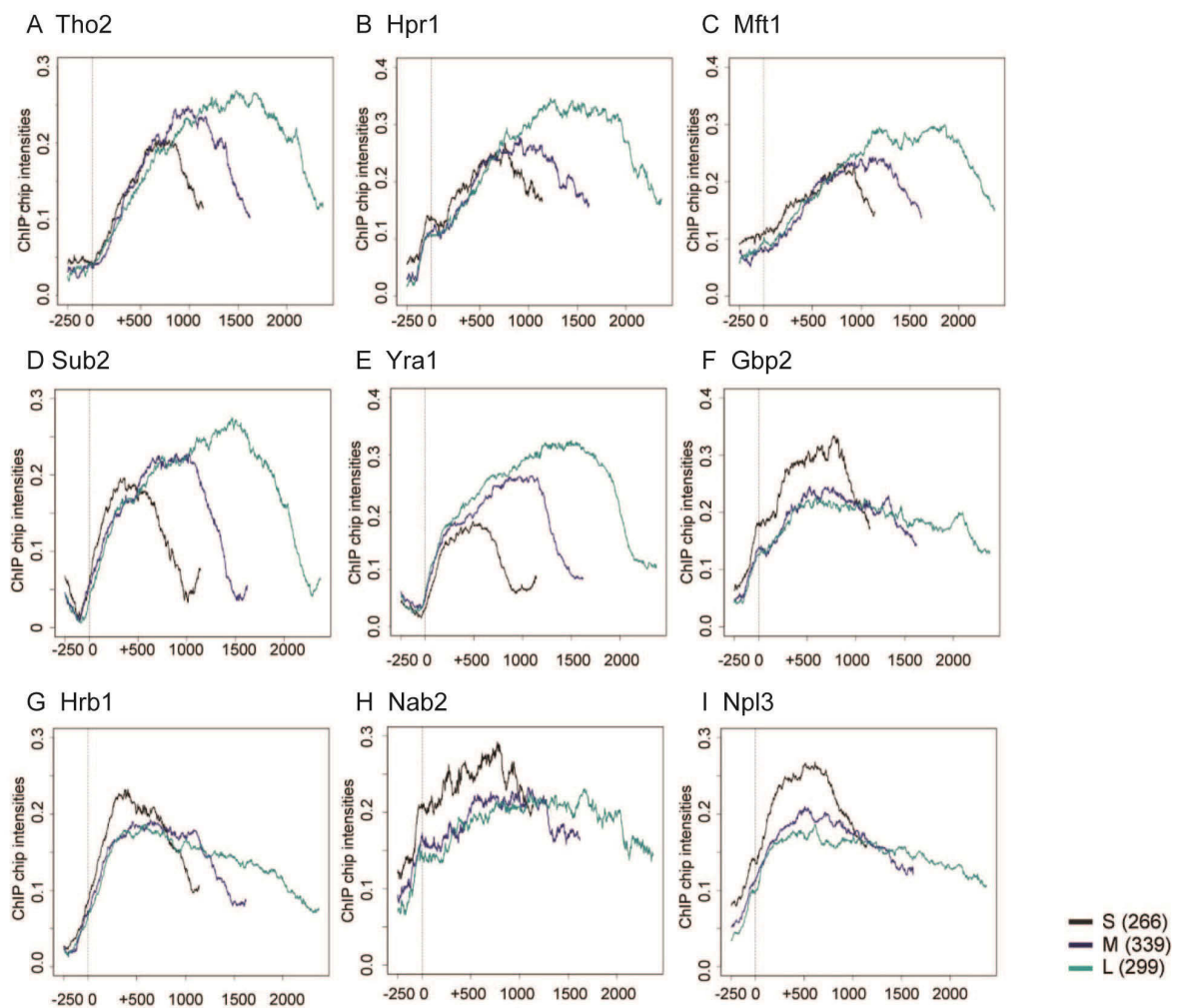
Figure 8: Recruitment profiles of THO, Sub2 and Yra1 are highly similar and increase with gene length while Gbp2, Hrb1, Nab2 and Npl3 do not. Meta profiles of gene occupancy were calculated of THO / TREX subunits (A - G), Nab2 (H), and Npl3 (I) for genes grouped into three different length classes. These classes were defined as in Mayer 2010: S (512-937bp; 266 genes), M (938-1537 bp, 339 genes) and L (1538-2895 bp, 299 genes). [Analysis by Dominik Meinel (Sträßer lab)]

Correlation coefficients between the peak occupancies of the individual proteins also reflect this difference in recruitment. While THO, Sub2 and Yra1 correlate well with each other but

not so highly with general elongation factors and the other mRNA binding proteins in our study, these other proteins (Gbp2, Hrb1, Npl3, and Nab2) correlate better with general elongation factors, whose occupancy also does not increase with length, and less with the core TREX subunits (data not shown).

Since other transcription elongation factors such as Spt5, Spt6 or Paf1 do not increase with gene length the observed 5' → 3' increase in core TREX recruitment is unique and intriguing. It could either result from increasing recruitment as the transcription complex progresses on a gene, with TREX reaching a maximal occupancy at some point independent of gene length, or TREX occupancy becoming constantly more and more the longer the gene gets. To distinguish between these scenarios, genes were divided into eight different length classes (see legend to Figure 9) and peak occupancies that were normalized to the respective Rpb3 peak occupancies to control for varying transcriptional activity were plotted for each length class (Figure 9).

These plots show that occupancy of THO and TREX subunits Yra1 and Sub2 becomes indeed higher the longer a gene is (especially pronounced for genes with up to 1500 bp in length but still clearly increasing further for longer genes), while the recruitment of the elongation factor Spt5 remains constant (Figure 9 A). Gpb2, Hrb1, Npl3, and Nab2 show similar behavior as Spt5 and do not increase significantly with length (Figure 9 B).
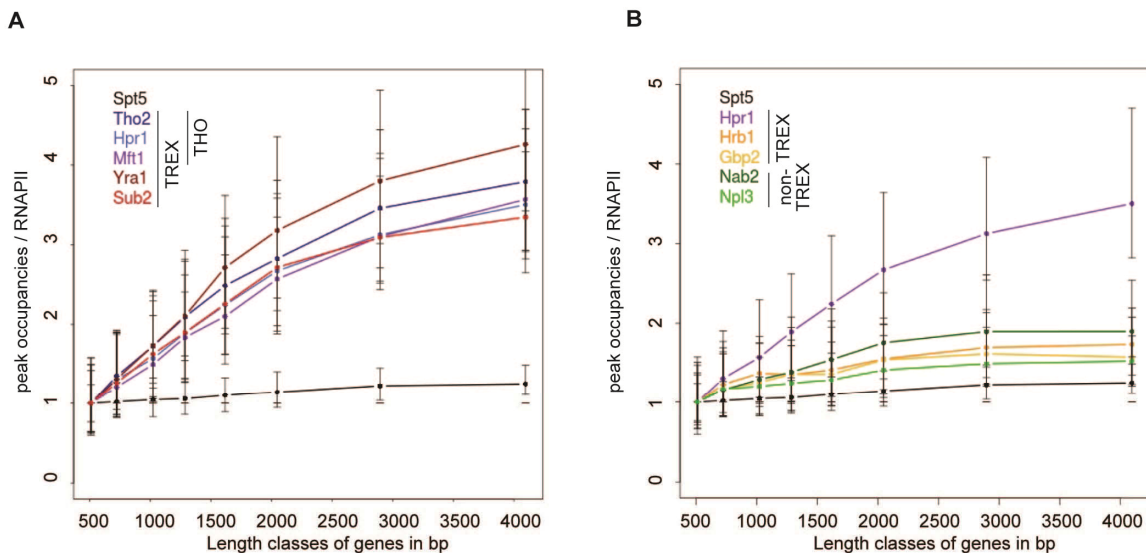
Figure 9: TREX recruitment increases with gene length. (A) The peak occupancies of TREX components Tho2, Hpr1, Mft1, Yra1 and Sub2 increase with gene length, while transcription elongation factor Spt5 occupancy remains constant. [Data for Spt5 was taken from Mayer 2010] (B) Same plot as in (A); the recruitment of SR-like proteins Hrb1, Gbp2, and Npl3 as well as Nab2 - contrary to THO, Sub2 and Yra1 - does not increase with gene length. Genes were subdivided in different length classes and the peak occupancy normalized to RNAPII occupancy within each length class was plotted. Length classes are: A (512-723 bp), B (724-1023 bp),C (1024-1286 bp), D (1287-1617 bp),E (1618-2047 bp),F (2048-2895 bp),G (2896-4095 bp),H (4096-5793 bp). [Analysis by Dominik Meinel (Sträßer lab)]

3.1.3. The length-dependent increase of TREX occupancy correlates with the increase in S2- and Y1-CTD phosphorylation

Two reasons for the observed length-dependent increase in TREX occupancy are conceivable: On the one hand, it might be the nascent RNA, to which more and more TREX complexes can bind as it grows longer. On the other hand, it could be the CTD of Rpb1 with its phosphorylation pattern that changes during the transcription cycle, thus facilitating an increasing recruitment of TREX.

Dominik Meinel (Sträßer lab) employed a ribozyme-encoding reporter gene assay to assess whether the increase in TREX towards the 3' end is the result of an interaction with the growing RNA. Upon transcription, the ribozyme folds and cleaves itself, releasing the upstream part of nascent RNA with all bound proteins from the site of transcription. In comparison with a mutated ribozyme construct that does not cleave itself, this assay revealed that TREX occupancy does partially depend on the presence of RNA but that the observed 5' → 3' increase is not caused by an increase in nascent RNA length during elongation (Meinel 2013).

Comparison with the genome-wide distribution profiles of Y1 and S2 CTD phosphorylation (Mayer 2010, Mayer 2012) revealed that THO occupancy follows the distribution of these phosphomarks within the ORF and drops before the transcription termination site together with Y1P, while S2P persists longer (Figure 10).
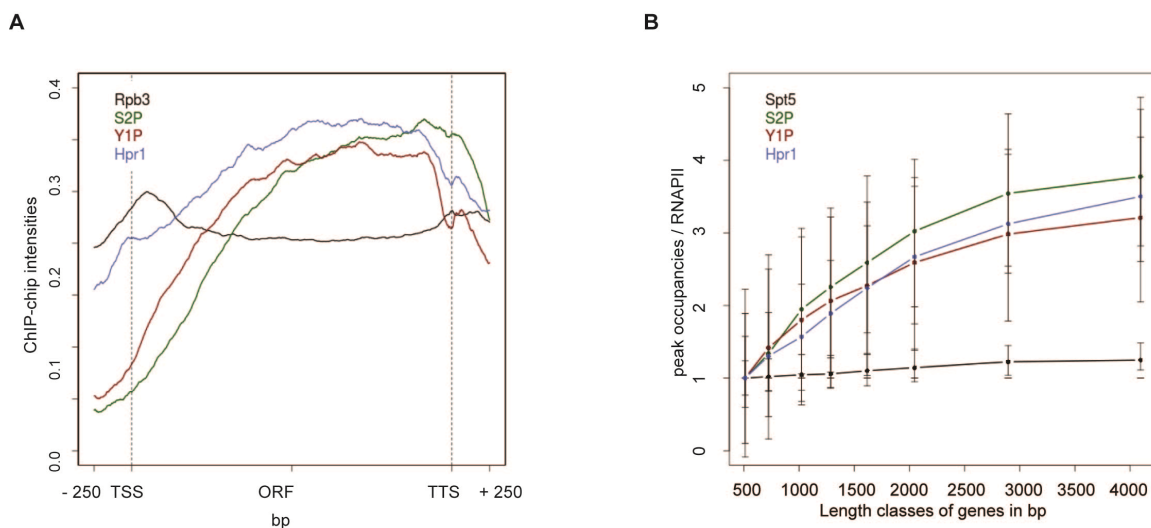
Figure 10: Hpr1 occupancy correlates with distribution of S2 and Y1 CTD phosphorylation. (A) Meta profiles of Hpr1, Rpb3, S2P, and Y1P **(B)** length dependency plot for Hpr1, Spt5, S2P, and Y1P [Spt5, S2P, and Y1P ChIP data are from Mayer 2010 and Mayer 2012; analysis by Dominik Meinel (Sträßer lab)]

Further experiments showed that Y1 and / or S2 phosphorylation of the CTD is necessary for TREX recruitment *in vivo* and that the THO complex is indeed able to bind directly to the S2/S5-diphosphorylated CTD of Rpb1 *in vitro* (Meinel 2013). Taken together, these results indicate that TREX is recruited to the transcription machinery by direct interaction of THO with the S2/S5 diphosphorylated CTD of Rpb1.

3.1.4. A C-terminal TAP-tag on Tho2 impairs its normal length-dependent recruitment to transcribed genes

Our ChIP-chip experiments led to the intriguing observation that a C-terminal TAP-tag impairs normal recruitment of Tho2. Tho2-TAP is recruited normally in the 5' region of genes but lacks the length-dependent increase in occupancy observed for the other THO subunits, Yra1, and Sub2.
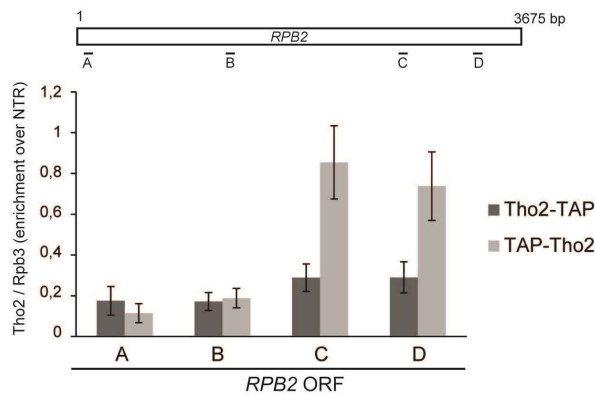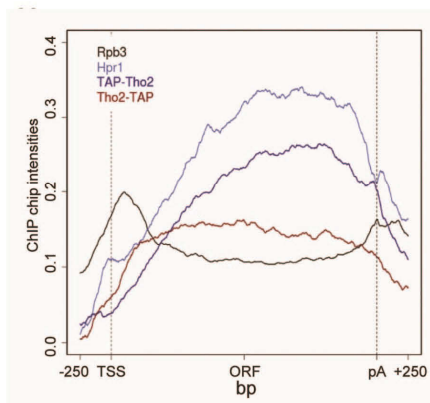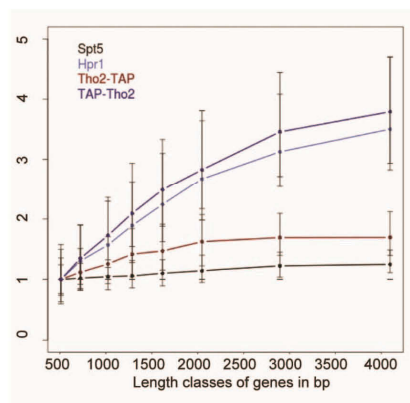
Figure 11: C-terminally TAP-tagged Tho2 shows impaired recruitment in the 3' region. (A) Recruitment of Tho2-TAP and TAP-Tho2 to the *RPB2*-ORF (primer locations are indicated on top) **(B)** Genome-wide meta profiles of Rpb3 (RNAPII), Hpr1, Tho2-TAP, and TAP-Tho2. **(C)** Length dependency plots for transcription elongation factor Spt5 [data from Mayer 2010], whose occupancy does not increase with gene length, and for Hpr1-TAP, Tho2-TAP and TAP-Tho2. [Analysis of the genome-wide data (B, C) by Dominik Meinel (Sträßer lab)]

The abnormal recruitment profile can be observed on a single exemplary gene (Figure 11 A) as well as on genome-wide profiles (Figure 11 B and C). Tagging on the N- instead of the C-terminus restores normal recruitment of Tho2 that closely matches the recruitment profiles of the other THO complex members (Figure 11 A, B, C and Figure 8).

Only at the *RPB2* gene, which is not so strongly expressed, the occupancy of the N-terminally tagged protein is a bit lower than that of the C-terminally tagged one (which was used in the genome-wide study). All in all, however, the results show a similar recruitment of both protein versions. Thus, the introduction of a strong artificial bias into our ChIP-chip data by location of the TAP tag on Thp2 and Gbp2 is unlikely.

We then used the *THO2-TAP* strain to specifically assess the effect of abolishing the 5' → 3' increase in TREX recruitment, since the complex otherwise assembles normally and is recruited as usual to the 5' end of genes in this strain (Dominik Meinel; data not shown). Expression analyses in *THO2-TAP* versus *TAP-THO2* yeast strains by Dominik Meinel (Sträßer lab) in collaboration with the lab of Frank Holstege (University Medical Center Utrecht, The Netherlands) showed that abrogation of the length-dependent increase in the Tho2-TAP strain leads to reduced expression of long genes, while other gene classes (e. g. highly transcribed, GC-rich) remain unaffected (Meinel 2013). The 5' → 3' increase in TREX recruitment is thus physiologically relevant for the efficient expression of long genes.

3.1.5. N- or C-terminal location of the TAP tag does not influence recruitment of Thp2 and Gbp2 to selected loci

Given the abnormal recruitment behavior of C-terminally TAP-tagged Tho2 I performed control ChIP experiments for another THO subunit (Thp2) and another TREX subunit (Gbp2) to exclude the possibility of artefacts introduced by the presence of the TAP tag on the analyzed proteins.

I performed chromatin immunoprecipitations with both C- and N-terminally TAP-tagged versions of both proteins and, by subsequent qPCR, analyzed their recruitment to two loci within three exemplary genes (*RPB2*, *ADH1*, and *PMA1)*, which are weakly, moderately, and strongly expressed, respectively (Figure 12).
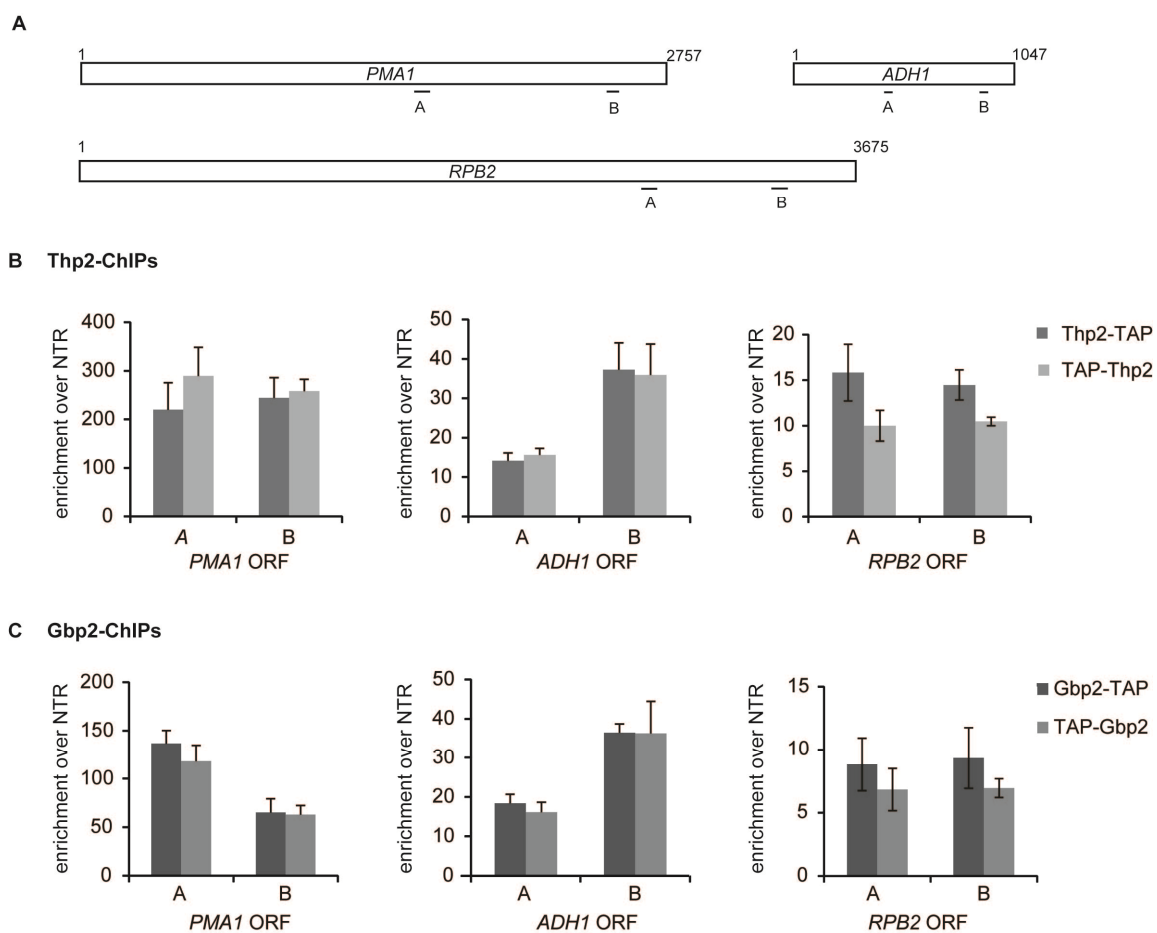
Figure 12: Comparison of the recruitment of C- or N-terminally TAP-tagged Thp2 and Gbp2 to selected loci. (A) Location of real-time primers within the analyzed ORFs. **(B)** ChIP occupancies (enrichment calculated over non-transcribed region, NTR) of Thp2-TAP vs. TAP-Thp2 at six loci in three different genes. **(C)** As in B, but for Gbp2. Results are the mean ± SD of three independent experiments.

3.2. A C-terminal TAP tag on Yra1 impairs normal function

3.2.1. A C-terminal TAP tag on Yra1 confers synthetic sickness with deletion of the *HPR1* and *THO2* genes

The C-terminal TAP tag fused to Yra1p does not influence growth in three different *S. cerevisiae* laboratory wild-type strains (BY4741, DS2-1b, and W303) at 20°C and 30°C and only minimally impairs growth at 37°C in the DS2-1b background (Figure 13).
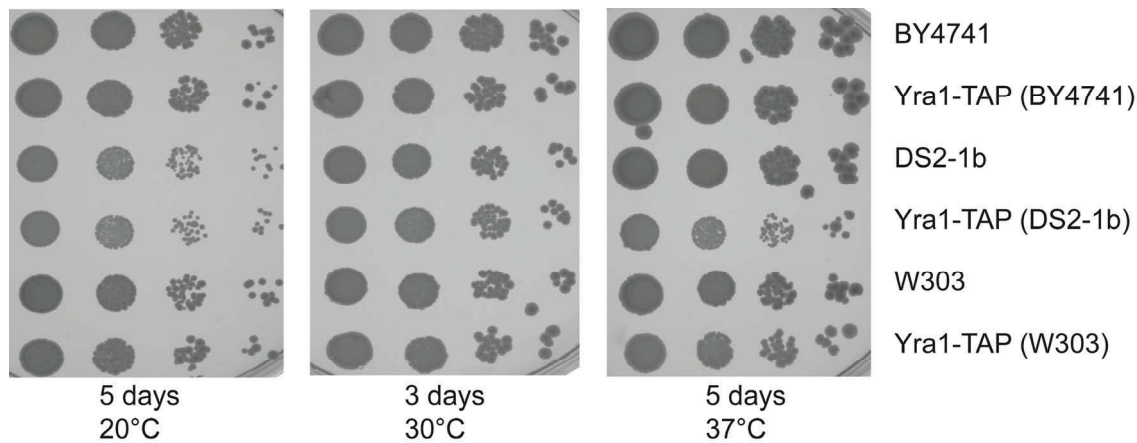
Figure 13: A C-terminal TAP tag on Yra1 has only minimal or no influence on growth of wild-type yeast strains. Growth was assessed by spot dilution assay on full medium (YPD) at different temperatures in three different wild-type *S. cerevisiae* strains and with additional expression of C-terminally TAP-tagged Yra1p.

However, there is a genetic interaction of *YRA1-TAP* with deletion of the *HPR1* and *THO2* genes (Figure 14), consistent with a functional relationship of these proteins, and indicating that the C-terminal TAP tag on Yra1 negatively impacts its functionality. Expression of a TAP tag fused to the C-terminus of Yra1p does not impair growth at any of the tested temperatures in the wild-type W303 yeast strain but mildly increases the already strong heat sensitivity of the *tho2*Δ strain. In the *hpr1*Δ strain it induces cold-sensitivity at 20°C and leads to synthetic lethality at 37°C (Figure 14). Therefore, an antibody directed against Yra1 was used for the ChIP-chip experiments.
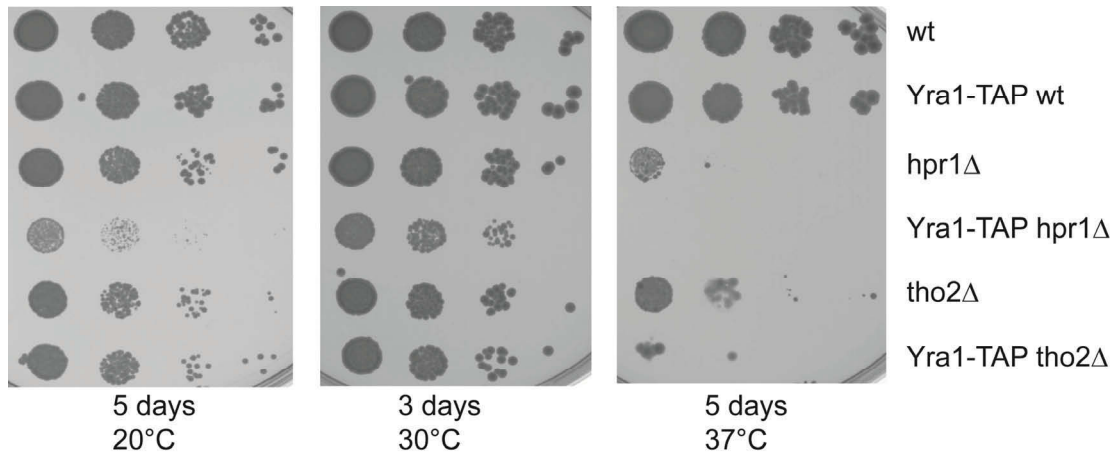
Figure 14: A C-terminal TAP-tag on Yra1 causes synthetic sickness with deletion of *HPR1* at normal and low temperature and synthetic lethality at high temperature. Spot dilution assay on full medium (YPD) to assess how expression of a C-terminal TAP tag fused to Yra1 influences growth at different temperatures in wt, *hrp1Δ*, and *tho2Δ* yeast strains (all W303 background).

3.2.2. Yra1 recruitment to transcribed loci is reduced when Hpr1 or Tho2 are absent

Since the *YRA1-TAP* allele interacts genetically with *THO2* and *HPR1* I wanted to examine the effect of *HPR1* and *THO2* deletion on Yra1 recruitment to transcribed genes and at the same time assess if the presence of a C-terminal TAP-tag influences Yra1 recruitment. To this end, I performed chromatin immunoprecipitations of Yra1 in wild-type, *hpr1Δ*, or *tho2Δ* backgrounds, using the TAP tag for immunoprecipitation on the one hand and an antibody raised against Yra1 in untagged strains on the other hand.
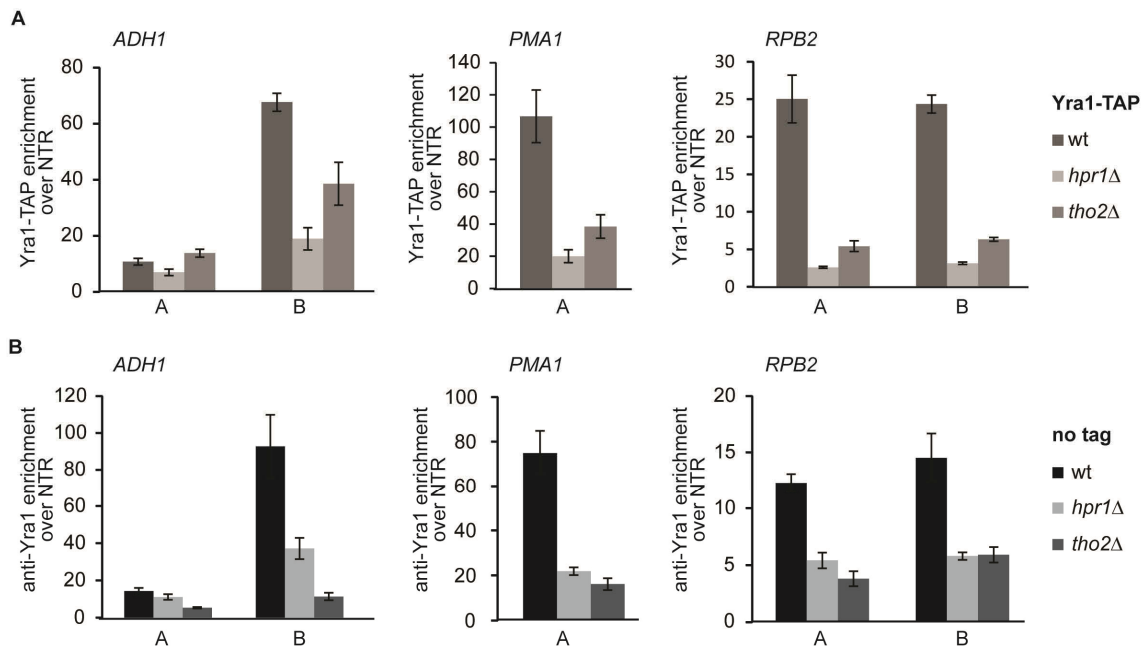
Figure 15: (A) Enrichment of Yra1-TAP over a non-transcribed region on three different genes was assessed by ChIP and subsequent real-time PCR using the TAP-tag on Yra1 for IP. **(B)** As in A, but Yra1 was immunoprecipitated by an antibody directed against Yra1 and Yra1 was not TAP-tagged. Results shown are the mean ± SD of 3 independent experiments. qPCR primers are the same as in Fig. 12.

In the absence of both THO subunits, Hpr1 and Tho2, the recruitment of Yra1 to the analysed genes is drastically reduced (Figure 15). Comparison of the ChIP data from immunoprecipitations using an antibody against Yra1 itself (Figure 15 B) with IPs using a C-terminal TAP tag (Figure 15 A), however, suggests that absence of Hpr1 in combination with the presence of a C-terminal TAP tag on Yra1 has an especially negative effect on Yra1 occupancy, which fits together with the stronger genetic interaction of YRA1-TAP with *hpr1Δ* than with *tho2Δ* (Figure 14). Results of the anti-Yra1-ChIPs, which likely reflect the "true" situation of Yra1 occupancy, show either equally reduced occupancy in both mutants (on *RPB2*-3'region) or a stronger negative effect of Tho2 absence (on *RPB2-M, ADH1* and *PMA1*) (Figure 15 B).

However, transcription is reduced in *hpr1Δ* and *tho2Δ* backgrounds, and reduced recruitment could be caused solely by overall reduced recruitment of the transcription machinery. Therefore I also quantified RNAPII occupancy at the selected genes and normalized the Yra1 recruitment levels obtained in Yra1-TAP- and anti-Yra1-ChIPs accordingly (Figure 16).
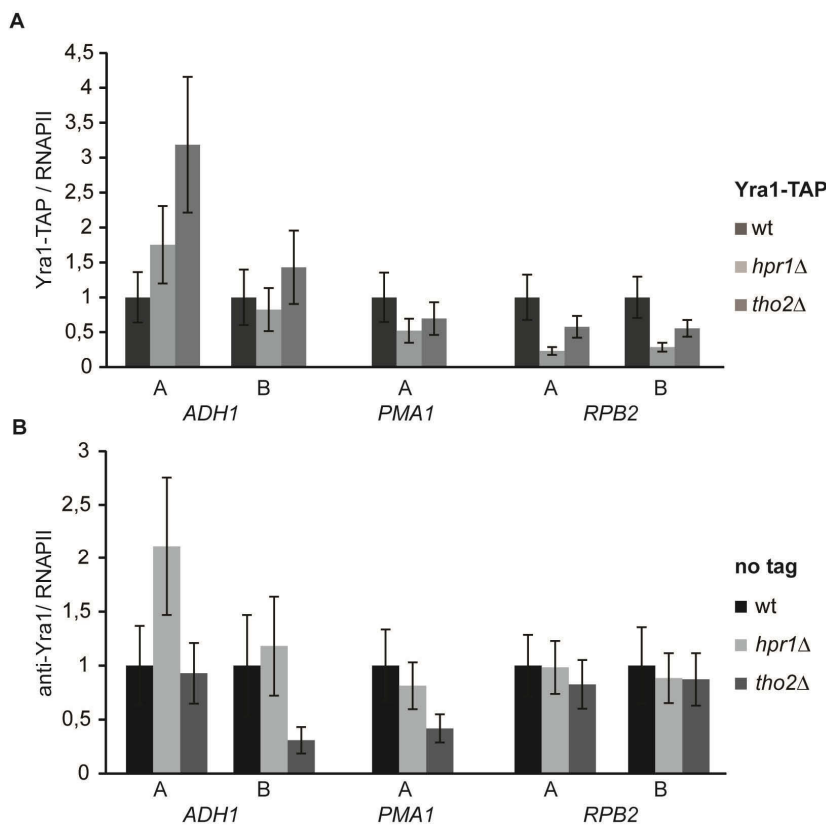
Figure 16: Yra1 recruitment normalized to transcription levels.
Same as in Figure 15, but Yra1 recruitment was first normalized to RNAPII occupancy, and the obtained values for the deletion strains were then normalized to the corresponding wt values.

Upon normalization to transcription levels, the presence of a C-terminal TAP tag on Yra1 together with deletion of *HPR1* still has the strongest negative effect on Yra1 recruitment to *PMA1* and *RPB2*, although the reduction is - due to the decrease in RNAPII occupancy to about 50 % of the wild-type in *hpr1Δ* and *tho2Δ* - no longer that pronounced (Figure 16 A).

On *ADH1*, transcription-normalized recruitment levels in the deletion mutants are even higher than in the wild-type. This is also true for recruitment of untagged Yra1 in the *hpr1Δ* background (Figure 16 B). Without the TAP tag and when the overall reduced rate of transcription in *hpr1Δ* and *tho2Δ* strains is taken into account only deletion of *THO2* has a clearly negative impact on Yra1 recruitment, whereas *HPR1* deletion only very slightly affects Yra1 levels on the gene (Figure 16 B; see also section 2.3.2.).

3.2.3. Steady-state Yra1 protein levels are upregulated when THO subunits are missing

Given the fact that transcription and the recruitment of Yra1 to several transcribed loci were more or less affected in deletion mutants of the THO complex (Figures 15 and 16) I wanted to check whether Yra1 was expressed at normal levels in these cells. Protein levels were assessed by quantitative Western Blot using whole cell protein extracts from wild-type, *hpr1Δ* and *tho2Δ* yeast strains.
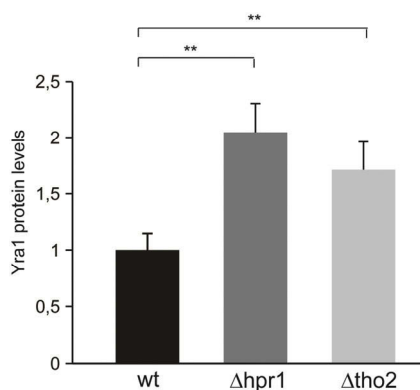
Figure 17: Yra1 protein levels are increased upon deletion of *HPR1* or *THO2*. Protein levels were quantified in whole cell extracts from untagged strains by Western Blot with an anti-Yra1 antibody and anti-Pgk1 as loading control. The graph shows the mean ± SD of three independent experiments.

Yra1 becomes significantly upregulated at the protein level upon deletion of THO complex subunits Hpr1 or Tho2 (Figure 17). Together with the ChIP data (Figure 15 and 16) this suggests that the cells are - more or less successful - trying to compensate for impaired Yra1 recruitment with increased expression of the protein.

Yra1 has been reported to bind directly to the S2,S5-diphosphorylated CTD of Rbp1 (MacKellar 2011) and to be recruited by direct interaction with 3' end processing factor Pcf11 (Johnson 2009). This data now underlines that the THO complex is important for stabilization of Yra1 on the gene and that the C-terminal region of Yra1 might be important for this interaction and its recruitment.

3.3. Deletion of single THO subunit differentially impairs recruitment of TREX subunits

3.3.1. RNAPII recruitment is reduced in deletion mutants of the THO complex

Mutation of THO complex subunits is known to affect the cell in many ways; one of them is the impairment of RNAPII processivity (Mason 2005). In order to quantify to what extent RNAPII recruitment is reduced in yeast strains lacking one THO subunit, I performed chromatin immunoprecipitations of Rpb3-TAP in the wild type and in four mutant yeast strains lacking one of the four THO subunits each.
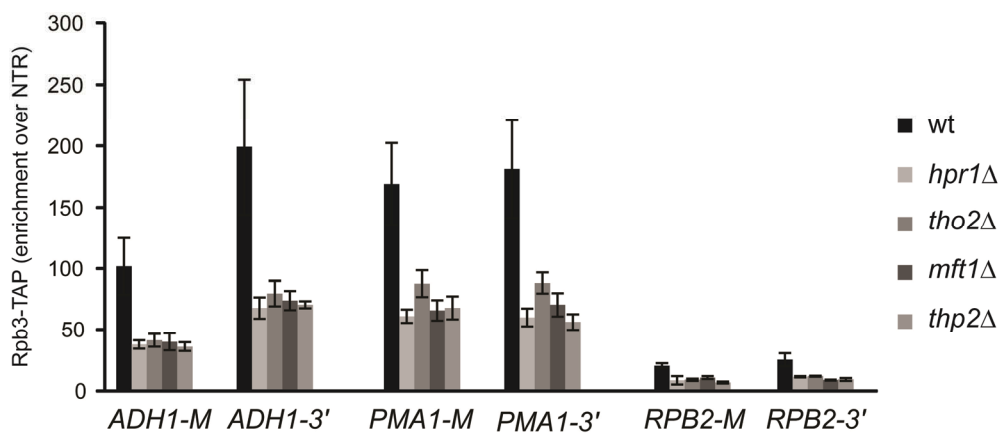
Figure 18: RNAPII recruitment is reduced when subunits of the THO complex are missing. Rpb3-TAP occupancy was assessed by chromatin immunoprecipitation in wild-type and THO-deficient yeast cells. Enrichment was calculated over a non-transcribed region on Chr. V. Results shown are the mean ± SD of three independent experiments per strain. qPCR primers are the same as in Fig. 12, with 'A' and 'B' corresponding to the middle ('M') and 3' region of the ORF in this figure, except for *RPB2*: the middle primer (M) is located approximately 1300 bp upstream of primer A.

Deletion of any of the THO subunits diminished RNAPII recruitment as assessed by Rpb3 occupancy at two loci each of three different RNAPII-transcribed genes by more than half in comparison to the wild-type situation (Figure 18). The characteristics of recruitment, *i.e.* an increase of occupancy from the middle to the 3' region of the *ADH1* and *RPB2* genes remained unaffected by the mutations. For the following ChIP experiments of TREX components in deletion mutants of THO their recruitment was therefore normalized to Rpb3 occupancy to account for the reduction in transcription which is caused by the absence of the single THO subunits.

3.3.2. Deletion of single THO subunits differentially affects TREX recruitment

In an attempt to find out if any one subunit of THO is especially important for TREX recruitment I performed ChIPs of THO / TREX subunits in wild-type yeast strains and strains lacking one of four THO subunits. Although THO is a very stable complex and deletion of Hpr1 and Mft1 has been reported to greatly reduce the stability of the whole complex, some residual complexes (approximately more than ten-fold less than in the wild-type) do form in the absence of single subunits (Huertas 2006 and data not shown). Deletion of different single THO subunits has previously been described to affect cells to a different extent (Chavez 2000, Garcia-Rubio 2008). Thus, ChIP experiments in single deletion mutants of THO might provide some hints which subunit(s) mediate(s) TREX recruitment.

Factor enrichments over a non-transcribed region obtained from the ChIP experiments were normalized to RNAPII occupancy (Rpb3-ChIPs) to account for the reduced transcriptional activity in the different THO deletion mutants (see Figure 18), and recruitment to three exemplary genes (*ADH1, PMA1, RPB2*) was analyzed (Figure 19).

Hpr1 recruitment is equally affected in all deletion strains: it remains more or less unchanged at *ADH1-M*, is reduced to about 75 % of the wild-type level at *ADH1-3'*, and to 25 - 50 % at *PMA1* and *RPB2* (Figure 19 A). Of note, the recruitment of Hpr1 to the anyway not strongly transcribed RPB2 gene is practically completely abolished in the deletion mutants since the absolute enrichments over the non-transcribed control region are barely above the background level of a control mock IP (not shown).

In contrast, the recruitment of Thp2 seems to be affected most by deletion of *THO2* and / or *MFT1* (Figure 19 B). The same effect is also seen on recruitment of Mft1, where *THO2* deletion has the biggest impact among THO subunit deletions (data not shown).

The recruitment pattern for the two TREX subunits Yra1 and Sub2 in the different yeast strains is highly similar, and again deletion of *THO2* leads to the biggest decrease in recruitment (Figure 19 C and D).

In summary, Tho2 and probably Mft1 seem to be the most important proteins for complex recruitment. Based on this experiment alone, however, it is difficult to reach a conclusion which THO subunit might mediate complex recruitment.
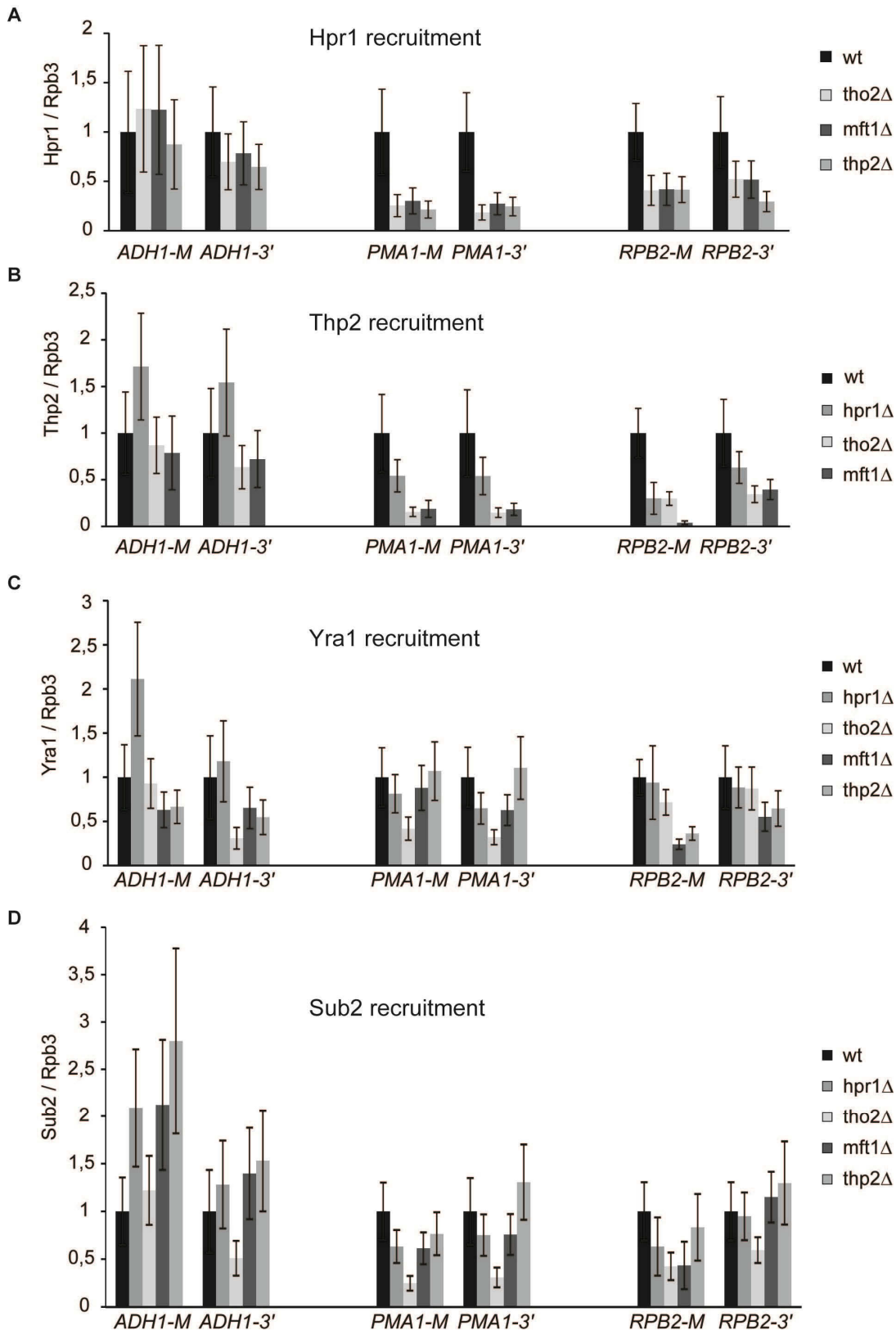
Figure 19: The deletion of single THO subunits differentially affects the recruitment of Thp2, Yra1, and Sub2. Recruitment of **(A)** Hpr1, **(B)** Thp2 (both ChIPped by C-terminal TAP tag), **(C)** Yra1, and **(D)** Sub2 (both ChIPped by antibody raised against the protein) to three different genes was analyzed by ChIP. Enrichments were first normalized to RNAPII occupancy (Rpb3-ChIP) and values for the deletion strains were then normalized to the wild-type value. Results represent the mean ± SD from three independent experiments. qPCR primers are the same as in Fig. 12, except for *RPB2*: the middle primer (M) is located approximately 1300 bp upstream of primer A; the 3' primer is identical with primer B.

4. Discussion

4.1. TREX is globally recruited to RNAPII-transcribed genes

We analyzed the recruitment of mRNA export factors on a genome-wide scale and found that TREX, Nab2, and Npl3 are recruited to all protein-coding genes. No differential recruitment to specific gene classes could be identified. This has in the meantime been confirmed by a recently published study which also reported global presence of Hpr1 and Sub2 on active ORFs (Gomez-Gonzalez 2011). In addition, there is also recruitment to sn/snoRNA genes, but at a lower level than at protein-coding genes. This recruitment is consistent with a recent finding in fission yeast, where the THO complex has also been found at snoRNA loci. It ensures TRAMP complex occupancy there and thus negatively regulates snoRNA expression (Larochelle 2012).

4.2. TREX is increasingly recruited towards the 3' end and binds directly to the S2/S5-diphosphorylated CTD of Rpb1

Our genome-wide analysis as well as a recently published one (Gomez-Gonzalez 2011) confirm that core TREX occupancy generally increases from the 5' to the 3' end (Figure 7), as it had been reported previously for single genes (Zenklusen 2002, Abruzzi 2004). The exact mechanism of TREX recruitment had remained elusive.

We now find a close resemblance of TREX occupancy meta profiles and the genome-wide distribution of S2 and Y1 phosphorylation of the Rpb1 CTD and show that TREX interacts directly with the S2/S5-diphosphorylated CTD in vitro (Figure 10 and Meinel 2013). Furthermore, S2 and / or Y1 phosphorylation of the CTD are necessary for TREX recruitment (Meinel 2013).

4.3. The 5' - 3' increase in TREX occupancy is length-dependent, not caused by the growing RNA, and physiologically important for the expression of long genes

Our results show that the occupancy of the core TREX complex (THO, Yra1, and Sub2) increases the longer a gene becomes (Figures 8 and 9). This increase could theoretically be caused by binding of TREX to the nascent RNA, which also becomes longer as transcription progresses. However, we could exclude this possibility by ChIP experiments on a ribozyme reporter construct, although we see a partial dependence on RNA for the occupancy of all TREX subunits (Meinel 2013).

Previous studies (Abruzzi 2004), using ChIPs with or without RNase digestion, reported that only Sub2 and Yra1 but not Hpr1 (THO) recruitment depends on RNA. This discrepancy to our results might be explained by the fact that nascent RNA is immediately released by ribozyme cleavage during transcription (before crosslinking and harvesting of the cells) whereas the RNase digestion was performed only after formaldehyde crosslinking, which might stabilize some originally RNA-dependent interactions.

We find that the increase in TREX occupancy from 5' to 3' depends on gene length (Figures 8 and 9). This is noteworthy, since other general transcription elongation factors such as Spt5 or Paf1 do not increase in occupancy with gene length (Meinel 2013 and Figure 9). We furthermore discovered that a C-terminal TAP tag on Tho2 specifically abrogates the length-dependent increase in TREX recruitment (Figure 11) without affecting complex formation (Meinel 2013). Interestingly, it was recently published that Tho2 interacts with nucleic acids (DNA or RNA) via its flexible and intrinsically disordered C-terminus (Pena 2012, Gewartowski 2012). One might speculate that the TAP tag interferes with nucleic acid binding of Tho2 and thus impairs its recruitment, which is consistent with the partially RNA-dependent occupancy of TREX, although we found the RNA not to be responsible for the length-dependent increase across the gene. Interestingly, the length-dependent increase of TREX is physiologically important for the expression of long genes (Meinel 2013).

All in all, our results strongly suggest that the interaction of TREX with a CTD that retains residual S5 phosphorylation throughout the ORF and becomes increasingly phosphorylated on S2 during elongation (see General Introduction, sections 1.1.4.1 and 1.1.4.3) mediates the increasing recruitment of TREX to transcribed genes. The proteins, whose occupancy does not increase with gene length (Gbp2, Hrb1, Nab2, Npl3), are probably transferred to the nascent RNA and thus move away from the transcription site. Sub2 and Yra1 are most likely also handed over to the mRNP, which is illustrated by the meta occupancy profiles, according to which Yra1 and Sub2 occupancy drops a bit earlier than that of THO (Figure 6). The events leading to TREX dissociation at the poly(A) site need to be further elucidated, but the drop in Y1 phosphorylation and the concomitant increase in termination factor recruitment (Mayer 2012) likely plays a role.

The aforementioned insights leading to a model of TREX recruitment and dissociation during the transcription cycle are summarized in Figure 20.
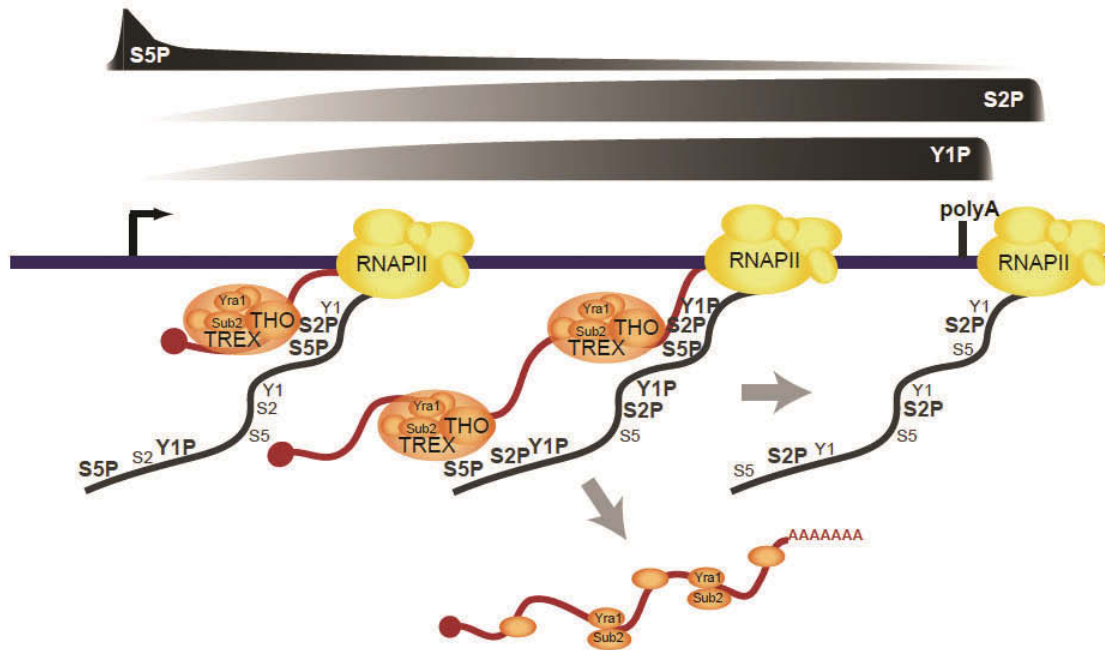
Figure 20: Model of TREX recruitment and dissociation (Meinel 2013). The TREX complex is recruited to transcribed genes, and its occupancy partially depends on RNA. Strikingly, TREX occupancy increases from 5' to 3'. This increase, however, is not caused by the growing chain of nascent RNA but most likely mediated by the concomitant increase in S2 phosphorylation of the CTD of Rpb1, since TREX is able to directly bind to the S2/S5-diphosphorylated CTD. It does not bind to Y1-phosphorylated CTD, but the drop in TREX occupancy at the polyadenylation site coincides with the drop in Y1P levels. Which mechanisms exactly mediate TREX dissociation remains to be elucidated. Yra1 and Sub2 are most likely transferred to the RNA and leave the site of transcription together with the mature mRNP.

Differential phosphorylation of the CTD during the transcription cycle thus not only serves to coordinate mRNA processing events with transcription but also ensures efficient coupling of transcription with mRNA export by recruiting the TREX complex.

4.4. A C-terminal TAP tag impairs Yra1 function and changes recruitment to actively transcribed genes

Expression of a TAP tag on the C-terminus of Yra1 results in anti-TAP ChIP profiles that are different from the profiles obtained in an untagged strain by an antibody raised against the Yra1 protein ("anti-Yra1") (Figure 15). Assuming that the anti-Yra1 ChIPs reflect the "natural" situation more accurately Tho2 seems to - either directly or indirectly - play a more important role in securing Yra1 occupancy than Hpr1 (Figures 15 and 16).

Interestingly, the presence of a C-terminal TAP tag on Yra1 to some degree even seems to rescue the defect in Yra1 recruitment in the *tho2Δ* background (Figure 15 A). Conversely, Yra1-TAP recruitment is reduced more in the *hpr1Δ* than in the *tho2Δ* background. This is

consistent with the observation that the genetic interaction of the *YRA1-TAP* allele with *HPR1* deletion is more severe than with *THO2* deletion (Figure 14).

Interestingly, a recent study briefly mentioned that C-terminal GFP tagging of Yra1 in their hands led to a temperature-sensitive growth phenotype in a wild-type W303 yeast strain (Johnson 2011). For the C-terminal TAP tag I do not observe any phenotype in wild-type W303 yeast (Figures 14 and 14), however, since the GFP tag is roughly one third bigger than the TAP tag it might lead to more pronounced effects.

All in all, the TAP tag at the C terminus probably interferes with interaction(s) necessary for normal recruitment of Yra1.

4.5. THO subunit deletion differentially affects TREX recruitment

Hpr1 has previously been shown to be important for Yra1 and Sub2 recruitment to *PMA1* (Zenklusen 2002, Huertas 2006), although the first study, analyzing Yra1 and Sub2 recruitment in wt and *hpr1Δ* strains, did not examine a possible reduction in transcription in the deletion mutant. Genetic interactions of Sub2 and Yra1 with all four THO subunits have been described (Strasser 2002), consistent with the existence of all these proteins as part of the TREX complex.

The present study extends the previous ChIP analyses on the PMA1 gene to include two more genes as well as more THO deletion strains. Tho2 and also Mft1 seem to be most important for TREX occupancy. However, based on these experiments alone it is impossible to reach any conclusion as to which THO subunit is responsible for complex recruitment to transcribed genes. Most likely, more than one subunit is part of the interaction interface. To identify these, more experiments such as CTD pull-down assays (as in Meinel 2013) with THO complexes lacking one or the other subunit or binding assays of individual purified subunits with CTD peptides are necessary.

THO-independent initial recruitment mechanisms for Yra1 have been described (Johnson 2009, MacKellar 2011), however, the present observations point to an important function of the THO complex in stabilizing Yra1 on the gene. This might occur directly or indirectly via Sub2 recruitment.

5. Specific Introduction to Part Two

5.1. The ubiquitin proteasome system (UPS)

5.1.1. Molecular mechanism and functions of ubiquitylation

Posttranslational modification of proteins with either a single ubiquitin (monoubiquitylation) or a chain of several ubiquitins (polyubiquitylation) plays an important role in a large number of diverse cellular processes, both proteolytic and non-proteolytic. It functions, for example, in targeted protein degradation (see below), receptor endocytosis (Haglund 2012), cell-cycle control (Mocciaro 2012), and DNA replication and repair (Ulrich 2011).

Ubiquitin is a 76 amino acids long and highly conserved protein, which is expressed in all eukaryotic cells. It has a rather compact structure of one alpha helix opposite of a five-stranded beta sheet, connected with some flexible loops (Vijay-Kumar 1987 and Figure 21). Most interactions with ubiquitin-binding proteins are mediated by a hydrophobic patch around Ile44 (Winget 2010).
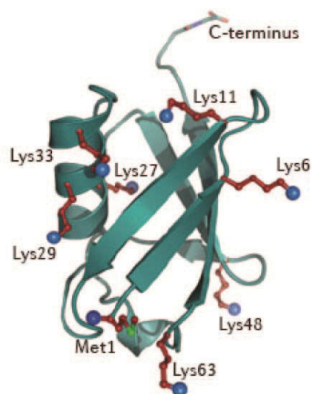
Figure 21: Structure of the ubiquitin molecule (Kulathu 2012).
Ribbon model of the structure of ubiquitin (Vijay-Kumar 1987; Protein Data Bank Identifier (PDB ID) 1UBQ). The lysine residues and the initiator methionine, which are all available for polyubiquitin chain formation, are indicated (see text further below).

The attachment of a ubiquitin molecule to its substrate is mediated by the action of three enzymes: In an ATP-consuming step the ubiquitin-activating enzyme E1 first forms a high-energy thioester bond with the carboxyl group of ubiquitin's C-terminal glycine residue. The activated ubiquitin is then transferred to a ubiquitin-conjugating enzyme (E2) by transesterification, and an E3 ubiquitin ligase catalyzes the final isopeptide bond formation between the carboxyl group of the C-terminal glycine of ubiquitin and, most commonly, the ε-amino group of a lysine residue in the substrate protein (Finley 2012 and Figure 22).

There are two types of E3 ligases: HECT (homologous to the E6AP carboxyl terminus) domain and RING (really interesting new gene) E3 ligases. Depending on the type of E3 involved, the ubiquitin is either transferred directly from the E2 to the substrate (RING type)

or another thioester intermediate of ubiquitin with the E3's active site cysteine is formed before its ligation to the substrate (HECT type) (Metzger 2012).
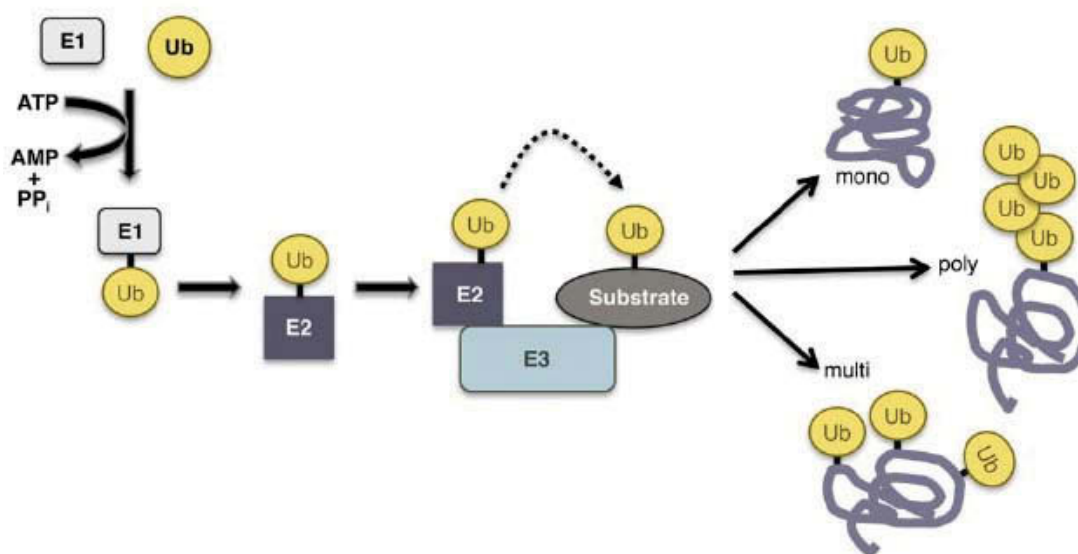
Figure 22: Enzymatic reactions leading to substrate ubiquitylation (from Finley et al. 2012). The substrate can be modified with a single ubiquitin at one (mono-) or more positions (multi-ubiquitylation), or several ubiquitin molecules can be attached to one another, forming a polyubiquitin chain. Ubiquitylation is a reversible modification which can be reversed by the action of deubiquitylating enzymes (DUBs). See text for details.

While most organisms possess only one E1 enzyme (Uba1 in yeast), there are 11 E2s and 60-100 E3s in yeast with different substrate specificities and preferences for specific types of chain linkage (see next paragraph) (Finley 2012). This diversity permits the large variety of ubiquitylation effects.

When several ubiquitin molecules are linked to one another, peptide bond formation can occur between the C-terminus of one ubiquitin and any of the seven lysines (K6, K11, K27, K29, K33, K48, K63) or the N-terminal methionine of the other ubiquitin, thus leading to different topologies of the resulting ubiquitin chains (Peng 2003, Walczak 2012, Xu 2009 and Figure 23). Polyubiquitin chains linked via Lys48, for example, are rather compact (Figure 23 A) while Lys63-linked chains adopt an extended conformation (Figure 23 B, C) (Tenno 2004, Eddins 2007, Datta 2009). Depending on the type of linkage, the overall structure and thus the accessibility of different surface regions of the ubiquitin molecule and the positioning of these regions to each other varies, which might be the basis for differential recognition and thus different effects in cellular metabolism.

E3 ligases either collaborate with a single E2 to catalyze both mono-ubiquitylation of the substrate as well as chain elongation (Petroski 2005) or utilize two different E2 sequentially (Rodrigo-Brenni 2007). In other cases, polyubiquitin chain formation is mediated by one

E2 / E3 pair that uses a monoubiquitin on the substrate previously attached by a different enzyme complex (Hoege 2002).
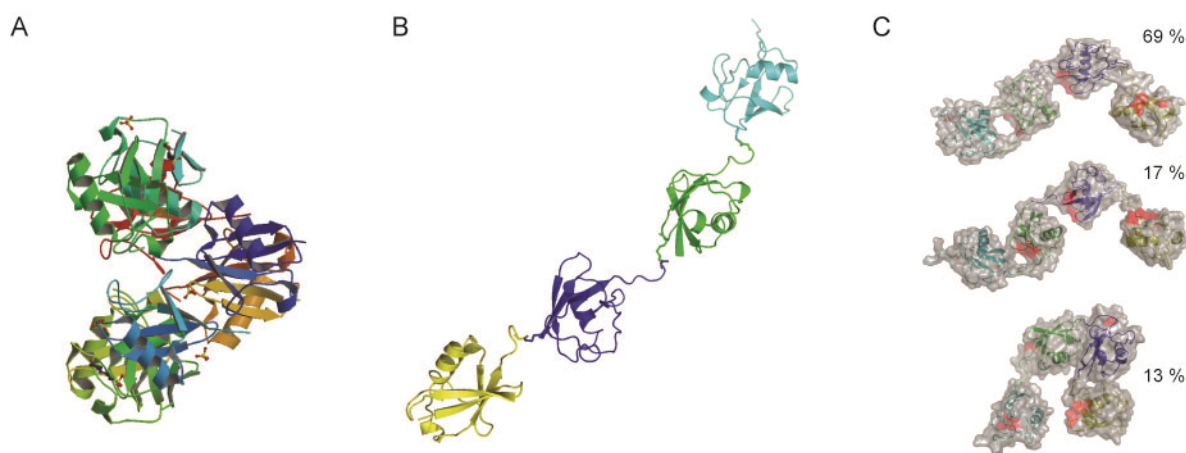
Figure 23: Polyubiquitin chains linked via different lysines of the ubiquitin molecule adopt different conformations. A: K48-linked tetraubiquitin forms a rather compact and globular structure (crystal structure published by Eddins 2007, PDB ID 2O6V). B: K63-linked tetraubiquitin shows a highly extended chain topology (crystal structure published by Datta 2009, PDB ID 3HM3) C: In solution, however, K63 chain conformation will probably be more flexible and compact than the one in the crystal, as explained by Minimal Ensemble Search (EMS) modeling. Numbers show the percentages the different conformations in the ensemble were assigned to best fit the data (Datta 2009).

The most abundant forms of polyubiquitin chains *in vivo* - as judged by a mass spectrometry-based quantification in log-phase yeast cells - are K48- and K11-linked chains with 29.1 % and 28 %, respectively, followed by K63-linked chains (16.3 %); the other linkage types are less abundant (Xu 2009).

The functions of the three most abundant forms are quite well characterized: K48-linked chains have been known for the longest time and lead to proteasomal degradation of their substrates, K11 chains are important for cell-cycle control and the ERAD (endoplasmic reticulum associated protein degradation) pathway, and K63 chains function, for example, in DNA repair and cytokine signaling. Less is known about the other types of chains, but the so-called "linear chains" (N-terminal methionine linked to C-terminal glycine) are connected to NF-KB signaling, K27 chains are implicated in mitochondrial biology, and K6 chains might play a role in the DNA damage response (Trempe 2011, Kulathu 2012).

5.1.2. Degradation by the proteasome and the proteolytic function of ubiquitin chains of different topology

The ubiquitin-proteasome system (UPS) is responsible for the removal of cellular proteins in a regulated and specific manner. The 26S proteasome is a 2.5 MDa, 32 subunit complex consisting of a barrel-shaped 20S core particle (CP), which houses the proteolytic activity, and one or two 19S regulatory particles (RP) flanking the core, which mediate substrate recognition and control entry into the proteolytic cavity of the CP (Tomko 2013 and Figure 24). Within the RP, six ATPases arranged in a circle are responsible for unfolding and translocation of the substrate into the core, while ubiquitin receptors mediate substrate recognition and binding (Finley 2009).
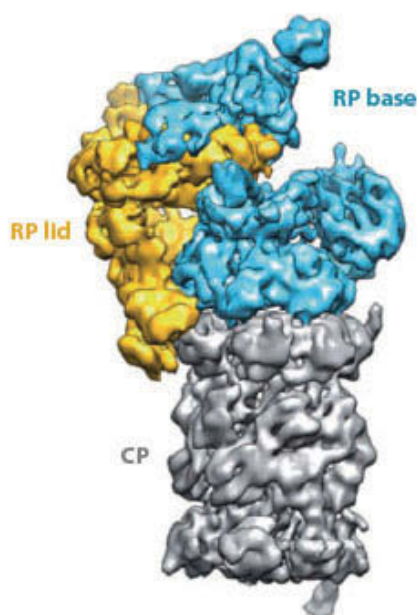
Figure 24: Architecture of the yeast 26S proteasome (from Tomko 2013; cryo EM density map adapted from Lander 2012).
The core particle (CP, in grey) has cylindrical shape with an inner cavity and is formed by a stack of four rings of seven subunits each (the outer rings are named α rings, the inner ones β rings). Proteolytic activity resides inside the barrel: 3 subunits of the β ring are threonine proteases. The α ring regulates access to the inner proteolytic chamber and serves as docking site for the regulatory particle.
The regulatory particle (RP) can be subdivided into the base (cyan) and lid (yellow). Two subunits of the base (Rpn10 and Rpn13) are ubiquitin receptors which bind and recognize ubiquitylated substrates. A hexameric ring of AAA+ ATPases converts energy from ATP hydrolysis into movement threading the substrate through the α ring towards the proteases (reviewed in Finley 2012, Tomko 2013).

While the structure of the CP has been known for some time (Groll 1997) only recent electron microscopy studies (Lander 2012, Lasker 2012, Sakata 2012, Beck 2012) provided insight into subunit composition of the RP and allowed speculation about a mechanistic model for substrate degradation (Figure 25, Matyskiela 2012).
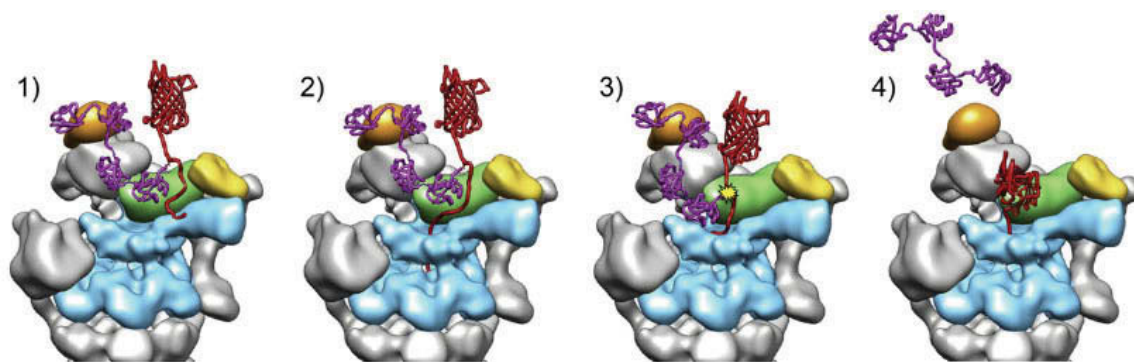
Figure 25: Mechanistic model for substrate degradation by the 26S proteasome (according to Matyskiela 2012). In the first step a substrate (*red*) bearing a chain of four or more ubiquitin molecules (purple) is tethered to the proteasome by binding of the ubiquitin chain to the proteasome's ubiquitin receptor Rpn13 (orange). Next (step 2), the ATPase ring ("unfoldase", *cyan*) engages the unstructured part of the substrate. Subsequently (step 3), the substrate is being moved by the action of the ATPases and this brings the isopeptide bond between ubiquitin and substrate lysine into the active center of the deubiquitylase Rpn11 (*green*), which can now cleave the bond. In the last step (4) the ubiquitin chain is released and the substrate is unfolded and translocated into the core particle.

Proteins that are to be degraded are marked by a polyubiquitin chain with a minimum length of four ubiquitin molecules (Thrower 2000) and are thus targeted to the proteasome. Shuttling ubiquitin receptors such as Dsk2 and Rad23, which can bind both ubiquitylated proteins and the proteasome (Elsasser 2005), might enhance substrate delivery, but their function is not essential (Finley 2012). In addition to the ubiquitin chain, unstructured regions in the substrate proteins enhance efficiency of proteasomal degradation (Prakash 2004).

The canonical chain topology leading to proteasomal degradation is the K48-G76 linkage (Chau 1989, Pickart 1997), however, there is evidence that other polyubiquitin chains (see below) or even multiple mono-ubiquitylation (Dimova 2012) might be sufficient to target proteins to the proteasome and trigger their degradation. Studies globally analyzing ubiquitylated proteins have found that chains of all linkage types except K63 accumulate upon proteasomal inhibition and thus seem to be processed by the proteasome *in vivo* (Meierhofer 2008, Bedford 2011). However, in specific cases K63-linked chains have also been described to be sufficient for proteasomal degradation (Saeki 2009).

5.1.3. Deubiquitylation and ubiquitin chain remodeling

Deubiquitylases (DUBs) are the antagonists of ubiquitin ligases and accordingly their actions have similarly diverse effects in cellular signaling and metabolism (Clague 2012). Twenty DUBs exist in yeast. They are not only needed to recycle ubiquitin chains from proteins before their degradation (both the lysosome and the proteasome have associated DUBs) and

participate in cellular signaling by controlling ubiquitylation status of substrates, but also to generate single ubiquitin molecules in the first place (Finley 2012). Ubiquitin is translated as a precursor protein, in which ubiquitin is fused to ribosomal proteins (L40 in the case of the two identical genes UBI1 and UBI2 and S31 in the case of UBI3) (Finley 1989). The fourth ubiquitin gene UBI4, which is induced under stress conditions, contains six tandem repeats of the ubiquitin coding sequence (Ozkaynak 1984). DUB activity - although it is not yet known of which enzyme(s) exactly - is thus also needed for ubiquitin synthesis.

Ubp6 is a deubiquitylase associated with the cap of yeast proteasomes and shortens ubiquitin chains on proteins bound to the proteasome from their distal ends. In addition, Ubp6 also delays proteasomal degradation non-catalytically (Hanna 2006). This has been proposed to function as a "timer", helping substrates, which take too long to be unfolded and would thus clog the proteasome, escape by trimming their ubiquitin chain below the required length (Kraut 2007).

Interestingly, the proteasome is also associated with the ubiquitin ligase Hul5, which extends ubiquitin chains on substrates, thus opposing Ubp6 and increasing the likelihood of degradation. This might provide another means of regulation by fine-tuning these two opposing activities according to the needs of the cell (Crosas 2006, Kraut 2007).

5.1.4. Diverse functions of the UPS in transcription

Interestingly, numerous functions of the ubiquitin proteasome system in the regulation of transcription have been uncovered over the past years, both proteolytic and non-proteolytic. The UPS for example controls the activity of transcriptional activators, regulates transcription through histone ubiquitylation, promotes transcription elongation, removes stalled polymerase complexes (see below), and represses cryptic transcription (Kwak 2011, Geng 2012).

Genome-wide ChIP studies find both 19S and 20S proteasome subunits to be recruited to actively transcribed genes, with only little difference between both complexes. Thus, the whole 26S proteasome most likely presents the functional unit recruited during transcription (Sikder 2006, Geng 2012). In that context, the so-called "Swiss army knife" model has been put forward, which postulates that active genes recruit the whole 26S proteasome, and the transcription machinery then uses its different proteolytic or non-proteolytic (*i.e.* ATPase chaperone) activities as needed in the respective situation (Geng 2012), just as one uses different functions of the Swiss army knife under different circumstances.

5.2. Transcription-coupled DNA repair and Rpb1 degradation in response to DNA damage

5.2.1. Transcription-coupled repair

DNA integrity is constantly threatened, for example by reactive oxygen species forming during normal metabolism, by exposure to chemicals or to UV light. Cells have accordingly developed elaborate repair machineries to deal with these assaults. DNA damage is obviously potentially dangerous as it can lead to the accumulation of mutations if it is not repaired. But lesions in actively transcribed genes can in addition cause immediate problems because they might block progression of RNAPII and thus the expression of the respective gene.

To cope with this, transcription-coupled nucleotide-excision repair (TC-NER) preferentially targets the transcribed strand of DNA and repairs lesions in active genes, mediated by Rad26 in *S. cerevisiae* (Hanawalt 2008, Gaillard 2013). As TC-NER depends on the presence of an RNAPII complex, the stalled enzyme is thought to function as a DNA damage sensor and facilitate loading of the NER machinery onto the DNA (Gaillard 2013). In contrast, global genome repair (GG-NER) depends on specialized protein complexes, which are dispensable for TC-NER. GG-NER does not depend on RNAPII and repairs damage non-preferentially in the whole genome (Gaillard 2013).

5.2.2. Rpb1 degradation upon DNA damage-dependent stalling

In cases when TC-NER is unsuccessful an alternative pathway is required, which leads to removal of the irreversibly stalled RNAPII complex through ubiquitylation and proteasomal degradation of its biggest subunit Rpb1. This pathway represents an independent and drastic "last resort" mechanism as an alternative to TC-NER (Lommel 2000, Wilson 2013).

First described as a response to DNA damage blocking RNAPII progression, Rpb1 ubiquitylation and degradation has subsequently been shown to occur in various other situations in which RNAPII is persistently stalled, such as NTP depletion upon 6-AU treatment or mutation of TFIIS (Somesh 2005) as well as inhibition of transcription elongation by α-amanitin treatment (Mitsui 1999, Anindya 2007).

Upon DNA damage-dependent stalling Rpb1 is polyubiquitylated in a sequential mechanism. The HECT domain ligase Rsp5, which binds to Rpb1 via its WW domain and was shown to mediate the DNA damage-induced degradation of Rpb1 (Huibregtse 1997, Beaudenon 1999), is needed for the initial ubiquitylation of Rpb1. The deubiquitylase Ubp2, which is associated with Rsp5 *in vivo*, can hydrolize K63-linked ubiquitin chains attached by Rsp5 (Kee 2005, Harreman 2009), resulting in monoubiquitylated Rpb1. This substrate is then efficiently polyubiquitylated by the E3 ubiquitin ligase complex Ela1-Elc1-Cul3, which attaches K48-

linked ubiquitin chains onto pre-monoubiquitylated Rpb1 (Harreman 2009). The proposal of this sequential mechanism consolidates the previously published requirements for Rsp5 (Huibregtse 1997, Beaudenon 1999) on the one hand and for Elc1 on the other hand (Ribar 2006, Ribar 2007).

Ubiquitylation of Rpb1 depends on its CTD, and only the elongating form with high levels in S2 phosphorylation and lower S5P levels is ubiquitylated (Mitsui 1999, Somesh 2005). In contrast, the initiating form of RNAPII (marked by high levels of S5 phosphorylation) is spared from degradation, and only RNAPII incorporated into a ternary complex is an especially good substrate for ubiquitylation, suggesting that structural features only present in the elongating ternary complex, probably combined with conformational changes upon stalling, mediate recognition by the ubiquitylation machinery (Somesh 2005, Wilson 2013).

Def1, which forms a complex with Rad26 and is needed for the degradation of Rpb1 upon DNA damage *in vitro* and *in vivo* (Reid 2004, Woudstra 2002), also preferentially promotes Rpb1 ubiquitylation *in vitro* when RNAPII is assembled in a ternary complex (Somesh 2005). Interestingly, the action of Def1 itself in promoting Rpb1 degradation depends on ubiquitin- and proteasome-mediated processing. It was shown recently that limited proteolysis of Def1 upon DNA damage and transcription stress generates a processed N-terminal fragment of Def1 (pr-Def1), which accumulates in the nucleus, binds to RNAPII and recruits the elongin-cullin E3 ligase complex by binding to the UbH domain in Ela1 (Wilson 2013).

Ubiquitylation of Rpb1 upon UV occurs on chromatin, and the AAA ATPase Cdc48 was shown to facilitate degradation of Rpb1 at sites of stalled transcription, probably by extracting the ubiquitylated Rpb1 from the RNAPII holoenzyme (Verma 2011).

Lastly, the deubiquitylase Ubp3 has been described to rescue Rpb1 should degradation no longer be necessary. Ubp3 can be copurified with RNAPII and is able to directly deubiquitylate mono- as well as poly-ubiquitylated Rpb1 *in vitro*. In doing so it might provide elongation or repair factors with the time needed to restart RNAPII and thus help prevent any unnecessary degradation of Rpb1 (Kvint 2008).

5.3. Previous findings

This part of my thesis continues the work of Eleni Karakasili, another Ph.D. student from the group of Dr. Katja Sträßer. Therefore, I will shortly highlight selected previous findings from Eleni Karakasili's Ph.D. thesis (LMU Munich, 2010).

Since RNAPII does not transcribe genes in one smooth run but pauses or arrests rather frequently, a system of protein factors has evolved which helps the polymerase transcribe along the gene (see General Introduction). When the stalling cannot be resolved, the prolonged arrest of an RNAPII complex poses a potentially lethal threat for the cell. Ubiquitylation and proteasomal degradation of Rpb1, the largest subunit of RNAPII, are then employed as a "last resort" mechanism to resolve this problem when DNA damage causes RNAPII stalling (Woudstra 2002, Anindya 2007; see also section 1.2.2.). However, it has been suggested that the same mechanism occurs generally in all other conditions causing RNAPII arrest (Somesh 2005, Daulny 2009, Wilson 2013).

Ms. Karakasili studied the molecular mechanism of Rpb1 degradation in four different *S. cerevisiae* strains with impaired transcription elongation (*ctk1Δ, dst1Δ, tho2Δ, bur2Δ*), hypothesizing that RNAPII stalling will be enhanced in these mutants independently of DNA damage.

5.3.1. Rpb1 protein levels and RNAPII occupancy on transcribed genes are reduced when transcription elongation is impaired

Upon transcriptional impairment by deletion of the four transcription elongation factors mentioned above the steady state Rpb1 protein levels were reduced to about $50 - 70\,\%$ of the wild-type level while Rpb3 levels were not affected (Karakasili 2010, PhD thesis, Figure 12) and *RPB1* mRNA levels were not reduced (Karakasili 2010, PhD thesis, Figure 13). This was accompanied by a reduction in RNAPII occupancy to about $50\,\%$, as assessed by Rpb3-ChIP experiments and qPCR at three different genes (Karakasili 2010, PhD thesis, Figure 11).

5.3.2. Rpb1 is polyubiquitylated and proteasome association with RNAPII as well as recruitment to sites of transcription is increased when transcription elongation is impaired

Purification of RNAPII combined with anti-ubiquitin Western blots showed increased ubiquitin signals at the height of Rpb1 in the transcription elongation mutants, pointing to an increased ubiquitylation of Rpb1 upon transcriptional impairment (Karakasili 2010, PhD thesis, Figure 20). Concomitantly, Western Blot analysis of the 20S proteasome in RNAPII

purifications revealed a stronger association of the proteasome with RNAPII (Karakasili 2010, PhD thesis, Figure 23). ChIP experiments of four different proteasomal subunits showed elevated recruitment to transcribed genes in the transcription elongation mutants (Karakasili 2010, PhD thesis, Figure 24).

5.3.3. The ubiquitin ligase Rsp5 but not Elc1 mediates the increased Rpb1 ubiquitylation in transcription elongation mutants and the increase of K63-linked chains is more pronounced than of K48-linked chains

Two E3 ligases, Rsp5 and Elc1, are needed for DNA damage-dependent degradation of Rpb1 (see specific introduction, 1.2.2.). Here, Ms. Karakasili used deletions of either *RSP5* or *ELC1* in combination with the deletion of *DST1* to impair transcription and subsequently analyzed Rpb1 polyubiquitylation to find out whether one or both E3 ligases are needed in the transcription elongation mutant (Karakasili 2010, PhD thesis, Figure 36). Neither of the two deletions by itself affected Rpb1 ubiquitylation. While *ELC1* deletion did not abolish the increase in the *dst1*Δ strain the ubiquitylation level of Rpb1 in the *dst1*Δ*rsp5*Δ double mutant dropped to a level comparable to that of the wild-type strain, indicating that upon transcription elongation impairment by *DST1* deletion the E3 ligase Rsp5 and not Elc1 is responsible for the increased Rpb1 ubiquitylation.

RNAPII purification and subsequent Western Blot analysis using ubiquitin linkage-specific antibodies showed an increase in both K48-linked and K63-linked polyubiquitin chains on Rpb1 upon transcriptional impairment in comparison to the wild-type, with the increase in K63-linked chains being more pronounced than the increase in K48-linked chains (Karakasili 2010, PhD thesis, Figure 30).

5.3.4. Other pathway components are the same as in DNA damage-induced stalling and ubiquitylation of RNAPII

Purification of RNAPII and quantification of Rpb1 polyubiquitin levels by Western blot were used to address whether the two E2 enzymes responsible for the damage-mediated degradation, Ubc4 and Ubc5 (Somesh 2005), were also involved in the damage-independent ubiquitylation of Rpb1. Deletion of either *UBC4* or *UBC5* in a *dst1*Δ strain background resulted in a reduction of the elevated Rpb1 polyubiquitin levels, indicating that both E2 enzymes (which have high sequence identity) are implicated in the Rpb1 ubiquitylation upon transcriptional impairment (Karakasili 2010, PhD thesis, Fig. 34).

The ubiquitylation promoting protein Def1, which is needed for DNA damage-induced degradation of Rpb1 but not for transcription-coupled repair (Woudstra 2002), is also needed for Rpb1 ubiquitylation when transcription elongation is impaired since the *def1*Δd*st1*Δ double

mutant exhibited reduced Rpb1 ubiquitylation levels compared to the *dst1*Δ strain (Karakasili 2010, PhD thesis, Figure 38A).

5.3.5. Deubiquitylases Ubp6 and Ubp2, but not Ubp3 are implicated in remodeling the ubiquitin chains on Rpb1 formed in transcription elongation mutants

RNAPII purifications from single and double deletion strains and subsequent quantification of Rpb1 polyubiquitylation levels determined that Ubp2 but not Ubp3 (as in the DNA damage induced pathway) deubiquitylates Rpb1 in the transcription elongation mutant *dst1*Δ. Furthermore, deletion of *UBP6* was also found to decrease Rpb1 ubiquitylation levels in *dst1*Δ, *i. e.* to compromise deubiquitylation (Karakasili, Figure 40).

5.4. Aim of the present study

As detailed above, Ms. Karakasili elucidated the molecular mechanism for degradation of transcriptionally stalled RNAPII. In comparison with the well-known DNA damage-dependent degradation she found evidence for a largely overlapping set of enzymes mediating Rpb1 ubiquitylation upon transcriptional impairment, yet with some distinct differences to the pathway taking effect upon DNA damage.

The present work aimed to corroborate the existence of these distinct sub-pathways of Rpb1 ubiquitylation according to different causes of RNAPII stalling and to further analyze Rpb1 polyubiquitylation upon transcription impairment.

6. Results

6.1. Both E3 ligases Rsp5 and Elc1 are recruited to a transcribed gene

Two ubiquitin ligases, Rsp5 and Elc1, are known to act sequentially in the DNA damage-induced ubiquitylation and degradation of Rpb1. Rsp5 ubiquitylates Rpb1 with K63-linked ubiquitin chains, which are subsequently remodeled by Ubp2, resulting in monoubiquitylated Rpb1. Elc1 then attaches K48-linked ubiquitin chains onto this substrate. (Harreman 2009). Since our lab had previously found evidence that Elc1 is dispensable for the polyubiquitylation of Rpb1 in transcription elongation mutants (*i. e.* independent of DNA damage) (Karakasili 2010, PhD thesis, Figure 36B), I wanted to know whether the two ubiquitin ligases are recruited differentially in wild-type cells and cells with transcription elongation problems (*dst1Δ*).
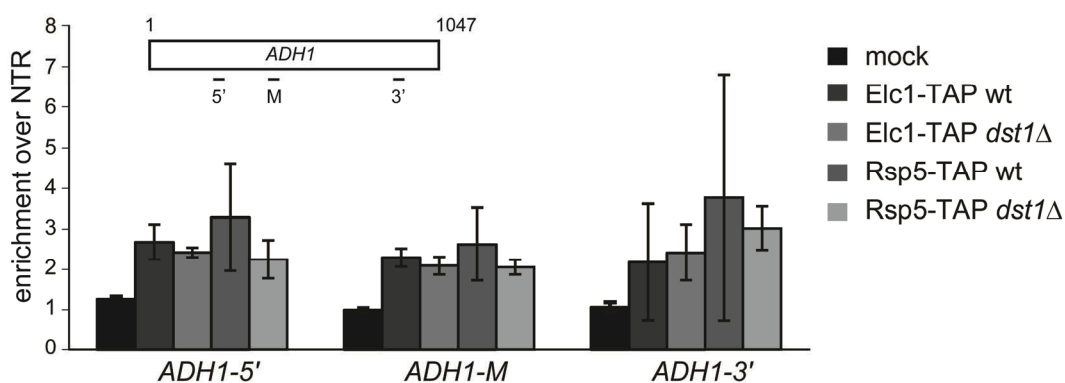
Figure 26: Elc1 and Rsp5 are recruited to *ADH1* in both wt and *dst1Δ* cells. Chromatin immunoprecipitations of TAP-tagged Elc1 and Rsp5 were performed in wt and *dst1Δ* backgrounds and in an untagged strain as negative control (mock IP). Both ubiquitin ligases are recruited to three loci within the *ADH1* gene. Enrichments on *ADH1* over a nontranscribed region (NTR) on Chr. V were calculated and mean values from 3 independent experiments ± SD were plotted.

Chromatin immunoprecipitation experiments, however, show that both E3 ubiquitin ligases Rsp5 and Elc1 are recruited at a low but detectable level across the ORF of the *ADH1* gene (Figure 26). There are neither significant differences between the two enzymes nor between the different genetic backgrounds (wt or *dst1Δ*). This indicates that both E3 ligases are present near the transcription elongation complex. Thus, the differential involvement of Elc1 and Rsp5 in Rpb1 ubiquitylation upon transcriptional impairment is probably not regulated at the level of recruitment to the transcription site.

6.2. The observed polyubiquitin signal is specific for ubiquitylation of Rpb1

When RNAPII is purified from wild-type cells and the transcription elongation mutants *ctk1Δ*, *dst1Δ*, *tho2Δ*, and *bur2Δ*, there is an increased anti-ubiquitin signal in the mutants compared to the wild-type in Western Blots at approximately 200 kDa and above (the height at which Rpb1 and polyubiquitylated Rpb1 run in an SDS-polyacrylamide gel) (Karakasili 2010, PhD thesis, Figure 20). Theoretically, high-molecular weight conjugates contaminating the purification and running at the same height as Rpb1 might contribute to the observed signal. To exclude this possibility, I purified equal amounts of RNAPII with the usual salt concentration of 100 mM NaCl and with highly stringent washing (1 M NaCl), and monitored the copurification of Tfg2, a subunit of the GTF TFIIF, which is tightly associated with RNAPII during transcription initiation and elongation (Figure 27).
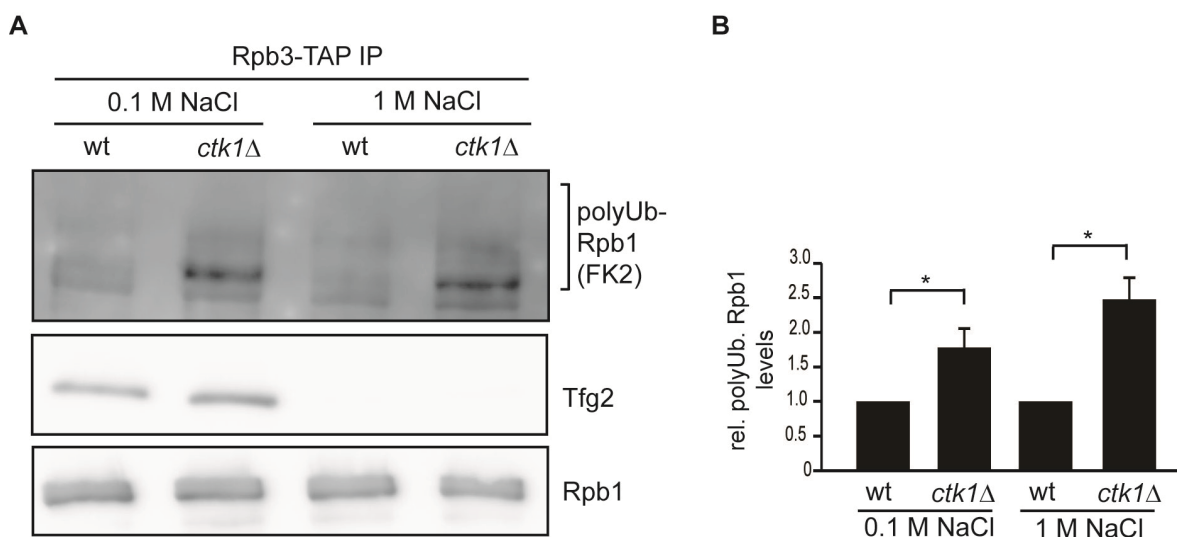
Figure 27: Analysis of Rpb1 polyubiquitylation in RNPII purifications from wt and *ctk1Δ* yeast strains. **A:** Equal amounts of RNAPII were purified with low salt or high salt washing and Rpb1, polyubiquitylated Rpb1 as well as association of Tfg2 were detected by Western Blotting (one representative experiment) **B:** Quantification of polyubiquitylation from three biologically independent experiments (mean ± SD; * p < 0.05, t test).

The loss of association of Tfg2p under high salt washing indicates the high purity of the isolated RNAPII complexes. Even with high salt washing, however, the polyubiquitylation signal is still increased in the transcription elongation mutant *ctk1Δ* compared to the wild-type (Figure 27), suggesting that the observed ubiquitin signal is indeed caused by polyubiquitin chains attached directly to Rpb1.

6.3. The half-life of Rpb1 is reduced when transcription elongation is impaired

Our lab has previously shown that Rpb1 protein levels from whole cell extracts are specifically reduced in four transcription elongation mutants while *RPB1* mRNA levels remain unaffected (Karakasili 2010, PhD thesis, Figures 12 and 13). In order to test whether this observed reduction in steady-state protein levels is indeed caused by increased turnover of the protein I performed cycloheximide chase assays. In this assay, *de novo* protein synthesis is abolished by addition of the drug cycloheximide (CHX), which blocks the translocation step in translation elongation (Schneider-Poetsch 2010). Aliquots of cells are taken immediately before addition as well as at different time points after addition of CHX, protein extracts are prepared, and levels of the protein of interest at each time point are quantified. Protein half-life can then be calculated from plotting the logarithmised ratios of protein at each time point relative to the amount of protein present before CHX addition.
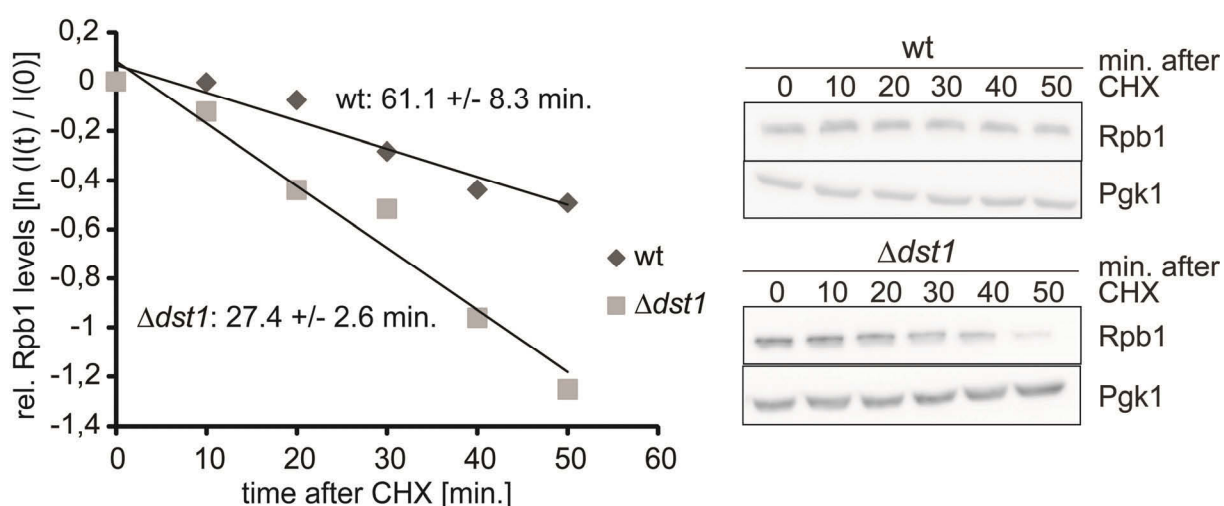
Figure 28: The half-life of Rpb1p is reduced when transcription elongation is impaired. Rpb1 protein levels were quantified in a cycloheximide chase assay. Logarithmised protein ratios were plotted and the protein half-life was calculated from linear regression. Quantification is based on 8 independent experiments.

The quantification of Rpb1 levels in the cycloheximide time course experiment yields Rpb1 half-lives of 61.1 ± 8.3 min. in the wild-type yeast strain and 27.4 ± 2.6 min. in the *dst1Δ* strain (Figure 28). This shows that the half-life of Rpb1p is indeed diminished to less than fifty percent of the wild-type value upon transcription elongation impairment, indicating that increased turnover of Rpb1p by proteasomal degradation is the cause for the observed decrease in steady-state protein levels in transcription elongation mutants.

6.4. Treatment with the transcription inhibitor 6-azauracil increases proteasome recruitment to a transcribed gene

Previously, our lab performed ChIP experiments in wild-type cells and transcription elongation mutants and found a decreased RNAPII occupancy on several transcribed loci with a concomitant increase in proteasome recruitment upon transcription elongation impairment by mutation of the aforementioned transcription factors (Karakasili 2010, PhD thesis, Figures 11 and 24).

I subsequently wanted to find out whether the impairment of transcription elongation by a different method, namely the treatment of wild-type cells with the drug 6-azauracil, has a similar effect in our assay system. 6-AU inhibits the GTP biosynthesis enzyme IMP dehydrogenase, thus depleting cellular GTP pools (Exinger 1992). 6-AU sensitivity in mutant yeast strains is widely used as an indicator that the mutated protein has a function in transcription elongation. Here, I performed ChIP experiments of RNAPII subunit Rpb3 and proteasome subunit Pre1 (both C-terminally TAP-tagged) upon treatment of wild-type cells with the transcription inhibitor 6-AU (250 μg / ml for 2.5 h prior to crosslinking) in comparison to solvent-treated cells.
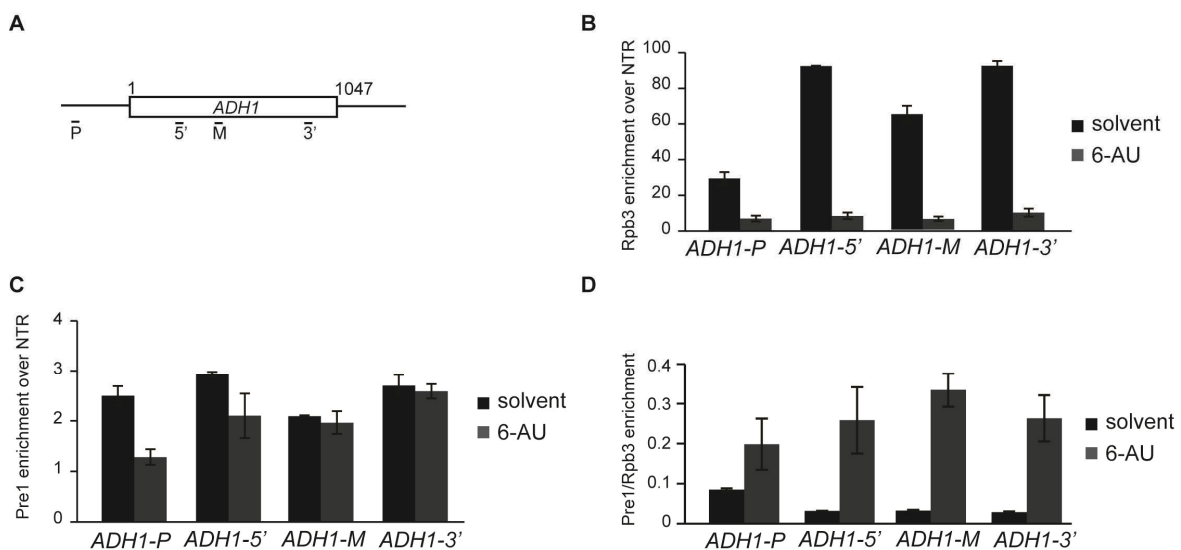
Figure 29: Impairment of transcription in wild-type yeast cells by 6-azauracil (6-AU) treatment leads to increased recruitment of the proteasome to a transcribed gene. Recruitment to the *ADH1* ORF (primer locations in **(A)**) was analyzed by chromatin immunoprecipitation and subsequent qPCR for RNAPII subunit Rpb3-TAP **(B)** and proteasomal subunit Pre1-TAP **(C)** and enrichments calculated over a non-transcribed region on Chr. V. **(D)** Quantification of proteasome recruitment normalized to transcription (*i. e.* RNAPII occupancy). Graphs show the results from at least three independent experiments (mean ± SD).

6-AU treatment indeed caused a drop in RNAPII occupancy and, normalized to the reduced transcriptional activity, an increased recruitment of the 26S proteasome to the transcribed

gene (Figure 29). This shows that transcription impairment by a different "route", namely nucleotide depletion, has a similar effect on RNAPII occupancy and proteasome recruitment as the deletion of transcription elongation factors.

6.5. Deletion of *ELC1* abrogates the UV-induced increase in Rpb1 ubiquitylation and has little effect on the increase caused by transcriptional impairment

UV-induced DNA damage leads to RNAPII stalling and subsequent polyubiquitylation and degradation of Rpb1, which is mediated through the attachment of K48-linked polyubiquitin chains by the ubiquitin ligase Elc1 (Beaudenon 1999, Huibregtse 1997, Chen 2007, Harreman 2009). Since we found no requirement for Elc1 upon transcription impairment by deletion of transcription elongation factors I wanted to gain some further insight as to whether two separate sub-pathways of recognition of stalled RNAPII and subsequent Rpb1 ubiquitylation exist. I compared the extent of Rpb1 polyubiquitylation caused by deletion of a transcription elongation factor on the one hand and UV irradiation (*i. e.* DNA damage) on the other hand and combined this with analyzing the additional effect of *ELC1* deletion.

To this end, I irradiated wt, *dst1Δ*, *elc1Δ* and *elc1Δdst1Δ* strains with UV or not, purified equal amounts of RNAPII in the presence of inhibitors for proteases, DUBs, and the proteasome, and quantified to what extent Rpb1 was polyubiquitylated under the different conditions (Figure 30).
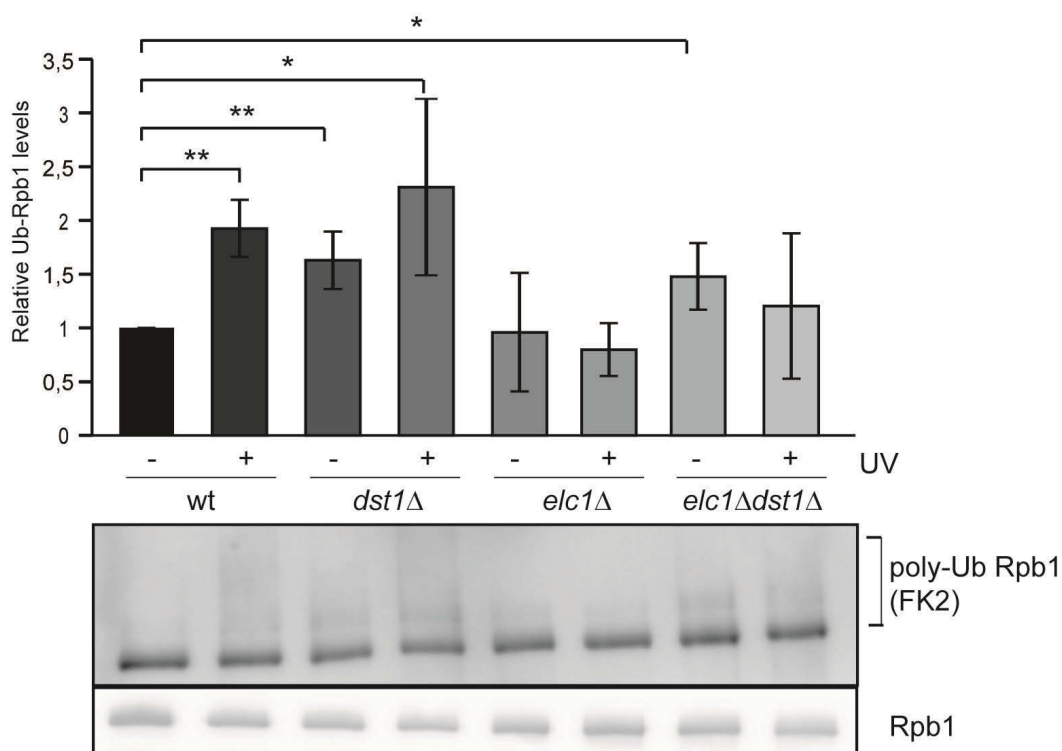
[previous page]
Figure 30: UV irradiation and deletion of DST1 increase Rpb1 polyubiquitylation. RNAPII was purified in equal amounts via TAP-tagged Rpb3 from non-treated or UV-irradiated (400 J / m^2 with 30 min. of recovery) wt, *dst1Δ*, *elc1Δ* and *elc1Δdst1Δ* strains. Levels of Rpb1 polyubiquitylation were quantified by Western Blot (n = 3; mean ± SD; * p < 0.05, ** p < 0.01, t test).

As expected, treatment of wild-type yeast cells with UV resulted in an approximately two-fold increase in Rpb1 ubiquitylation compared to the untreated cells. Rpb1 ubiquitylation was also clearly elevated by the sole deletion of *DST1*, consistent with previous results (Karakasili 2010, PhD thesis) and further increased by UV irradiation of the Dst1-deficient cells, although that difference is not statistically significant (Figure 30, first four lanes). Yeast cells lacking Elc1, on the other hand, exhibited a level of Rpb1 ubiquitylation comparable to the wt control cells, which – as expected from the published role of Elc1 in Rpb1 ubiquitylation upon UV – was not increased further by irradiation. Rpb1 ubiquitylation in cells lacking both Elc1 and Dst1 was increased compared to the wt control cells to a level almost comparable to the one in *dst1Δ* cells and was not further influenced by UV irradiation. This might point towards the existence of two independent branches of the ubiquitylation pathway; one caused by UV induced DNA damage and one by transcriptional impairment by the lack of Dst1.

6.6. K63R mutation of ubiquitin in combination with *DST1* deletion leads to a temperature-sensitive growth phenotype and to synthetic lethality upon 6-AU treatment

Previous observations from our lab point to a role of K63-linked ubiquitin chains in the degradation of DNA-damage independently stalled Rpb1, either direct or indirect: (1) Not only K48-linked but also K63-linked ubiquitylation of Rpb1 increases in the transcription elongation mutants (Karakasili 2010, PhD thesis, Figures 30) and (2) expression of K63R instead of wild-type ubiquitin seems to somewhat abolish the decrease in steady-state Rpb1 protein levels in a *dst1Δ* background (Karakasili 2010, PhD thesis, Figures 31).

To gain further information on the importance of K63-linked ubiquitylation I used strains expressing either normal ubiquitin or K63R ubiquitin (Spence 1995) and analyzed the growth phenotype of wt and *dst1⊿* cells in these backgrounds.

YPD
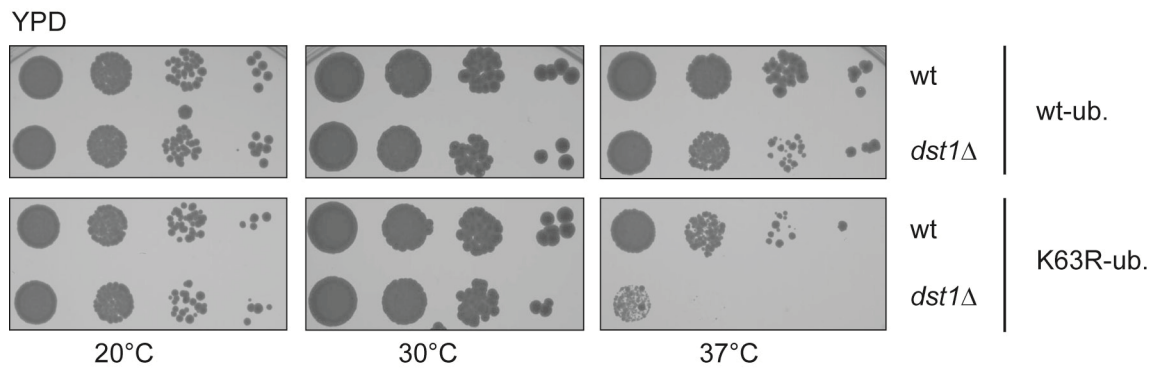
Figure 31: Expression of K63R-ubiquitin combined with the deletion of *DST1* leads to a temperature-sensitive growth phenotype at 37°C. Spot dilution assay of wt and *dst1Δ* cells, expressing either wild-type or K63R ubiquitin on full medium (YPD) at the indicated temperatures.

Deletion of *DST1* is known to have no influence on growth in otherwise wild-type yeast strains at normal temperature. This is also seen in the present analysis on full medium, when wild-type ubiquitin is expressed. Growth at 37°C is slightly impaired (Figure 31, upper panel). Expression of K63R instead of wt ubiquitin, which precludes the formation of K63-linked polyubiquitin chains, also slightly impairs growth at 37°C. However, when the K63R mutation is combined with the impairment of transcription elongation by deletion of *DST1* there is a pronounced growth defect when cells are grown at the elevated temperature (Figure 31, lower panel).

Sensitivity to the drug 6-azauracil (6-AU), which depletes UTP and GTP pools in the cell, in mutant yeast strains is generally taken as an indicator for a function of the mutated protein in transcription elongation (Hampsey 1997). Next, I analyzed the effect of 6-AU treatment on the growth of the aforementioned strains. As expected, *DST1* deletion induces 6-AU sensitivity (Figure 32). Interestingly, the expression of K63R instead of wild-type ubiquitin slightly increases the 6-AU sensitivity of *dst1Δ* cells at 20°C (Figure 32, upper panel) and even leads to near-complete inhibition of cell growth at 30°C (Figure 32, lower panel).
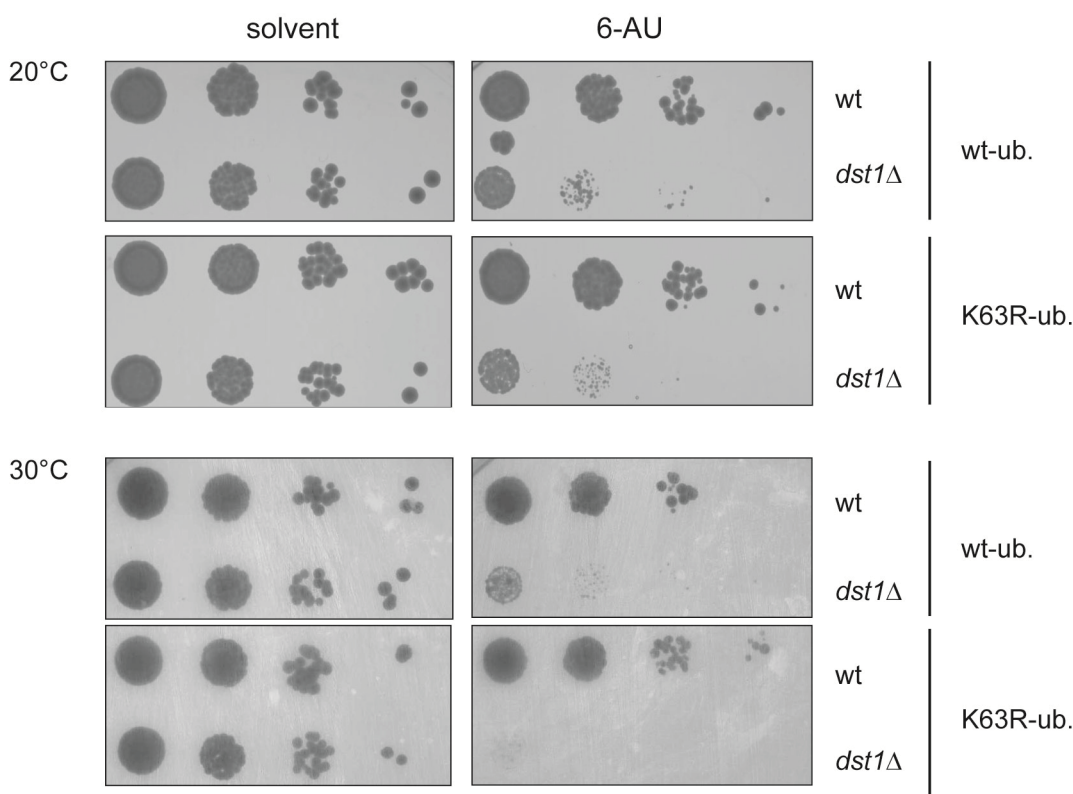
Figure 32: Expression of K63R-ubiquitin is synthetically lethal with deletion of DST1 in the presence of 6-azauracil. Spot dilution assay of wt and *dst1Δ* cells, expressing either wild-type or K63R ubiquitin at the indicated temperatures. Strains were transformed with pRS316 to allow growth on SDC-ura medium supplemented with either 75 µg/ml 6-azauracil or the corresponding amount of solvent (DMSO). All strains were unable to grow at 37°C (both solvent and 6-AU plates).

All in all, this genetic interaction argues for a relevant connection between the functions of Dst1 and K63-linked polyubiquitylation.

6.7. K63R mutation of ubiquitin slightly reduces the polyubiquitylation of Rpb1 upon transcriptional impairment

Since we had previously seen a more pronounced increase in K63-linked than in K48-linked polyubiquitylation upon transcription impairment, I next analyzed the effect of the K63R ubiquitin mutation on the extent of Rpb1 polyubiquitylation in *ctk1Δ* cells (which have the strongest phenotype among the four transcription elongation mutants used in Ms. Karakasili's study). To this end, I purified equal amounts of RNAPII from the different yeast strains in the presence of protease, DUB, and proteasome inhibitors and quantified the extent of total Rpb1 polyubiquitylation (Figure 33).

A   **B**
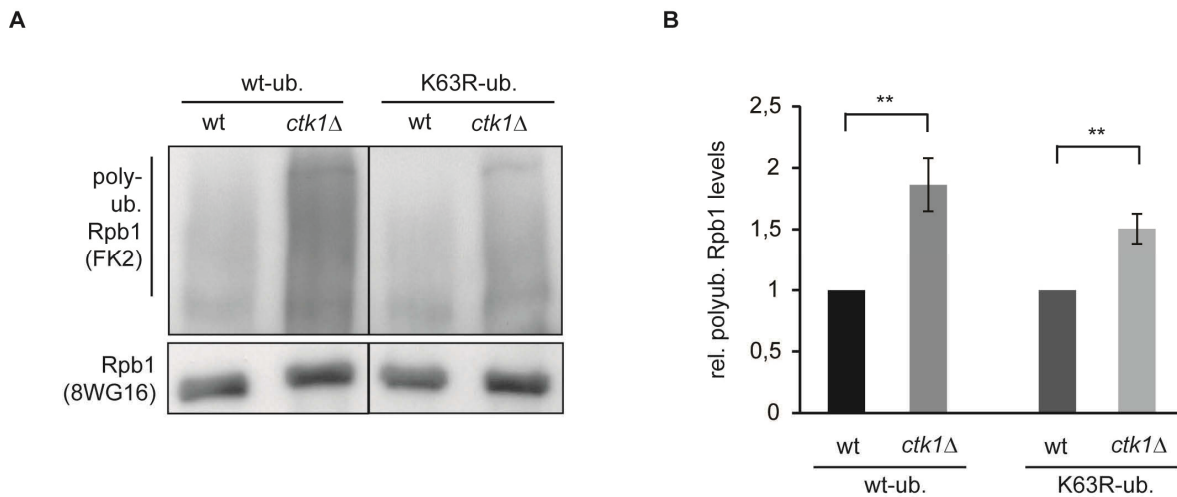
Figure 33: The increase in Rpb1 polyubiquitylation in transcription elongation mutants is slightly less pronounced when only K63R ubiquitin is available. RNAPII was purified in equal amounts using the anti-Rpb1 antibody 8WG16 from wt and *ctk1Δ*, in both wild-type and K63R ubiquitin backgrounds. **(A)** Exemplary Western Blots showing the amount of Rpb1 purified (lower panel) and the extent of Rpb1 polyubiquitylation (upper panel) in the different strains. **(B)** Quantification of Rpb1 polyubiquitylation normalized to the amount of Rpb1 present in each purification (n = 3; mean ± SD; ** $p < 0.01$; t test).

Consistent with previous results, transcription elongation impairment by deletion of *CTK1* led to a significant increase in Rpb1 polyubiquitylation levels (Figure 33, compare first two lanes / columns). When the formation of K63-linked polyubiquitin chains was precluded by expressing K63R-ubiquitin, this increase was slightly less pronounced than in a wt-ubiquitin background (Figure 33, compare the last two with the first two lanes / columns). This, together with the previous results, illustrates that a certain amount of K63-linked ubiquitin chains are formed upon transcription impairment. However, it does not support a major function of K63-linked polyubiquitin chains upon transcription impairment by deletion of *CTK1*.

6.8. K63R mutation of ubiquitin does not abolish the reduction in steady state Rpb1 protein levels upon deletion of *CTK1*

The canonical ubiquitin signal leading to proteasomal degradation consists of polyubiquitin chains linked via K48 (see introduction Part II, section 1.1.2.). However, we found evidence that Elc1, which synthesizes K48-linked ubiquitin chains, is dispensable for Rpb1 polyubiquitylation in transcription elongation mutants, while Rsp5, which preferentially synthesizes K63-linked chains, is required (Karakasili 2010, PhD thesis, Fig. 36).

To analyze the importance of K63-linked ubiquitin chains for the degradation of Rpb1 I quantified steady state Rpb1 protein levels in wild-type yeast and the transcription elongation

mutant *ctk1Δ* and compared cells expressing wild-type ubiquitin with cells expressing K63R-mutated ubiquitin (Figure 34).
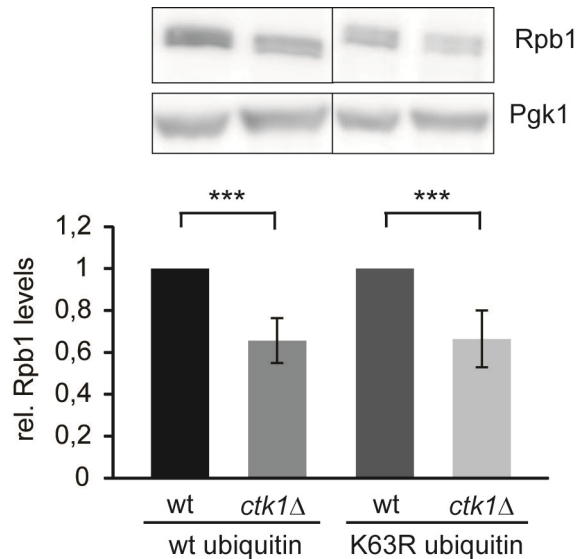
Figure 34: The reduction in steady-state Rpb1 protein levels in transcription elongation mutants is not abolished when only K63R ubiquitin is available. Rpb1 levels were assessed by quantitative Western Blot in wild-type and *ctkΔ*, both in strains expressing wild-type ubiquitin (left) and K63R-ubiquitin (right).
The graphs show quantifications of twelve independent experiments each (mean ± SD; *** $p < 0.001$; t test).

In *ctk1Δ* cells the Rpb1 levels are reduced, as expected, to about 60 % of the wild-type level, when normal ubiquitin is present. When there is only K63R ubiquitin available and thus no K63-linked ubiquitin chains can be formed, the observed reduction in Rpb1 levels in the *ctk1Δ* strain is not different from the wt ubiquitin background (Figure 34).

Preventing the formation of K63-linked polyubiquitin chains therefore does not result in less pronounced degradation of Rpb1. This indicates that K63-linked polyubiquitylation does not play a role in the degradation of Rpb1 upon impairment of transcription elongation by deletion of *CTK1*.

7. Discussion

7.1. Rpb1 ubiquitylation and degradation is a universal and conserved rescue mechanism in cases of persistent stalling of RNAPII

Transcription normally is a discontinuous process, with RNAPII pausing frequently (Darzacq 2007). If RNAPII stalls persistently, however, this can be very problematic, since the stalled polymerase blocks subsequent transcription complexes, so that the affected gene will no longer be transcribed.

Targeted Rpb1 degradation has been known for some time and was first described when RNAPII was stalled at helix-distorting DNA lesions caused by UV irradiation or cisplatin treatment (Bregman 1996, Ratner 1998, Beaudenon 1999, Jung 2006).

In the present project we utilized different mutant *S. cerevisiae* strains (*dst1⊿, ctk1⊿, bur2⊿, tho2⊿*), which were selected because they exhibit impaired transcription elongation and therefore likely a concomitant increase in RNAPII stalling, to analyze the cellular mechanisms dealing with DNA damage-independently stalled RNAPII complexes.

The final outcome - clearing of the stalled complex by degradation of Rpb1 - turned out to be the same as in DNA damage-dependent stalling. My colleague, Eleni Karakasili, already found that Rpb1 is polyubiquitylated and degraded by the proteasome under these conditions of DNA damage-independent stalling and that most of the involved enzymes (Uba1, Ubc4, Ubc5, Rsp5, Def1, and Ubp2) are the same as described for DNA damage-dependent stalling (Karakasili 2010 PhD thesis).

I determined that the observed polyubiquitylation upon transcriptional impairment by deletion of *CTK1* is specific for Rpb1 (Figure 27). Moreover, cycloheximide chase assays reveal an increased turnover, *i.e.* a decreased half-life of the Rpb1 protein upon transcription impairment (Figure 28), which is reflected in the observed reduction of Rpb1 protein levels.

As in the transcription elongation mutants, we find a similar decrease in Rpb1 levels, increase in Rpb1 polyubiquitylation, and increase in recruitment of the proteasome to the transcription site upon treatment with the transcription elongation inhibitor 6-AU (Karakasili 2010 PhD thesis Figures 16 and 21, and this thesis, Figure 29). The drug depletes UTP and GTP pools in the cell (Hampsey 1997), which impairs transcription elongation and might mimic naturally occurring situations of starvation. Our results are in agreement with previously published data showing increased polyubiquitylation of Rpb1 upon 6-AU treatment (Somesh 2005). Rpb1 ubiquitylation and degradation is therefore similarly affected by nucleotide depletion and deletion of transcription elongation factors.

Thus, work from the past decade together with the present study suggests that the clearing of irreversibly stalled RNAPII complexes through removal of Rpb1 via ubiquitylation and proteasomal degradation is a universal "last resort" rescue mechanism in a variety of situations from yeast to mammalian cells (Wilson 2013 and references therein, Karakasili 2010 PhD thesis, and this thesis).

Importantly, however, we found that the E3 ubiquitin ligase Elc1 (responsible for UV-induced Rpb1 degradation) is dispensable for Rpb1 polyubiquitylation in DNA damage-independent stalling and, unexpectedly, that there is a pronounced increase in K63-linked ubiquitylation on Rpb1 (Karakasili 2010 PhD thesis). This is an important distinction from the degradation pathway acting upon DNA damage and provides first evidence that cells might discriminate between RNAPII complexes stalled either dependently or independently of DNA damage.

7.2. Elc1 is not responsible for Rpb1 polyubiquitylation upon damage-independent impairment of transcription but is also present at the site of transcription

Previous results of our lab showed that *ELC1* deletion in a *dst1Δ* background did not abolish the increase in ubiquitylation caused by deletion of *DST1* (in fact, it rather increased it), while deletion of *RSP5* in that background resulted in reduced wild-type ubiquitylation levels (Karakasili 2010 PhD thesis, Figure 36). This indicates that Rps5 but not Elc1 is the E3 ligase responsible for ubiquitylation of Rpb1 upon DNA damage-independent stalling. Chromatin immunoprecipitations, however, did not reveal any differential recruitment of the two ubiquitin ligases (Figure 24), suggesting that their differing involvement is not regulated at the level of their recruitment to the transcription complex. On the other hand, it is not surprising that not only Rsp5 but also Elc1 is detected by ChIP in wild-type and *dst1Δ* cells since Elc1 is the yeast homolog of mammalian Elongin C, which is a part of RNAPII transcription factor Elongin that suppresses transient RNAPII pausing (Bradsher 1993, Aso 1997), and plays a role in global genome repair (LeJeune 2009). Which factor determines the activity of Elc1 remains to be determined.

7.3. K63-linked ubiquitylation increases in DNA damage-independently stalled Rpb1 but only slightly influences total Rpb1 polyubiquitylation levels

Eleni Karakasili previously found that the increase in K63-linked polyubiquitylation is much more pronounced than the increase in K48-linked polyubiquitylation in the four transcription elongation mutants compared to the wild-type (Karakasili 2010 PhD thesis, Figure 30). This is surprising, on the one hand, since K48-linked polyubiquitin is the canonical signal for proteasomal degradation while K63-linked ubiquitin chains are thought to have purely non-degradative functions (see Part II, section 1.1.2.) On the other hand, the 26S proteasome is

able to bind and degrade K63-linked polyubiquitin chains (and even heterogeneous ubiquitin chains of mixed linkages) both *in vitro* and *in vivo* (Kirkpatrick 2006, Kim 2007, Saeki 2009). Interestingly, there is a genetic interaction at 37°C between the K63R mutation in ubiquitin, which precludes formation of K63-linked chains, and transcription impairment by deletion of *DST1* (Figure 31). Furthermore, expression of K63R-ubiquitin and concomitant deletion of *DST1* becomes lethal in the presence of the transcription elongation drug 6-azauracil (Figure 32). This argues for an involvement of K63-linked chains in the cellular mechanism dealing with damage-independently stalled RNAPII.

I found that expression of K63R-mutant ubiquitin only slightly reduces the increase in total Rpb1 polyubiquitylation upon deletion of the transcription elongation factor Ctk1 (Figure 33), and the expression of K63R ubiquitin does not abolish the decrease in Rpb1 levels (Figure 34) The modification of Rpb1 by K63-linked ubiquitin chains might function in the degradation of Rpb1 but the effect of expressing K63R- instead of wt-ubiquitin on the steady state Rpb1 protein levels was not substantial.

The data, however, indicate that K63-linked chains are to some extent part of the total Rpb1 polyubiquitylation which is formed upon DNA damage-independent transcription impairment by deletion of transcription elongation factors. A direct role for K63-linked polyubiquitylation of Rpb1 for its degradation is unlikely but its presence might play an indirect role in promoting Rpb1 degradation upon transcription impairment. We cannot exclude, however, that initially built K63-linked chains are later remodeled into K48-linked chains or that further K48-linked chains are added by another E3 ligase, which has yet to be identified.

It is important to note that we also do observe a smaller increase in K48-linked polyubiquitylation of Rpb1 upon deletion of the transcription elongation factors, which might be sufficient for the enhanced degradation of Rpb1, even in the absence of DNA damage.

Interestingly, mammalian cells also utilize targeted Rpb1 ubiquitylation and degradation when RNAPII is arrested by treatment with α-amanitin (Nguyen 1996, Anindya 2007). Rpb1 in α-amanitin-arrested complexes was found *in vitro* to be polyubiquitylated with K63-linked chains, although the α-amanitin-dependent species of ubiquitylated Rpb1 was observed to be stable (Lee 2004). In that instance it was speculated that these K63-linked chains might fulfill a nondegradative function in signaling for other factors, *e. g.* DNA repair proteins (Lee 2004).

Our study presents a first hint that K63-linked polyubiquitylation of Rpb1 occurs upon transcription impairment. The exact function of these K63-linked chains remains to be elucidated.

All in all, we describe a mechanism of Rpb1 degradation that takes effect upon damage-independent stalling of RNAPII and is overlapping, yet distinct from the pathway acting upon damage-dependent stalling (see Figure 35 for a summary). This provides first evidence that the cell might be able to discriminate between different causes of RNAPII stalling.
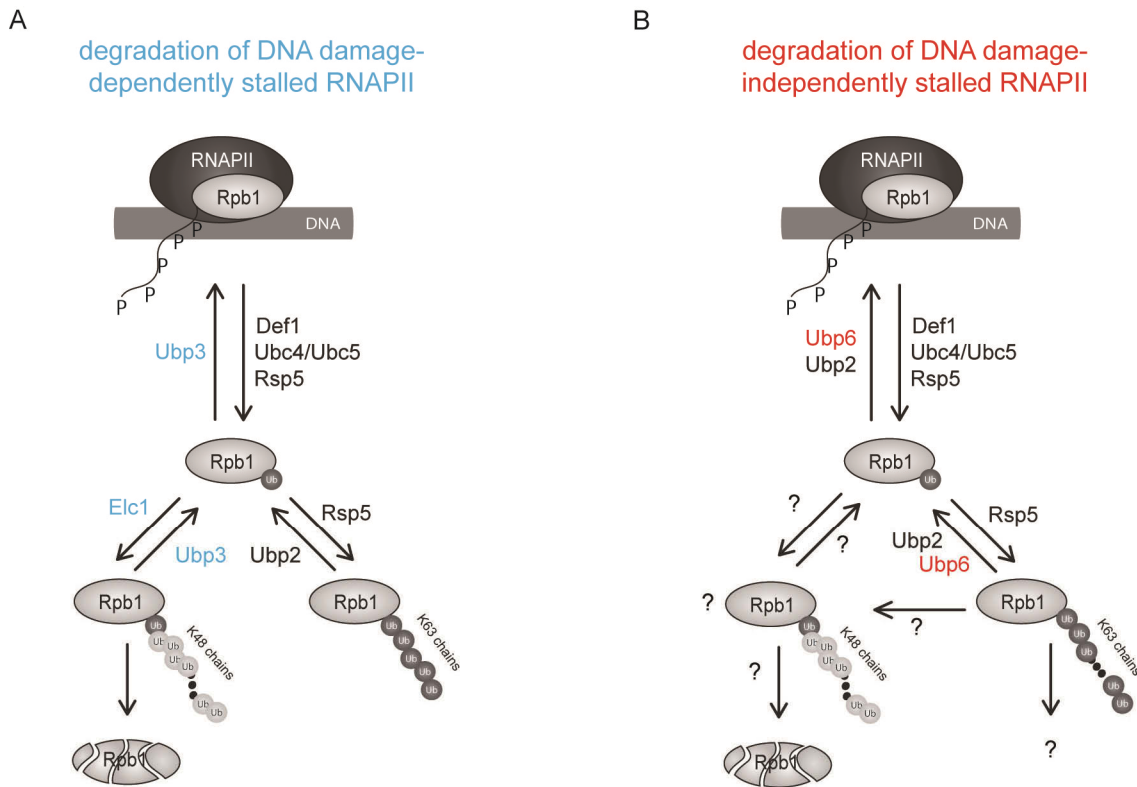
Figure 35: Illustrations comparing the degradation of Rpb1 caused by DNA damage (A) and by DNA damage-independent transcription impairment (B) (modified from Karakasili 2010, PhD thesis, Figure 45). See text for details.

8. Materials and Methods

8.1. Materials

8.1.1. Strains

Table 1: *Escherichia coli*

strain	genotype	company
DH5α	*fhuA2 lac(del)U169 phoA glnV44 Φ80′ lacZ(del)M15 gyrA96 recA1 relA1 endA1 thi-1 hsdR17*	Invitrogen (Karlsruhe)

Table 2: Parental wild-type *S. cerevisiae* strains

Strain	Genotype	Source
RS453 (MATa)	*ura3-1 trp1-1 his3-11,15 leu2-3,112 ade2-1 can1-100 GAL+*	R. Serrano
RS453 (MATα)	*ura3-1 trp1-1 his3-11,15 leu2-3,112 ade2-1 can1-100 GAL+*	R. Serrano
W303 (MATa)	*leu2-3,112 trp1-1 can1-100 ura3-1 ade2-1 his3-11,15 [phi+]*	Wallis 1989
W303 (MATα)	*leu2-3,112 trp1-1 can1-100 ura3-1 ade2-1 his3-11,15 [phi+]*	Wallis 1989
BY4741 (MATa)	*his3⊿1 leu2⊿0 met15⊿0 ura3⊿0*	Open Biosystems

Table 3: *S. cerevisiae* strains used in this study

Strain	Description	Reference
RPB3-TAP	*RPB3-TAP::HIS3*; MATa; *his3⊿1; leu2⊿0; met15⊿0; ura3⊿0*	Meinel 2013
HPR1-TAP	*HPR1-TAP::URA3*; MATa; *his3⊿1; leu2⊿0; met15⊿0; ura3⊿0*	Meinel 2013
TAP-THO2	*TAP-THO2*, MATa; *his3⊿1; leu2⊿0; met15⊿0; ura3⊿0*	Meinel 2013
THO2-TAP	*THO2-TAP::URA3*, MATa; *ade2-1; his3-11,15; ura3-52; leu2-3,112; trp1-1; can1-100; GAL+*	Meinel 2013
MFT1-TAP	*MFT1-TAP::URA3*; MATa; *his3⊿1; leu2⊿0; met15⊿0; ura3⊿0*	Meinel 2013
GBP2-TAP	*GBP2-TAP::URA3*; MATa; *his3⊿1; leu2⊿0; met15⊿0; ura3⊿0*	Meinel 2013
HRB1-TAP	*HRB1-TAP::URA3*; MATa; *his3⊿1; leu2⊿0; met15⊿0; ura3⊿0*	Meinel 2013
TAP-NPL3	*TAP::NPL3;* MATa; *his3⊿1; leu2⊿0; met15⊿0; ura3⊿0*	Meinel 2013
NAB2-TAP	*NAB2-TAP::URA3;* MATa; *his3⊿1; leu2⊿0; met15⊿0; ura3⊿0*	Meinel 2013

hpr1Δ	*hpr1::HIS3; MATa; ura3-1, ade2-1, his3-11,5, trp1-1, leu2-3,112, can1-100*	Andres Aguilera lab
tho2Δ	*tho2::KANMX6; MATa; ura3-1, ade2-1, his3-11,5, trp1-1, leu2-3,112, can1-100*	Andres Aguilera lab
mft1Δ	*mft1::KAN MX6; MATa; ade2-1, his3-100, leu2-112, ura3-1, trp1-1, can1-100*	Andres Aguilera lab
thp2Δ	*thp2::KANMX6; MATa; his3⊿1 leu2⊿0 met15⊿0 ura3⊿0*	Andres Aguilera lab
RPB3-TAP	*RPB3-TAP::TRP1; MATa; ura3-1 trp1-1 his3-11,15 leu2-3,112 ade2-1 can1-100*	Katja Sträßer lab
RPB3-TAP HPR1 shuffle	*hpr1::HIS3; RPB3-TAP::TRP1; pRS316-HPR1[URA3]; ura3, ade2-1, his3-11,15, trp1-1, leu2-3,112, can1-100*	Katja Sträßer lab
RPB3-TAP THO2 shuffle	*tho2::KANMX6; RPB3-TAP::TRP1; pRS316-THO2[URA3]; MATα; ade2-1, trp1-1,can1-100, leu2,3-112, his3-11,15, ura3*	Katja Sträßer lab
RPB3-TAP MFT1 shuffle	*mft1::KANMX6; RPB3-TAP::TRP1; pRS316-MFT1[URA3]; ura3, ade2-1, his3-11,15, trp1-1, leu2-3,112, can1-100*	Katja Sträßer lab
RPB3-TAP THP2 shuffle	*thp2::KANMX6; RPB3-TAP::TRP1; pRS316-THP2[URA3]; MATa; ura3, ade2-1, his3-11,15, trp1-1, leu2-3,112, can1-100*	Katja Sträßer lab
HPR1-TAP	*HPR1-TAP::TRP1; MATα; ura3-1 trp1-1 his3-11,15 leu2-3,112 ade2-1 can1-100*	Katja Sträßer lab
HPR1-TAP THO2 shuffle	*HPR1-TAP::TRP1; tho2::KANMX6; pRS316-THO2; MATα; ura3-1 trp1-1 his3-11,15 leu2-3,112 ade2-1 can1-100*	Katja Sträßer lab
HPR1-TAP MFT1 shuffle	*HPR1-TAP::TRP1; mft1::KANMX6; pRS316-MFT1; MATa; leu2-3,112 trp1-1 can1-100 ura3-1 ade2-1 his3-11,15*	Katja Sträßer lab
HPR1-TAP THP2 shuffle	*HPR1-TAP::TRP1; thp2::KANMX6; pRS316-THP2; MATa; ura3-1 trp1-1 his3-11,15 leu2-3,112 ade2-1*	Katja Sträßer lab
MFT1-TAP	*MFT1-TAP::TRP1; MATα; ura3-1 trp1-1 his3-11,15 leu2-3,112 ade2-1 can1-100*	Katja Sträßer lab
MFT1-TAP HPR1 shuffle	*MFT1-TAP::TRP1; hpr1::HIS3; pRS316-HPR1; MATα; leu2-3,112 trp1-1 can1-100 ura3-1 ade2-1 his3-11,15*	Katja Sträßer lab
MFT1-TAP THO2 shuffle	*MFT1-TAP::TRP1; tho2::KANMX6; pRS316-THO2; MATα; leu2-3,112 trp1-1 can1-100 ura3-1 ade2-1 his3-11,15*	Katja Sträßer lab
MFT1-TAP THP2 shuffle	*MFT1-TAP::TRP1; thp2::KANMX6; pRS316-THP2; MATa; leu2-3,112 trp1-1 can1-100 ura3-1 ade2-1 his3-11,15*	Katja Sträßer lab
RPB3-TAP	*RPB3::TAP::TRP1; leu2-3,112 trp1-1 can1-100 ura3-1 ade2-1 his3-11,15 [phi+]*	Karakasili PhD thesis 2010
RPB3-TAP CTK1 shuffle	*CTK1::HIS3, RPB3::TAP::TRP1; pRS316-CTK1[URA3]; MATa; leu2-3,112 trp1-1 can1-100 ura3-1 ade2-1 his3-11,15 [phi+]*	Karakasili PhD thesis 2010
RPB3-TAP DST1 shuffle	*DST1::HIS3, RPB3::TAP::TRP1; RS316-DST1[URA3]; MATa; leu2-3,112 trp1-1 can1-100 ura3-1 ade2-1 his3-11,15 [phi+]*	Karakasili PhD thesis 2010

PRE1-TAP	*PRE1::TAP::TRP1;* MATa; *leu2-3,112 trp1-1 can1-100 ura3-1 ade2-1 his3-11,15 [phi+]*	Karakasili PhD thesis 2010
PRE1-TAP DST1 shuffle	*DST1::HIS3, PRE1::TAP::TRP1;* RS316-*DST1[URA3]* ; MATa; *leu2-3,112 trp1-1 can1-100 ura3-1 ade2-1 his3-11,15 [phi+]*	Karakasili PhD thesis 2010
RSP5-TAP	*RSP5-TAP::TRP1;* MATa; *leu2-3,112 trp1-1 can1-100 ura3-1 ade2-1 his3-11,15 [phi+]*	Karakasili PhD thesis 2010
RSP5-TAP DST1 shuffle	*RSP5-TAP::TRP1;* pRS316-*DST1[URA3]*; MATa; *leu2-3,112 trp1-1 can1-100 ura3-1 ade2-1 his3-11,15 [phi+]*	Karakasili PhD thesis 2010
ELC1-TAP	*ELC1-TAP::TRP1;* MATa; *leu2-3,112 trp1-1 can1-100 ura3-1 ade2-1 his3-11,15 [phi+]*	Karakasili PhD thesis 2010
ELC1-TAP DST1 shuffle	*ELC1-TAP::TRP1;* pRS316-*DST1[URA3]*; MATa; *leu2-3,112 trp1-1 can1-100 ura3-1 ade2-1 his3-11,15 [phi+]*	Karakasili PhD thesis 2010
dst1Δ	*DST1::HIS3;* MATa; *leu2-3,112 trp1-1 can1-100 ura3-1 ade2-1 his3-11,15 [phi+]*	Karakasili PhD thesis 2010
elc1Δ	*ELC1::KANMX6;* MATa; *leu2-3,112 trp1-1 can1-100 ura3-1 ade2-1 his3-11,15 [phi+]*	Karakasili PhD thesis 2010
RPB3-TAP elc1Δ	*RPB3-TAP::TRP1; ELC1::KANMX6;* MATa; *leu2-3,112 trp1-1 can1-100 ura3-1 ade2-1 his3-11,15 [phi+]*	Karakasili PhD thesis 2010
dst1Δ elc1Δ	*DST1::HIS3; ELC1::KANMX6;* MATa; *leu2-3,112 trp1-1 can1-100 ura3-1 ade2-1 his3-11,15 [phi+]*	Karakasili PhD thesis 2010
RPB3-TAP dst1Δ elc1Δ	*RPB3-TAP::TRP1; DST1::HIS3;* ELC1::KANMX6; MATa; *leu2-3,112 trp1-1 can1-100 ura3-1 ade2-1 his3-11,15 [phi+]*	Karakasili PhD thesis 2010
SUB280	MATa; *lys2-801 leu2-3,112 ura3-52 his3-D200 trp1-1[am] ubi1-D1::TRP1 ubi2-D2::ura3 ubi3-Dub-2 ubi4-D2::LEU2;* [pUB39-WTUB] [pUB100]	Spence 1995
SUB413	MATa; *lys2-801 leu2-3,112 ura3-52 his3-D200 trp1-1[am] ubi1-D1::TRP1 ubi2-D2::ura3 ubi3-Dub-2 ubi4-D2::LEU2;* [pUB39-K63RUB] [pUB100]	Spence 1995
SUB280 *DST1* shuffle	*DST1::KANMX6;* pRS316-*DST1[URA3]*; MATa; *lys2-801 leu2-3,112 ura3-52 his3-D200 trp1-1[am] ubi1-D1::TRP1 ubi2-D2::ura3 ubi3-Dub-2 ubi4-D2::LEU2;* [pUB39-WTUB] [pUB100]	this study
SUB413 *DST1* shuffle	*DST1::KANMX6;* pRS316-*DST1[URA3]*; MATa; *lys2-801 leu2-3,112 ura3-52 his3-D200 trp1-1[am] ubi1-D1::TRP1 ubi2-D2::ura3 ubi3-Dub-2 ubi4-D2::LEU2;* [pUB39-K63RUB] [pUB100]	this study
SUB280 *CTK1* shuffle	*CTK1::KANMX6;* pRS316-*CTK1[URA3]*; MATa; *lys2-801 leu2-3,112 ura3-52 his3-D200 trp1-1[am] ubi1-D1::TRP1 ubi2-D2::ura3 ubi3-Dub-2 ubi4-D2::LEU2;* [pUB39-WTUB] [pUB100]	this study
SUB413 *CTK1* shuffle	*CTK1::KANMX6;* pRS316-*CTK1[URA3]*; MATa; *lys2-801 leu2-3,112 ura3-52 his3-D200 trp1-1[am] ubi1-D1::TRP1 ubi2-D2::ura3 ubi3-Dub-2 ubi4-D2::LEU2;* [pUB39-K63RUB] [pUB100]	this study

8.1.2. Plasmids

Table 4: Plasmids used in this study

plasmid name	description	reference
pRS316	encoding URA3 marker; enabling growth on SDC-ura medium - for 6-AU experiments	Sikorski 1989
pRS316-DST1	for expression of *DST1* in shuffle strains; the *DST1* ORF plus 500 bp of promoter and terminator region were cloned into pRS316	K. Sträßer (unpubl. work)
pRS316-CTK1	for expression of *CTK1* in shuffle strains; the *CTK1* ORF plus 500 bp of promoter and terminator region were cloned into pRS316	Röther 2007
pBS1479	for C-terminal TAP tagging with *TRP1* marker	Puig 2001
pBS1539	for C-terminal TAP tagging with *URA3* marker	Puig 2001
pBS1761	for N-terminal TAP tagging with *TRP1* marker	Puig 2001
pBS1766	encoding Cre recombinase for excision of the selection marker in N-terminal TAP tagging	Puig 2001
pKS1386	pBSIIKS+-5'-Δctk1-KANMX6-3' for disruption of *CTK1* with KANMX6	Karakasili PhD thesis 2010
pKS1388	pBSIIKS+-5'-Δdst1-KANMX6-3' for disruption of *DST1* with KANMX6	Karakasili PhD thesis 2010

8.1.3. Oligonucleotides

All oligonucleotides were purchased from Thermo Fisher Scientific (Ulm).

Table 5: qPCR primers used in this study

primer name	sequence
YER fw	TGCGTACAAAAAGTGTCAAGAGATT
YER rev	ATGCGCAAGAAGGTGCCTAT
ADH1-5' fw	GTTGTCGGCATGGGTGAAA
ADH1-5' rev	GGCGTAGTCACCGATCTTCC
ADH1-M fw	AGCCGCTCACATTCCTCAAG
ADH1-M rev	ACGGTGATACCAGCACACAAGA
ADH1-3' fw	TTGGACTTCTTCGCCAGAGG
ADH1-3' rev	GCCGACAACCTTGATTGGAG
PMA1-M fw	AAATCTTGGGTGTTATGCCATGT
PMA1-M rev	CCAAGTGTCTAGCTTCGCTAACAG
PMA1-3' fw	CGTCTTCGCTGTCGACATCA
PMA1-3' rev	TTTTCAGACCACCAACCGAAT
RPB2-5' fw	CGAGGATGAAAGTGCACCAA
RPB2-5' rev	GCCCCTTCTCGCGAAAA
RPB2-M fw	CCCAACTTTTCAAGACATTGTTCA
RPB2-M rev	TGGTTTTTGCGTTAATCGCTAA
RPB2-M to 3' fw	ACGTACAAACACCTTAAGAATGAACA
RPB2-M to 3' rev	CAGGCGCAATTAGACCATCA
RPB2-3' fw	TTGAAGGAGAGATTAATGGAAGCA
RPB2-3' rev	AGCCCGCAAATACCACAAAT

Table 6: TAP tagging oligos used in this study

oligo name	sequence
TAP-THP2 oligo 1	GTTTATCAGGTTTACACTGCTCAAGTTATCAAGTTCATAGC GAACAAAAGCTGGAGCTCAT
TAP-THP2 oligo 2	AGAGAGATTCAAAATACGTACGACCTTCTTCCTTTGTCAT CTTATCGTCATCATCAAGTG
TAP-THO2 oligo 1	CAGTTGATACATATTCGCACCAGTATACATTTTCAGGACTTT GAACAAAAGCTGGAGCTCAT
TAP-THO2 oligo 2	GAAAGAGCGTTCAATTTGGAAAGTAGCGTCTGTTCTGCCAT CTTATCGTCATCATCAAGTG
TAP-GBP2 oligo 1	GGCGAAAAGGAAACAAACATCAGCTGGATTTTTTCGCCAAG GAACAAAAGCTGGAGCTCAT
TAP-GBP2 oligo 2	CTACTCCTATCATTTCCATACATCCCTAGCTCTCTCTCCAT CTTATCGTCATCATCAAGTG

Table 7: colony PCR primers used in this study for verification of gene disruption

primer name	sequence
CTK1_del_600 up_fw	CCAAAGATTTACGACAACTA
DST1_del_600 up_fw	CGAACATCATTTTCAAATTGATCA
KAN_del_up_rev	GAAACGTGAGTCTTTTCCTTACCC

8.1.4. Antibodies

Table 8: Antibodies used in this study

antibody	dilution	host	source
PAP (peroxidase-anti-peroxidase)	1 : 5 000 (WB)	rabbit	P1291 (SIGMA)
α-Sub2	15 μl (ChIP)	rabbit	Katja Sträßer
α-Yra1	15 μl (ChIP)	rabbit	Katja Sträßer
8WG16 (α-Rpb1-CTD)	1 : 500 (WB) 10 μl (IP)	mouse	MMS-126R (Covance)
α-Pgk1	1 : 10 000 (WB)	mouse	A6457 (Molecular Probes)
FK2 (α-mono- and polyubiquitin	1 : 1 000 (WB)	mouse	PW8810 (Biomol)
α-mouse-HRP	1 : 3 000 (WB)	goat	170-6516 (BioRad)

8.2 Methods

8.2.1. Standard Methods

Standard methods such as restriction digests, transformation of vectors into E. coli, and agarose gel electrophoresis were performed according to Sambrook and Russell (2001).

8.2.1.1. PCR reactions

For TAP taggings according to Puig et al. (2001) 100 µl KNOP PCR reactions were performed in a T3 Personal Thermocycler (Biometra / Analytik Jena) and purified for yeast transformation as described in 8.2.1.2.

100 µl	KNOP PCR reaction	PCR program	
78 µl	ddH$_2$0	.	
10 µl	10x KNOP buffer (50 mM Tris-HCl pH 9.2, 16 mM (NH$_4$)$_2$SO$_4$, 2.25 mM MgCl$_2$)	94°C, 2 min.	
1 µl	template DNA (100 - 300 ng)	94°C, 1 min.	
0.5 µl	fw primer	45 - 50°C, 0.5 min.	35 x
0.5 µl	rev primer	68°C, 2.5 - 3 min.	
8 µl	dNTP mix (25 mM each)	68°C, 10 min.	
2 µl	KNOP polymerase mix (2 U Taq, 0.56 U Vent polymerase)		

For verification of gene disruptions colony PCR was performed in 25 µl volume with one primer annealing in the marker used for disruption and one primer annealing in the flanking genomic region. Some yeast cells were added to the PCR mix without Taq polymerase and boiled for 15 min. at 95°C in order to lyse the cells. Polymerase was then added and the PCR program resumed. The PCR product was analyzed by agarose gel electrophoresis.

25 µl	colony PCR reaction	PCR program	
19.6 µl	ddH$_2$0	95°C 15 min.	
2.5 µl	10x Taq buffer (Fermentas)	+ Taq.	
1.5 µl	MgCl$_2$ [25 mM]	95°C, 0.5 min.	
0.25 µl	fw primer	45°C, 0.5 min.	25 x
0.25 µl	rev primer	72°C, 1 min.	
0.6 µl	dNTP mix (25 mM each)	72°C, 2 min.	
some	yeast cell mass from colony		
0.3 µl	Taq polymerase(Fermentas)		

8.2.1.2. Phenol-Chloroform extraction of DNA

Digested gene disruption cassettes or PCR fragments for genomic tagging of yeast proteins were purified by phenol-chloroform extraction. The digest or PCR reaction was mixed with one volume of phenol:chloroform:isoamylalcohol (25:24:1), centrifuged at top speed for 10 min., and the aqueous phase extracted with an equal volume of chloroform (mixing and centrifuging for another 10 min.). The DNA in the aqueous phase was precipitated at - 20°C for at least an hour by addition of 1/10 of the volume of 3 M NaOAc, pH 5.2, and 2 volumes of 100 % ethanol. The pellet was washed with 70 % ethanol, dried, and resuspended in approximately 30 - 50 μl TE buffer (1 mM EDTA, 10 mM Tris-HCl, pH 8.0). A 0.5 μl aliquot was analyzed on an agarose gel, and 10 - 40 μl were used for transformation of S. cerevisiae (see 8.2.2.2.).

8.2.2. Yeast Techniques

8.2.2.1. Yeast Cell Culture

Yeast cells were cultivated in either in yeast extract / peptone full medium with glucose as carbon source (YPD) or in synthetic complete medium with glucose (SDC-x as selective medium lacking an amino acid or uracil to select for prototrophy or SDC+all as full medium).

Full medium (YPD)	1% yeast extract 2 % Bacto-peptone 2 % glucose
Synthetic complete medium (SDC)	0.67 % yeast nitrogen base 0.06 % complete synthetic mix containing all essential amino acids except those needed to select for prototrophy ("SDC-x") or containing all of them ("SDC+all") 2 % glucose

Precultures were inoculated in liquid medium from single colonies on a freshly restreaked plate, incubated on a shaking platform overnight at 30 °C, and the next day diluted in fresh medium to an OD_{600} of 0.1 – 0.2. Cultures were grown under agitation at 30 °C and used for experiments (transformation, ChIP, small-scale IP,…) at $OD_{600} \approx 0.6 – 0.8$.

Yeast strains expressing wild-type or K63R ubiquitin (strain backgrounds SUB280 and SUB413; see Table 3) were grown in SDC+all medium and ubiquitin expression was induced by addition of 100 μM $CuSO_4$ for 1.25 h prior to harvesting or 45 min. prior to CHX treatment in the CHX chase experiments.

8.2.2.2. Transformation of yeast cells

Cells were collected by centrifugation at appr. OD_{600} 0.5 - 0.8, washed once with water and once with solution I (10 mM Tris pH 7.5, 1 mM EDTA, 100 mM lithium acetate). The transformation mixture contained cells corresponding to ≈ 8 ml of culture, resuspended in solution I, 5 µg salmon sperm DNA as carrier DNA, the DNA to be transformed, and 300 µl of solution II (10 mM Tris pH 7.5, 1 mM EDTA, 100 mM lithium acetate, 40 % PEG). The mixture was incubated on a turning wheel at room temperature for 30 min., heat-shocked at 42 °C for 10 min., cooled on ice for 3 min., diluted by addition of 1 ml H_2O and centrifuged (1200 rcf, 3 min.). In the case of plasmid transformations, the cells were then immediately resuspended in 100 µl of sterile H_2O and plated on selective agar plates. For genomic integrations (*i.e.* TAP taggings or gene disruptions), the cells were resuspended in full medium and incubated on a turning wheel for recovery at room temperature for 1 - 6 h, before being plated on selective agar plates.

8.2.2.3. Genomic integration of a TAP tag

The TAP tagging procedure was performed as described by Puig et al. (2001). Briefly, for C-terminal tagging a PCR product containing the TAP tag sequence and a selection marker is created using the plasmids pBS1479 (*TRP1*) or pBS1539 (*URA3*) as templates ("KNOP PCR", see 8.2.1.1.). The primers used for this PCR additionally contain 50 nt-long 5' overhangs which represent the last nucleotides of the ORF before the stop codon (oligo 1) and the region downstream of the stop codon (oligo 2; see Table 6). The PCR product is purified by phenol-chloroform extraction (see 8.2.1.2.) and will be genomically integrated by homologous recombination upon transformation into yeast cells (see 8.2.2.2.). Correct integration is verified by Western Blotting of whole cell extracts (see 8.2.3.1. and 8.2.3.5) against the TAP tag (PAP antibody).

For N-terminal TAP tagging PCR primers are designed such that integration by homologous recombination will take place at the beginning of the target gene, with oligo 1 containing an overhang of the 50 nt immediately upstream of and excluding the start codon and oligo 2 containing an overhang of the start codon and the next 50 nt. Plasmid pBS1761 is used as a template for amplification of the N-terminal TAP tagging cassette. This cassette contains *TRP1* as selection marker, the *GAL1* promoter (both flanked by loxP sites) and the TAP tag. Upon correct integration into the yeast genome the selection marker is at first placed under control of the target gene promoter, while the target gene is expressed from the *GAL1* promoter. To put the target gene again under control of its native promoter, the positive transformants are transformed with plasmid pBS1766 encoding Cre recombinase, which excises the original selection marker and the GAL1 promoter by site-specific recombination at the loxP sites.

8.2.2.4. Gene deletion

Genes are disrupted by replacing the coding sequence with a selectable marker. As for the integration of a TAP tag one makes use of yeast's active homologous recombination and transforms them with a DNA fragment containing the marker flanked by promoter and terminator region of the targeted gene. Correct integration is verified by colony PCR (see 8.2.1.1.) using primers which anneal to the genomic region outside the targeted ORF and within the selection marker.

8.2.2.5. Spot dilution assays (dot spots)

One loop of freshly growing yeast cells (*i.e.* restreaked the previous day) was resuspended in 1 ml of H_2O and then diluted 1:10 four times. 5 µl of each dilution were spotted onto YPD or SDC-ura plates (supplemented with DMSO or 75 µg/ml 6-AU, as indicated) and incubated at the indicated temperature for 3 – 5 days.

8.2.2.6. Long-term storage of yeast strains

Freshly growing cells (growing on plate for no longer than 2 days) were collected by careful scraping off the plate, resuspended in 1 ml of 50 % sterile glycerol, vortexed gently and flash-frozen in liquid nitrogen. Samples were subsequently stored at – 80 °C.

8.2.3. Special Techniques

8.2.3.1. Protein extract preparation (yeast whole cell lysate) by alkaline lysis

Cells were diluted in the morning and grown to an $OD_{600} \approx 0.6 - 0.8$. 5 OD of cells were collected by centrifugation (3600 rpm, 3 min, 4°C), washed once with 1 ml cold H_2O, pelleted and flash-frozen in liquid nitrogen for short-term storage at $-80\,°C$. The cell pellet was resuspended in 500 µl of cold H_2O and lysed by incubation on ice for 20 min. with 150 µl of pre-treatment solution (1.85 M NaOH and 7.5 % β-mercapthoethanol). Proteins were then precipitated by addition of 150 µl 55 % TCA solution (≈ 10 % final concentration), incubated on ice for 20 min. and centrifuged at 16100 rcf for 20 min. The protein pellet was dissolved in 60 µl 1x SB and neutralized with 20 µl 1 M Tris base, heated for 1 min. at 65°C and centrifuged at top speed for 3 min. For quantitative WB, absorption at 280 nm was measured and samples diluted to an equal total protein concentration. Samples were either used for SDS-PAGE immediately or stored at -20°C.

8.2.3.2. UV treatment of yeast cells

Cells were diluted from overnight precultures in the morning and grown to an $OD_{600} \approx 0.5$. Cycloheximide was added to a final concentration of 50 µg / ml for 45 min. prior to UV treatment. The cell suspension was then centrifuged in 50 ml conical tubes, the cycloheximide-containing medium kept in the cell culture flasks for after the treatment, and each pellet from 50 ml of culture resuspended in an equal volume of cold PBS. This suspension was irradiated in a circular petri dish (diameter ≈ 14 cm) with 400 J / m2 in a XL-1500 UV crosslinker (Spectronics Corporation, Westbury, NY, USA), pipetted back into the 50 ml conical tubes, pelleted (3600 rpm, 3 min, 4°C), and resuspended in the original growth medium. "No UV" control samples were treated likewise but were not poured into the petri dish and not irradiated. After treatment, cells were allowed to recover in the incubator for 30 min. Cells were collected by centrifugation (3600 rpm, 3 min, 4°C), washed once with ice-cold PBS, once with ice-cold TAP-LB (50 mM Tris-HCl, pH 7.5, 1.5 mM $MgCl_2$, 0.15 % NP-40, 100 mM NaCl) with 1x protease inhibitor cocktail, flash-frozen in liquid nitrogen and stored at -80°C. Cell pellets were subsequently used for pull-down assays as described in section 8.2.3.3.

8.2.3.3. Pull-down assays ("small-scale IP") for analysis of Rpb1 polyubiquitylation

100 OD of yeast cells were harvested and stored at - 80° C for up to one week. Each 100 OD cell pellet was resuspended in 800 µl TAP lysis buffer (50 mM Tris-HCl, pH 7.5, 1.5 mM $MgCl_2$, 0.15 % NP-40, 100 mM NaCl; supplemented with 1x protease inhibitor cocktail, 2 mM NEM (deubiquitinase inhibitor), and 20 µM lactacystin or 20 µM MG132 (proteasome inhibitor)) and

lysed in 2 ml tubes by vortexing with 800 µl glass beads for 4 x 3 min. with 3 min. incubations on ice in between. Bottom and lid of the 2 ml tube were punctured with a hot syringe needle and the cell lysate was collected by centrifugation (2000 rpm, 2 min.) into a 15 ml tube. The lysates were brought to an equal volume of 1.5 ml by addition of ≈ 250 µl lysis buffer and were then centrifuged for 20 min. in a table-top centrifuge (top speed, 4 °C).

800 - 900 µl of the extract were used for immunoprecipitation (avoiding aspiration of both the cell debris pellet and the fatty phase on top). Equal amounts of RNAPII complexes were either immunoprecipitated from strains expressing Rpb3-TAP using 50 µl IgG sepharose at 4 °C for 1.5 h or from untagged strains using 10 µl anti-Rpb1 antibody 8WG16 (Covance) for 1 h and subsequent incubation with 50 µl Protein G-Dynabeads (Invitrogen) for 30 min. at 4 °C. Beads with immunoprecipitated complexes were washed four times with cold lysis buffer (50 mM Tris-HCl, pH 7.5, 1.5 mM $MgCl_2$, 0.15 % NP-40, and 100, 500 or 1000 mM NaCl as indicated) and the bound complexes eluted by heating the beads with 60 - 80 µl 2x sample buffer (IgG sepharose) or 1x sample buffer (Dynabeads) at 65°C for 2 min. with vortexing.

For the analysis of Tfg2 association (which runs at the height of the IgG heavy chain) with RNAPII purified from strains expressing Rpb3-TAP, bound complexes were eluted by TEV protease cleavage (incubation with 3 µl TEV in 100 µl low salt lysis buffer at 16°C for 1 h) and mixed with the appropriate volume of 4x SB.

Samples for ubiquitylation analysis were immediately used for SDS-PAGE (8.2.3.5.)

8.2.3.4. Cycloheximide chase assay for Rpb1 half-life determination

Cells were diluted from overnight precultures to an OD_{600} of 0.2. At an OD_{600} of approximately 0.6 - 0.7, an aliquot of 5 OD of cells was removed and harvested (see 8.2.3.1., preparation of alkaline lysis extracts). After removal of this t = 0 sample, translation was inhibited by addition of cycloheximide to the culture to a final concentration of 100 µg / ml, and 5 OD samples were withdrawn at regular time intervals as specified over the next 50 or 60 min.. Alkaline lysis extracts were prepared (see 8.2.3.1) and Rpb1 protein levels were determined by quantitative Western Blotting (see 8.2.3.6.). The logarithmised protein ratios for each time point after cycloheximide addition relative to t = 0 were plotted against the time, and the half-life was calculated by linear regression.

8.2.3.5. SDS-PAGE and protein transfer

Extracts for quantitative WB or detection of Rpb1, Tfg2, Pgk1 were separated on 10 % SDS polyacrylamide gels (after an initial sample concentration at 100 V for 5 min.) for 1 h at 200 V, and samples for analysis of Rpb1 polyubiquitylation on 6 % polyacrylamide gels for 1.5 - 2 h at 200 V (in the cold-room; using pre-cooled gels and buffer). SDS-PAGE was carried out in the

Mini-Protean apparatus (Biorad), using SDS running buffer (25 mM Tris; 0.1% (w/v) SDS; 0.19 mM glycine).

Proteins were subsequently transferred to nitrocellulose membranes (qWB) or activated PVDF membranes (ubiquitin detection) using a wet blotting apparatus (Biorad). A sandwich was assembled consisting of 2 layers of sponge material, 3 layers of Whatman paper, the membrane, the gel, 3 layers of Whatman paper, 2 layers of sponge material (all pre-soaked in wet blotting buffer) and submerged in a tank filled with pre-cooled wet blotting buffer (25 mM Tris, 192 mM glycine, 20 % methanol). Proteins were transferred at 100 V for 1 h (qWB) or at 80 V for 1.75 h (ubiquitin detection). In the latter case, wet blotting was performed in the cold room.

8.2.3.6. Quantitative Western Blotting

For quantitative Western Blot, protein concentration of alkaline lysis extracts was determined by measuring the absorption at 280 nm, and all samples were diluted to an equal concentration of total protein, before loading equal amounts on gel. After SDS-PAGE and Blot (see 5.2.11.), Western Blot was performed simultaneously against the protein of interest and Pgk1 as loading control. Blots were routinely blocked with 2 % milk in PBS, except for blots with the anti-ubiquitin antibody FK2, which were blocked with 5 % BSA in TBST (TBS with 0.1 % Tween-20). Incubation with primary antibodies was normally done overnight in the cold room, secondary antibody incubation at room temperature for 1 h (for anti-ubiquitin Western Blots at least 2 h). Signals were detected using ECL solution (for ubiquitin detection, SuperSignal West Dura, Pierce) and the Fujifilm LAS-3000 mini image reader (raytek, Sheffield, UK). MultiGauge software (ver 3; ScienceLab2005; Fujifilm Life Sciences) was used to quantify the signals.

8.2.3.7. Chromatin immunoprecipitation for single loci (ChIP-qPCR)

ChIP buffers

FA lysis buffer low salt	FA lysis buffer high salt	TLEND
50 mM HEPES-KOH, pH 7.5	50 mM HEPES-KOH pH, 7.5	10mM Tris-HCl pH 8.0
150 mM NaCl	500 mM NaCl	0.25M LiCl
1 mM EDTA	1mM EDTA	1mM EDTA
1 % Triton X-100	1% Triton X-100	0.5% Nonidet P-40
0.1 % sodium deoxycholate	0.1% sodium deoxycholate	0.5% SDS
0.1 % SDS	0.1 % SDS	

Elution buffer	100 x protease inhibitor cocktail
50 mM Tris·Cl pH 7.5	28 ng/ml Leupeptin; 137 ng/ml Pepstatin A; 17 ng/ml
10 mM EDTA	PMSF; 0.33 mg/ml benzamidine; in 100 % ethanol p.a.

Formaldehyde crosslinking

100 ml of cells growing in mid-log phase were chemically crosslinked (at OD_{600} of appr. 0.80) by incubation with 1 % formaldehyde for 20 min. at 20°C, and the reaction was quenched by addition of glycine to a final concentration of 350 mM. Cells were harvested, washed with cold TBS and transferred to eppis in FA lysis buffer with 1x protease inhibitor cocktail; pellets were flash-frozen in liquid nitrogen and stored at - 80°C.

Lysis and sonication

The cell pellets were thawed, resuspended in 800 µl of FA lysis buffer with 1x protease inhibitor cocktail and lysed by vortexing with 800 µl glass beads for 5 x 3 min. with 3 min. on ice in between. Successful lysis (> 85 %) was verified under the microscope. The lysate was sonicated in a Bioruptor UCD-200 (Diagenode) at an output of 200 W for 3 x 12 min. (30 sec. on / 30 sec. off) with intermittent cooling on ice for 4 min., resulting in an average chromatin size of 250 - 300 bp (monitored by agarose gel electrophoresis). The lysate was cleared by two successive centrifugation steps (13000 rpm, 4°C; 10 and 5 min.) and the supernatant (= soluble chromatin fraction) used for chromatin immunoprecipitation.

Chromatin immunoprecipitation

Protein concentration of the lysate was estimated by measuring the absorption at 280 nm. 5 A_{280} in a total volume of 1200 µl FA lysis buffer (low salt) were used for ChIP of Rpb3-TAP, 15 A_{280} for ChIP of Hpr1-TAP and Mft1-TAP, 18 A280 for ChIP of Pre1, and 20 A_{280} for ChIP of Tho2-TAP, Thp2-TAP, Yra1 and Sub2. TAP-tagged proteins of interest were immunoprecipitated with 15 µl of IgG-coupled Dynabeads tosylactivated M280 (Invitrogen) for 2.5 h at 20°C (Pre1 overnight at 4°C). Yra1 and Sub2 were precipitated with antibodies raised against the protein (15 µl each) for 2 h at 20°C, followed by an incubation with 15 µl Protein A-Dynabeads (Invitrogen) for 30 min. IP samples were washed 2x with FA lysis buffer low salt, 2x with FA lysis buffer high salt, 2x with TLEND, and 1x with TE, and eluted in 120 µl elution buffer by incubation at 65°C for 20 min. in a shaking thermomixer (850 rpm).

0.08 A280 of the corresponding lysates were saved as Input samples and, in a total volume of 120 µl elution buffer, processed in parallel with the IP samples for protein digestion and reversal of crosslinks.

Protein digestion and reversal of crosslinks

Eluates or Input samples were mixed with 80 µl TE and 20 µl Proteinase K (P4850; Sigma) and incubated at 37°C for 2 h for protein digestion and at 65°C for 10 - 12 h for reversal of

crosslinks. IP and INP DNA was subsequently purified with the Nucleospin Extract II kit (Macherey & Nagel) according to the manufacturer's instructions in an elution volume of 100 µl.

Fragment size control

Successful and consistent chromatin fragmentation was monitored using 100 µl of the soluble chromatin fraction after sonication (see end of step *lysis and sonication*). These were mixed with 92 µl TE and 8 µl Proteinase K and incubated as above for protein digestion and reversal of crosslinks. The sample was then mixed with 20 µl of LiCl [4 M], 1 µl glycogen and 120 µl phenol and centrifuged at 13000 rpm for 10 min. The aqueous phase was mixed with 400 µl of 100 % ethanol and nucleic acids precipitated at -20°C for 6 h. Subsequently, the sample was centrifuged (13000 rpm, 20 min., 4°C) and the pellet washed with 70 % ethanol, dried and resuspended in 20 µl TE. RNA was removed by RNase treatment (5 µl RNase A [10 mg/ml] for 1 h at 37°C). The sample was then analyzed on a 1.5 % agarose gel.

Quantitative PCR for selected target genes

Quantitative real-time PCR with Input and IP samples was performed in a StepOnePlus Real-Time PCR Cycler (Applied Biosystems, Darmstadt) using the *Power* SYBR Green PCR Mastermix (Life Technologies) according to the manufacturer's instructions (with the exception that the total reaction volume was only 10 µl). PCR efficiency (E) was determined with standard curves, and primer sequences are listed in table 5. A nontranscribed region (NTR) of chromosome V (174137-174447) served as control, and the enrichment of the protein of interest at selected loci over this NTR was calculated according to $[E^{\wedge}(C_T\,IP - C_T\,Input)]_{NTR}\,/\,[E^{\wedge}(C_T\,IP - C_T\,Input)]_{gene\,of\,interest}$. CT values were determined using Applied Biosystem's StepOne Software v2.1.

8.2.3.8. Chromatin immunoprecipitation followed by hybridization to tiling arrays (genome-wide ChIP-chip)

ChIP procedure

ChIP-chip experiments were essentially performed as described in (Mayer 2010). Rpb3-TAP, TAP-Tho2, Tho2-TAP, Hpr1-TAP, Mft1-TAP, Gbp2-TAP, Hrb1-TAP, TAP-Npl3, and Nab2-TAP were immunoprecipitated with 50 µl IgG Sepharose beads Fast Flow (GE Healthcare), Yra1 and Sub2 were immunoprecipitated with antibodies directed against the protein.

The basic ChIP procedure was similar as detailed in section 8.2.3.7. for ChIP-qPCR, with a few modifications: Starting material for one ChIP came from 600 ml of yeast culture and was equally distributed to three tubes in parallel for lysis, sonication, IP, and elution. Washing after IP included one additional washing step with FA lysis buffer high salt, and samples were eluted in 140 ml elution buffer by incubation for 1 h at 65°C in a shaking thermomixer (1000 rpm). DNA

was purified after Proteinase K digestion and reversal of crosslinks with the QIAquick PCR purification kit (Qiagen) according to the manufacturer's instructions and eluted in 50 µl nuclease-free water. For further processing, the samples were concentrated to 10 µl in a vacuum concentrator (SpeedVac, Thermo Scientific).

Whole genome amplification and hybridization to tiling arrays

Input and IP samples were further processed and hybridized to custom-made Affymetrix *S. cerevisiae* tiling arrays as described in the Affymetrix Chromatin Immunoprecipitation Assay Protocol P/N 702238. To this end, concentrated DNA was amplified and re-amplified using the GenomePlex™ Complete Whole Genome Amplification kit (WGA-2, Sigma), following the Farnham Lab WGA protocol for ChIP-chip, and purified with the QIAquick PCR purification kit (Qiagen). 0.4 mM dUTP were included in the second WGA reaction to allow for subsequent enzymatic cleavage. Purity of the sample and successful amplification were monitored using a NanoDrop1000 spectrophotometer and agarose gel electrophoresis.

Samples were then enzymatically fragmented and labeled using the GeneChip WT Double-Stranded DNA Terminal Labeling Kit (P/N 900812, Affymetrix) according to the manufacturer's instructions. 5.5 µg of fragmented and labeled DNA were hybridized to a custom-made Affymetrix tiling array (P/N 520055) for 16 h at 45°C in a GeneChip Hybridization Oven 640 (Affymetrix). Subsequently, arrays were washed and stained in the Affymetrix GeneChip Fluidics Station 450 using the FS45_0001 program and scanned in an Affymetrix GeneChip Scanner 3000 7G. The obtained .cel files were used for data analysis.

Data analysis

At least two independent biological replicates were measured for each protein. All data analyses were performed by Dominik Meinel (Sträßer lab), similar to the procedure described in (Mayer 2010) and (Mayer 2012) and as described in (Meinel 2013).

Briefly, outlier probes were determined and excluded, quantile normalization between replicate measurements was performed, replicate measurements were averaged, and data was normalized using an algorithm which combined mock IP and Input normalization (for details, see supplemental information to Mayer 2010).

Meta occupancy profiles were calculated from the top 50 % expressed genes, which were grouped into three length classes: short (512 - 937 bp; comprising 266 genes), medium length (938 - 1537 bp; 339 genes), and long genes (1538 - 2895 bp; 299 genes).

To analyze a possible length-dependent recruitment, peak occupancies of each factor (reflecting the 90 % quantile of factor recruitment) were calculated. The peak occupancies for any given

factor were normalized to the peak occupancies of Rpb3 (RNAPII) at the respective genes to normalize for variations in transcription frequency. Genes were grouped into eight length groups: A (512 - 723 bp), B (724 - 1023 bp), C (1024 - 1286 bp), D (1287 - 1617 bp), E (1618 - 2047 bp), F (2048 - 2895 bp), G (2896 - 4095 bp) and H (4096 - 5793 bp), the mean values and standard deviations calculated and plotted versus the gene length.

References

Abruzzi KC, Lacadie S, Rosbash M (2004). Biochemical analysis of TREX complex recruitment to intronless and intron-containing yeast genes. *EMBO J,* 23(13):2620-31.

Adelman K, Lis JT (2012). Promoter-proximal pausing of RNA polymerase II: emerging roles in metazoans. *Nat Rev Genet,* 13(10):720-31

Alexander RD, Innocente SA, Barrass JD, Beggs JD (2010). Splicing-dependent RNA polymerase pausing in yeast. *Mol Cell,* 40(4):582-93

Anindya R, Aygün O, Svejstrup JQ (2007). Damage-induced ubiquitylation of human RNA polymerase II by the ubiquitin ligase Nedd4, but not Cockayne syndrome proteins or BRCA1. *Mol Cell,* 28(3):386-97.

Ansari A, Hampsey M (2005). A role for the CPF 3'-end processing machinery in RNAP II-dependent gene looping. *Genes Dev,* 19(24):2969-78.

Ares M Jr, Grate L, Pauling MH (1999). A handful of intron-containing genes produces the lion's share of yeast mRNA. *RNA,* 5(9):1138-9.

Armache KJ, Mitterweger S, Meinhart A, Cramer P (2005). Structures of complete RNA polymerase II and its subcomplex, Rpb4/7. *J Biol Chem,* 280(8):7131-4.

Aso T, Conrad MN (1997). Molecular cloning of DNAs encoding the regulatory subunits of elongin from Saccharomyces cerevisiae and Drosophila melanogaster. *Biochem Biophys Res Commun,* 241(2):334-40.

Barta I, Iggo R (1995). Autoregulation of expression of the yeast Dbp2p 'DEAD-box' protein is mediated by sequences in the conserved DBP2 intron. *EMBO J,* 14(15):3800-8.

Bataille AR, Jeronimo C, Jacques PÉ, Laramée L, Fortin MÈ, Forest A, Bergeron M, Hanes SD, Robert F (2012). A universal RNA polymerase II CTD cycle is orchestrated by complex interplays between kinase, phosphatase, and isomerase enzymes along genes. *Mol Cell,* 45(2):158-70.

Batisse J, Batisse C, Budd A, Böttcher B, Hurt E (2009). Purification of nuclear poly(A)-binding protein Nab2 reveals association with the yeast transcriptome and a messenger ribonucleoprotein core structure. *J Biol Chem,* 284(50):34911-7.

Beaudenon SL, Huacani MR, Wang G, McDonnell DP, Huibregtse JM (1999). Rsp5 ubiquitin-protein ligase mediates DNA damage-induced degradation of the large subunit of RNA polymerase II in Saccharomyces cerevisiae. *Mol Cell Biol,* 19(10):6972-9.

Beck F, Unverdorben P, Bohn S, Schweitzer A, Pfeifer G, Sakata E, Nickell S, Plitzko JM, Villa E, Baumeister W, Förster F (2012). Near-atomic resolution structural model of the yeast 26S proteasome. *Proc Natl Acad Sci U S A,* 109(37):14870-5.

Bedford L, Layfield R, Mayer RJ, Peng J, Xu P (2011). Diverse polyubiquitin chains accumulate following 26S proteasomal dysfunction in mammalian neurones. *Neurosci Lett,* 491(1):44-7.

Berretta J, Morillon A (2009). Pervasive transcription constitutes a new level of eukaryotic genome regulation. *EMBO Rep,* 10(9):973-82.

Blobel G (1985). Gene gating: a hypothesis. *Proc Natl Acad Sci U S A,* 82(24):8527-9.

Bradsher JN, Tan S, McLaury HJ, Conaway JW, Conaway RC (1993). RNA polymerase II transcription factor SIII. II. Functional properties and role in RNA chain elongation. *J Biol Chem,* 268(34):25594-603.

Bregman DB, Halaban R, van Gool AJ, Henning KA, Friedberg EC, Warren SL (1996). UV-induced ubiquitination of RNA polymerase II: a novel modification deficient in Cockayne syndrome cells. *Proc Natl Acad Sci U S A,* 93(21):11586-90.

Bucheli ME, Buratowski S (2005). Npl3 is an antagonist of mRNA 3' end formation by RNA polymerase II. *EMBO J,* 24(12):2150-60.

Buratowski S (2003). The CTD code. *Nat Struct Biol,* 10(9):679-80.

Buratowski S (2009). Progression through the RNA polymerase II CTD cycle. *Mol Cell,* 36(4):541-6.

Carrillo Oesterreich F, Preibisch S, Neugebauer KM (2010). Global analysis of nascent RNA reveals transcriptional pausing in terminal exons. *Mol Cell,* 40(4):571-81.

Chan S, Choi EA, Shi Y (2011). Pre-mRNA 3'-end processing complex assembly and function. *Wiley Interdiscip Rev RNA,* 2(3):321-35.

Chanarat S, Seizl M, Strässer K (2011). The Prp19 complex is a novel transcription elongation factor required for TREX occupancy at transcribed genes. *Genes Dev,* 25(11):1147-58.

Chanarat S, Burkert-Kautzsch C, Meinel DM, Sträßer K (2012). Prp19C and TREX: interacting to promote transcription elongation and mRNA export. *Transcription,* 3(1):8-12.

Chau V, Tobias JW, Bachmair A, Marriott D, Ecker DJ, Gonda DK, Varshavsky A (1989). A multiubiquitin chain is confined to specific lysine in a targeted short-lived protein. *Science,* 243(4898):1576-83.

Chávez S, Aguilera A (1997). The yeast HPR1 gene has a functional role in transcriptional elongation that uncovers a novel source of genome instability. *Genes Dev,* 11(24):3459-70.

Chávez S, Beilharz T, Rondón AG, Erdjument-Bromage H, Tempst P, Svejstrup JQ, Lithgow T, Aguilera A (2000). A protein complex containing Tho2, Hpr1, Mft1 and a novel protein, Thp2, connects transcription elongation with mitotic recombination in Saccharomyces cerevisiae. *EMBO J,* 19(21):5824-34.

Chávez S, García-Rubio M, Prado F, Aguilera A (2001). Hpr1 is preferentially required for transcription of either long or G+C-rich DNA sequences in Saccharomyces cerevisiae. *Mol Cell Biol,* 21(20):7054-64.

Chen X, Ruggiero C, Li S (2007). Yeast Rpb9 plays an important role in ubiquitylation and degradation of Rpb1 in response to UV-induced DNA damage. *Mol Cell Biol,* 27(13):4617-25.

Cheng H, Dufu K, Lee CS, Hsu JL, Dias A, Reed R (2006). Human mRNA export machinery recruited to the 5' end of mRNA. *Cell,* 127(7):1389-400.

Chinchilla K, Rodriguez-Molina JB, Ursic D, Finkel JS, Ansari AZ, Culbertson MR (2012).

Interactions of Sen1, Nrd1, and Nab3 with multiple phosphorylated forms of the Rpb1 C-terminal domain in Saccharomyces cerevisiae. *Eukaryot Cell,* 11(4):417-29.

Cho EJ, Takagi T, Moore CR, Buratowski S (1997). mRNA capping enzyme is recruited to the transcription complex by phosphorylation of the RNA polymerase II carboxy-terminal domain. *Genes Dev,* 11(24):3319-26.

Clague MJ, Coulson JM, Urbé S (2012). Cellular functions of the DUBs. *J Cell Sci,* 125(Pt 2):277-86.

Cloutier SC, Ma WK, Nguyen LT, Tran EJ (2012). The DEAD-box RNA helicase Dbp2 connects RNA quality control with repression of aberrant transcription. *J Biol Chem,* 287(31):26155-66.

Conaway RC, Conaway JW (2011). Function and regulation of the Mediator complex. *Curr Opin Genet Dev,* 21(2):225-30.

Cordin O, Banroques J, Tanner NK, Linder P (2006). The DEAD-box protein family of RNA helicases. *Gene,* 367:17-37.

Cramer P, Armache KJ, Baumli S, Benkert S, Brueckner F, Buchen C, Damsma GE, Dengl S, Geiger SR, Jasiak AJ, Jawhari A, Jennebach S, Kamenski T, Kettenberger H, Kuhn CD, Lehmann E, Leike K, Sydow JF, Vannini A (2008). Structure of eukaryotic RNA polymerases. *Annu Rev Biophys,* 37:337-52.

Crosas B, Hanna J, Kirkpatrick DS, Zhang DP, Tone Y, Hathaway NA, Buecker C, Leggett DS, Schmidt M, King RW, Gygi SP, Finley D (2006). Ubiquitin chains are remodeled at the proteasome by opposing ubiquitin ligase and deubiquitinating activities. *Cell,* 127(7):1401-13.

Cuenca-Bono B, García-Molinero V, Pascual-García P, Dopazo H, Llopis A, Vilardell J, Rodríguez-Navarro S (2011). SUS1 introns are required for efficient mRNA nuclear export in yeast. *Nucleic Acids Res,* 39(19):8599-611

Darzacq X, Shav-Tal Y, de Turris V, Brody Y, Shenoy SM, Phair RD, Singer RH (2007). In vivo dynamics of RNA polymerase II transcription. *Nat Struct Mol Biol,* 14(9):796-806.

Datta AB, Hura GL, Wolberger C (2009). The structure and conformation of Lys63-linked tetraubiquitin. *J Mol Biol,* 392(5):1117-24.

Daulny A, Tansey WP (2009). Damage control: DNA repair, transcription, and the ubiquitin-proteasome system. *DNA Repair (Amst),* 8(4):444-8.

David CJ, Boyne AR, Millhouse SR, Manley JL (2011). The RNA polymerase II C-terminal domain promotes splicing activation through recruitment of a U2AF65-Prp19 complex. *Genes Dev,* 25(9):972-83.

Dermody JL, Dreyfuss JM, Villén J, Ogundipe B, Gygi SP, Park PJ, Ponticelli AS, Moore CL, Buratowski S, Bucheli ME (2008). Unphosphorylated SR-like protein Npl3 stimulates RNA polymerase II elongation. *PLoS One,* 3(9):e3273.

Dieppois G, Iglesias N, Stutz F (2006). Cotranscriptional recruitment to the mRNA export receptor Mex67p contributes to nuclear pore anchoring of activated genes. *Mol Cell Biol,* 26(21):7858-70.

Dimova NV, Hathaway NA, Lee BH, Kirkpatrick DS, Berkowitz ML, Gygi SP, Finley D, King RW (2012). APC/C-mediated multiple monoubiquitylation provides an alternative degradation signal for cyclin B1. *Nat Cell Biol,* 14(2):168-76.

Dong S, Li C, Zenklusen D, Singer RH, Jacobson A, He F (2007). YRA1 autoregulation requires nuclear export and cytoplasmic Edc3p-mediated degradation of its pre-mRNA. *Mol Cell,* 25(4):559-73.

Drygin D, Rice WG, Grummt I (2010). The RNA polymerase I transcription machinery: an emerging target for the treatment of cancer. *Annu Rev Pharmacol Toxicol,* 50:131-56.

Eckmann CR, Rammelt C, Wahle E (2011). Control of poly(A) tail length. *Wiley Interdiscip Rev RNA,* 2(3):348-61.

Eddins MJ, Varadan R, Fushman D, Pickart CM, Wolberger C (2007). Crystal structure and solution NMR studies of Lys48-linked tetraubiquitin at neutral pH. *J Mol Biol,* 367(1):204-11.

Egloff S, O'Reilly D, Chapman RD, Taylor A, Tanzhaus K, Pitts L, Eick D, Murphy S (2007). Serine-7 of the RNA polymerase II CTD is specifically required for snRNA gene expression. *Science,* 318(5857):1777-9.

Egloff S, Murphy S (2008). Cracking the RNA polymerase II CTD code. *Trends Genet,* 24(6):280-8.

Egloff S (2012). Role of Ser7 phosphorylation of the CTD during transcription of snRNA genes. *RNA Biol,* 9(8):1033-8.

Elsasser S, Finley D (2005). Delivery of ubiquitinated substrates to protein-unfolding machines. *Nat Cell Biol,* 7(8):742-9.

Enriquez-Harris P, Levitt N, Briggs D, Proudfoot NJ (1991). A pause site for RNA polymerase II is associated with termination of transcription. *EMBO J,* 10(7):1833-42.

Exinger F, Lacroute F (1992). 6-Azauracil inhibition of GTP biosynthesis in Saccharomyces cerevisiae. *Curr Genet,* 22(1):9-11.

Fan HY, Merker RJ, Klein HL (2001). High-copy-number expression of Sub2p, a member of the RNA helicase superfamily, suppresses hpr1-mediated genomic instability. *Mol Cell Biol,* 21(16):5459-70.

Feuerbach F, Galy V, Trelles-Sticken E, Fromont-Racine M, Jacquier A, Gilson E, Olivo-Marin JC, Scherthan H, Nehrbass U (2002). Nuclear architecture and spatial positioning help establish transcriptional states of telomeres in yeast. *Nat Cell Biol,* 4(3):214-21.

Finley D, Bartel B, Varshavsky A (1989). The tails of ubiquitin precursors are ribosomal proteins whose fusion to ubiquitin facilitates ribosome biogenesis. *Nature,* 338(6214):394-401.

Finley D (2009). Recognition and processing of ubiquitin-protein conjugates by the proteasome. *Annu Rev Biochem,* 78:477-513.

Finley D, Ulrich HD, Sommer T, Kaiser P (2012). The ubiquitin-proteasome system of Saccharomyces cerevisiae. *Genetics,* 192(2):319-60.

Fischer T, Strässer K, Rácz A, Rodriguez-Navarro S, Oppizzi M, Ihrig P, Lechner J, Hurt E (2002). The mRNA export machinery requires the novel Sac3p-Thp1p complex to dock at the nucleoplasmic entrance of the nuclear pores. *EMBO J,* 21(21):5843-52.

Folkmann AW, Noble KN, Cole CN, Wente SR (2011). Dbp5, Gle1-IP6 and Nup159: a working model for mRNP export. *Nucleus,* 2(6):540-8.

Gaillard H, Wellinger RE, Aguilera A (2007). A new connection of mRNP biogenesis and export with transcription-coupled repair. *Nucleic Acids Res,* 35(12):3893-906.

Gaillard H, Aguilera A (2013). Transcription coupled repair at the interface between transcription elongation and mRNP biogenesis. *Biochim Biophys Acta,* 1829(1):141-50.

Galy V, Gadal O, Fromont-Racine M, Romano A, Jacquier A, Nehrbass U (2004). Nuclear retention of unspliced mRNAs in yeast is mediated by perinuclear Mlp1. *Cell,* 116(1):63-73.

García-Oliver E, García-Molinero V, Rodríguez-Navarro S (2012). mRNA export and gene expression: the SAGA-TREX-2 connection. *Biochim Biophys Acta,* 1819(6):555-65.

García-Rubio M, Chávez S, Huertas P, Tous C, Jimeno S, Luna R, Aguilera A (2008). Different physiological relevance of yeast THO/TREX subunits in gene expression and genome integrity. *Mol Genet Genomics,* 279(2):123-32.

Geng F, Wenzel S, Tansey WP (2012). Ubiquitin and proteasomes in transcription. *Annu Rev Biochem,* 81:177-201.

Gewartowski K, Cuéllar J, Dziembowski A, Valpuesta JM (2012). The yeast THO complex forms a 5-subunit assembly that directly interacts with active chromatin. *Bioarchitecture,* 2(4).

Ghavi-Helm Y, Michaut M, Acker J, Aude JC, Thuriaux P, Werner M, Soutourina J (2008). Genome-wide location analysis reveals a role of TFIIS in RNA polymerase III transcription. *Genes Dev,* 22(14):1934-47.

Gilbert W, Siebel CW, Guthrie C (2001). Phosphorylation by Sky1p promotes Npl3p shuttling and mRNA dissociation. *RNA,* 7(2):302-13.

Gilbert W, Guthrie C (2004). The Glc7p nuclear phosphatase promotes mRNA export by facilitating association of Mex67p with mRNA. *Mol Cell,* 13(2):201-12.

Gómez-González B, García-Rubio M, Bermejo R, Gaillard H, Shirahige K, Marín A, Foiani M, Aguilera A (2011). Genome-wide function of THO/TREX in active genes prevents R-loop-dependent replication obstacles. *EMBO J,* 30(15):3106-19.

González-Barrera S, Prado F, Verhage R, Brouwer J, Aguilera A (2002). Defective nucleotide excision repair in yeast hpr1 and tho2 mutants. *Nucleic Acids Res,* 30(10):2193-201.

Görnemann J, Barrandon C, Hujer K, Rutz B, Rigaut G, Kotovic KM, Faux C, Neugebauer KM, Séraphin B (2011). Cotranscriptional spliceosome assembly and splicing are independent of the Prp40p WW domain. *RNA,* 17(12):2119-29.

Graber JH, Nazeer FI, Yeh PC, Kuehner JN, Borikar S, Hoskinson D, Moore C (2013). DNA damage induces targeted, genome-wide variation of poly(A) sites in budding yeast. *Genome Res,* 23(10):1690-703.

Green DM, Marfatia KA, Crafton EB, Zhang X, Cheng X, Corbett AH (2002). Nab2p is required for poly(A) RNA export in Saccharomyces cerevisiae and is regulated by arginine methylation via Hmt1p. *J Biol Chem,* 277(10):7752-60.

Gromak N, West S, Proudfoot NJ (2006). Pause sites promote transcriptional termination of mammalian RNA polymerase II. *Mol Cell Biol,* 26(10):3986-96.

Grünberg S, Warfield L, Hahn S (2012). Architecture of the RNA polymerase II preinitiation complex and mechanism of ATP-dependent promoter opening. *Nat Struct Mol Biol,* 19(8):788-96.

Gu B, Eick D, Bensaude O (2013). CTD serine-2 plays a critical role in splicing and termination factor recruitment to RNA polymerase II in vivo. *Nucleic Acids Res,* 41(3):1591-603.

Gwizdek C, Hobeika M, Kus B, Ossareh-Nazari B, Dargemont C, Rodriguez MS (2005). The mRNA nuclear export factor Hpr1 is regulated by Rsp5-mediated ubiquitylation. *J Biol Chem,* 280(14):13401-5.

Gwizdek C, Iglesias N, Rodriguez MS, Ossareh-Nazari B, Hobeika M, Divita G, Stutz F, Dargemont C (2006). Ubiquitin-associated domain of Mex67 synchronizes recruitment of the mRNA export machinery with transcription. *Proc Natl Acad Sci U S A,* 103(44):16376-81.

Haag JR, Pikaard CS (2011). Multisubunit RNA polymerases IV and V: purveyors of non-coding RNA for plant gene silencing. *Nat Rev Mol Cell Biol,* 12(8):483-92.

Häcker S, Krebber H (2004). Differential export requirements for shuttling serine/arginine-type mRNA-binding proteins. *J Biol Chem,* 279(7):5049-52.

Haglund K, Dikic I (2012). The role of ubiquitylation in receptor endocytosis and endosomal sorting. *J Cell Sci,* 125(Pt 2):265-75.

Hampsey M (1997). A review of phenotypes in Saccharomyces cerevisiae. *Yeast,* 13(12):1099-133.

Hampsey M, Reinberg D (2003). Tails of intrigue: phosphorylation of RNA polymerase II mediates histone methylation. *Cell,* 113(4):429-32.

Hampsey M, Singh BN, Ansari A, Lainé JP, Krishnamurthy S (2011). Control of eukaryotic gene expression: gene loops and transcriptional memory. *Adv Enzyme Regul,* 51(1):118-25.

Hanawalt PC, Spivak G (2008). Transcription-coupled DNA repair: two decades of progress and surprises. *Nat Rev Mol Cell Biol,* 9(12):958-70.

Hanna J, Hathaway NA, Tone Y, Crosas B, Elsasser S, Kirkpatrick DS, Leggett DS, Gygi SP, King RW, Finley D (2006). Deubiquitinating enzyme Ubp6 functions noncatalytically to delay proteasomal degradation. *Cell,* 127(1):99-111.

Harel-Sharvit L, Eldad N, Haimovich G, Barkai O, Duek L, Choder M (2010). RNA polymerase II subunits link transcription and mRNA decay to translation. *Cell,* 143(4):552-63.

Harreman M, Taschner M, Sigurdsson S, Anindya R, Reid J, Somesh B, Kong SE, Banks CA, Conaway RC, Conaway JW, Svejstrup JQ (2009). Distinct ubiquitin ligases act sequentially for RNA polymerase II polyubiquitylation. *Proc Natl Acad Sci U S A,* 106(49):20705-10.

Heidemann M, Eick D (2012). Tyrosine-1 and threonine-4 phosphorylation marks complete the RNA polymerase II CTD phospho-code. *RNA Biol,* 9(9):1144-6.

Heidemann M, Hintermair C, Voß K, Eick D (2013). Dynamic phosphorylation patterns of RNA polymerase II CTD during transcription. *Biochim Biophys Acta,* 1829(1):55-62.

Hieronymus H, Silver PA (2003). Genome-wide analysis of RNA-protein interactions illustrates specificity of the mRNA export machinery. *Nat Genet,* 33(2):155-61.

Hilleren P, McCarthy T, Rosbash M, Parker R, Jensen TH (2001). Quality control of mRNA 3'-end processing is linked to the nuclear exosome. *Nature,* 413(6855):538-42.

Hintermair C, Heidemann M, Koch F, Descostes N, Gut M, Gut I, Fenouil R, Ferrier P, Flatley A, Kremmer E, Chapman RD, Andrau JC, Eick D (2012). Threonine-4 of mammalian RNA polymerase II CTD is targeted by Polo-like kinase 3 and required for transcriptional elongation. *EMBO J,* 31(12):2784-97.

Hobeika M, Brockmann C, Iglesias N, Gwizdek C, Neuhaus D, Stutz F, Stewart M, Divita G, Dargemont C (2007). Coordination of Hpr1 and ubiquitin binding by the UBA domain of the mRNA export factor Mex67. *Mol Biol Cell,* 18(7):2561-8.

Hocine S, Singer RH, Grünwald D (2010). RNA processing and export. *Cold Spring Harb Perspect Biol,* 2(12):a000752.

Hoege C, Pfander B, Moldovan GL, Pyrowolakis G, Jentsch S (2002). RAD6-dependent DNA repair is linked to modification of PCNA by ubiquitin and SUMO. *Nature,* 419(6903):135-41.

Hsin JP, Sheth A, Manley JL (2011). RNAP II CTD phosphorylated on threonine-4 is required for histone mRNA 3' end processing. *Science,* 334(6056):683-6.

Hsin JP, Manley JL (2012). The RNA polymerase II CTD coordinates transcription and RNA processing. *Genes Dev,* 26(19):2119-37.

Huertas P, Aguilera A (2003). Cotranscriptionally formed DNA:RNA hybrids mediate transcription elongation impairment and transcription-associated recombination. *Mol Cell,* 12(3):711-21.

Huertas P, García-Rubio ML, Wellinger RE, Luna R, Aguilera A (2006). An hpr1 point mutation that impairs transcription and mRNP biogenesis without increasing recombination. *Mol Cell Biol,* 26(20):7451-65.

Huibregtse JM, Yang JC, Beaudenon SL (1997). The large subunit of RNA polymerase II is a substrate of the Rsp5 ubiquitin-protein ligase. *Proc Natl Acad Sci U S A,* 94(8):3656-61.

Hurt E, Strässer K, Segref A, Bailer S, Schlaich N, Presutti C, Tollervey D, Jansen R (2000). Mex67p mediates nuclear export of a variety of RNA polymerase II transcripts. *J Biol Chem,* 275(12):8361-8.

Hurt E, Luo MJ, Röther S, Reed R, Strässer K (2004). Cotranscriptional recruitment of the serine-arginine-rich (SR)-like proteins Gbp2 and Hrb1 to nascent mRNA via the TREX complex. *Proc Natl Acad Sci U S A,* 101(7):1858-62.

Iglesias N, Tutucci E, Gwizdek C, Vinciguerra P, Von Dach E, Corbett AH, Dargemont C, Stutz F (2010). Ubiquitin-mediated mRNP dynamics and surveillance prior to budding yeast mRNA export. *Genes Dev,* 24(17):1927-38.

Jiao X, Xiang S, Oh C, Martin CE, Tong L, Kiledjian M (2010). Identification of a quality-control mechanism for mRNA 5'-end capping. *Nature,* 467(7315):608-11.

Jimeno S, Rondón AG, Luna R, Aguilera A (2002). The yeast THO complex and mRNA export factors link RNA metabolism with transcription and genome instability. *EMBO J,* 21(13):3526-35

Jimeno S, Luna R, García-Rubio M, Aguilera A (2006). Tho1, a novel hnRNP, and Sub2 provide alternative pathways for mRNP biogenesis in yeast THO mutants. *Mol Cell Biol,* 26(12):4387-98.

Jimeno-González S, Haaning LL, Malagon F, Jensen TH (2010). The yeast 5'-3' exonuclease Rat1p functions during transcription elongation by RNA polymerase II. *Mol Cell,* 37(4):580-7.

Johnson SA, Cubberley G, Bentley DL (2009). Cotranscriptional recruitment of the mRNA export factor Yra1 by direct interaction with the 3' end processing factor Pcf11. *Mol Cell,* 33(2):215-26.

Johnson SA, Kim H, Erickson B, Bentley DL (2011). The export factor Yra1 modulates mRNA 3' end processing. *Nat Struct Mol Biol,* 18(10):1164-71.

Johnson TL, Vilardell J (2012). Regulated pre-mRNA splicing: the ghostwriter of the eukaryotic genome. *Biochim Biophys Acta,* 1819(6):538-45.

Jung Y, Lippard SJ (2006). RNA polymerase II blockage by cisplatin-damaged DNA. Stability and polyubiquitylation of stalled polymerase. *J Biol Chem,* 281(3):1361-70.

Karakasili E (2010). Molecular mechanism for degradation of transcriptionally stalled RNA polymerase II in the yeast Saccharomyces cerevisiae. *Dissertation, LMU München*, http://edoc.ub.uni-muenchen.de/12174/.

Katahira J, Okuzaki D, Inoue H, Yoneda Y, Maehara K, Ohkawa Y (2013). Human TREX component Thoc5 affects alternative polyadenylation site choice by recruiting mammalian cleavage factor I. *Nucleic Acids Res,* 41(14):7060-72.

Kee Y, Lyon N, Huibregtse JM (2005). The Rsp5 ubiquitin ligase is coupled to and antagonized by the Ubp2 deubiquitinating enzyme. *EMBO J,* 24(13):2414-24.

Kelly SM, Corbett AH (2009). Messenger RNA export from the nucleus: a series of molecular wardrobe changes. *Traffic,* 10(9):1199-208.

Kettenberger H, Armache KJ, Cramer P (2004). Complete RNA polymerase II elongation complex structure and its interactions with NTP and TFIIS. *Mol Cell,* 16(6):955-65.

Kim Guisbert K, Duncan K, Li H, Guthrie C (2005). Functional specificity of shuttling hnRNPs revealed by genome-wide analysis of their RNA binding profiles. *RNA,* 11(4):383-

93.

Kim Guisbert KS, Li H, Guthrie C (2007). Alternative 3' pre-mRNA processing in Saccharomyces cerevisiae is modulated by Nab4/Hrp1 in vivo. *PLoS Biol,* 5(1):e6.

Kim HT, Kim KP, Lledias F, Kisselev AF, Scaglione KM, Skowyra D, Gygi SP, Goldberg AL (2007). Certain pairs of ubiquitin-conjugating enzymes (E2s) and ubiquitin-protein ligases (E3s) synthesize nondegradable forked ubiquitin chains containing all possible isopeptide linkages. *J Biol Chem,* 282(24):17375-86.

Kirkpatrick DS, Hathaway NA, Hanna J, Elsasser S, Rush J, Finley D, King RW, Gygi SP (2006). Quantitative analysis of in vitro ubiquitinated cyclin B1 reveals complex chain topology. *Nat Cell Biol,* 8(7):700-10.

Kraut DA, Prakash S, Matouschek A (2007). To degrade or release: ubiquitin-chain remodeling. *Trends Cell Biol,* 17(9):419-21.

Kress TL, Krogan NJ, Guthrie C (2008). A single SR-like protein, Npl3, promotes pre-mRNA splicing in budding yeast. *Mol Cell,* 32(5):727-34.

Kuehner JN, Pearson EL, Moore C (2011). Unravelling the means to an end: RNA polymerase II transcription termination. *Nat Rev Mol Cell Biol,* 12(5):283-94.

Kulaeva OI, Hsieh FK, Chang HW, Luse DS, Studitsky VM (2013). Mechanism of transcription through a nucleosome by RNA polymerase II. *Biochim Biophys Acta,* 1829(1):76-83.

Kulathu Y, Komander D (2012). Atypical ubiquitylation - the unexplored world of polyubiquitin beyond Lys48 and Lys63 linkages. *Nat Rev Mol Cell Biol,* 13(8):508-23.

Kvint K, Uhler JP, Taschner MJ, Sigurdsson S, Erdjument-Bromage H, Tempst P, Svejstrup JQ (2008). Reversal of RNA polymerase II ubiquitylation by the ubiquitin protease Ubp3. *Mol Cell,* 30(4):498-506.

Kwak J, Workman JL, Lee D (2011). The proteasome and its regulatory roles in gene expression. *Biochim Biophys Acta,* 1809(2):88-96.

Lander ES, Linton LM, Birren B, Nusbaum C, Zody MC et al. (2001). Initial sequencing and analysis of the human genome. *Nature,* 409(6822):860-921.

Lander GC, Estrin E, Matyskiela ME, Bashore C, Nogales E, Martin A (2012). Complete subunit architecture of the proteasome regulatory particle. *Nature,* 482(7384):186-91.

Larochelle M, Lemay JF, Bachand F (2012). The THO complex cooperates with the nuclear RNA surveillance machinery to control small nucleolar RNA expression. *Nucleic Acids Res,* 40(20):10240-53.

Lasker K, Förster F, Bohn S, Walzthoeni T, Villa E, Unverdorben P, Beck F, Aebersold R, Sali A, Baumeister W (2012). Molecular architecture of the 26S proteasome holocomplex determined by an integrative approach. *Proc Natl Acad Sci U S A,* 109(5):1380-7.

Lee MS, Henry M, Silver PA (1996). A protein that shuttles between the nucleus and the cytoplasm is an important mediator of RNA export. *Genes Dev,* 10(10):1233-46.

Lee KB, Sharp PA (2004). Transcription-dependent polyubiquitination of RNA polymerase

II requires lysine 63 of ubiquitin. *Biochemistry,* 43(48):15223-9.

Lei EP, Krebber H, Silver PA (2001). Messenger RNAs are recruited for nuclear export during transcription. *Genes Dev,* 15(14):1771-82.

Lei H, Zhai B, Yin S, Gygi S, Reed R (2013). Evidence that a consensus element found in naturally intronless mRNAs promotes mRNA export. *Nucleic Acids Res,* 41(4):2517-25.

Lejeune D, Chen X, Ruggiero C, Berryhill S, Ding B, Li S (2009). Yeast Elc1 plays an important role in global genomic repair but not in transcription coupled repair. *DNA Repair (Amst),* 8(1):40-50.

Lewis A, Felberbaum R, Hochstrasser M (2007). A nuclear envelope protein linking nuclear pore basket assembly, SUMO protease regulation, and mRNA surveillance. *J Cell Biol,* 178(5):813-27.

Libri D, Dower K, Boulay J, Thomsen R, Rosbash M, Jensen TH (2002). Interactions between mRNA export commitment, 3'-end quality control, and nuclear degradation. *Mol Cell Biol,* 22(23):8254-66.

Linder P, Jankowsky E (2011). From unwinding to clamping - the DEAD box RNA helicase family. *Nat Rev Mol Cell Biol,* 12(8):505-16.

Lommel L, Bucheli ME, Sweder KS (2000). Transcription-coupled repair in yeast is independent from ubiquitylation of RNA pol II: implications for Cockayne's syndrome. *Proc Natl Acad Sci U S A,* 97(16):9088-92.

Long JC, Caceres JF (2009). The SR protein family of splicing factors: master regulators of gene expression. *Biochem J,* 417(1):15-27.

Luo W, Johnson AW, Bentley DL (2006). The role of Rat1 in coupling mRNA 3'-end processing to transcription termination: implications for a unified allosteric-torpedo model. *Genes Dev,* 20(8):954-65.

Luse DS (2013). Promoter clearance by RNA polymerase II. *Biochim Biophys Acta,* 1829(1):63-8.

Lykke-Andersen S, Jensen TH (2007). Overlapping pathways dictate termination of RNA polymerase II transcription. *Biochimie,* 89(10):1177-82.

Lykke-Andersen S, Mapendano CK, Jensen TH (2011). An ending is a new beginning: transcription termination supports re-initiation. *Cell Cycle,* 10(6):863-5.

Ma WK, Cloutier SC, Tran EJ (2013). The DEAD-box protein Dbp2 functions with the RNA-binding protein Yra1 to promote mRNP assembly. *J Mol Biol,* 425(20):3824-38.

MacKellar AL, Greenleaf AL (2011). Cotranscriptional association of mRNA export factor Yra1 with C-terminal domain of RNA polymerase II. *J Biol Chem,* 286(42):36385-95.

Mapendano CK, Lykke-Andersen S, Kjems J, Bertrand E, Jensen TH (2010). Crosstalk between mRNA 3' end processing and transcription initiation. *Mol Cell,* 40(3):410-22.

Martinez-Rucobo FW, Cramer P (2013). Structural basis of transcription elongation. *Biochim Biophys Acta,* 1829(1):9-19.

Mason PB, Struhl K (2005). Distinction and relationship between elongation rate and

processivity of RNA polymerase II in vivo. *Mol Cell,* 17(6):831-40.

Masuda S, Das R, Cheng H, Hurt E, Dorman N, Reed R (2005). Recruitment of the human TREX complex to mRNA during splicing. *Genes Dev,* 19(13):1512-7.

Matyskiela ME, Martin A (2012). Design principles of a universal protein degradation machine. *J Mol Biol,* 425(2):199-213.

Mayer A, Lidschreiber M, Siebert M, Leike K, Söding J, Cramer P (2010). Uniform transitions of the general RNA polymerase II transcription complex. *Nat Struct Mol Biol,* 17(10):1272-8.

Mayer A, Heidemann M, Lidschreiber M, Schreieck A, Sun M, Hintermair C, Kremmer E, Eick D, Cramer P (2012).CTD tyrosine phosphorylation impairs termination factor recruitment to RNA polymerase II. *Science,* 336(6089):1723-5.

McBride AE, Cook JT, Stemmler EA, Rutledge KL, McGrath KA, Rubens JA (2005). Arginine methylation of yeast mRNA-binding protein Npl3 directly affects its function, nuclear export, and intranuclear protein interactions. *J Biol Chem,* 280(35):30888-98.

McCracken S, Fong N, Rosonina E, Yankulov K, Brothers G, Siderovski D, Hessel A, Foster S, Shuman S, Bentley DL (1997). 5'-Capping enzymes are targeted to pre-mRNA by binding to the phosphorylated carboxy-terminal domain of RNA polymerase II. *Genes Dev,* 11(24):3306-18.

Meierhofer D, Wang X, Huang L, Kaiser P (2008). Quantitative analysis of global ubiquitination in HeLa cells by mass spectrometry. *J Proteome Res,* 7(10):4566-76.

Meinel DM, Burkert-Kautzsch C, Kieser A, O'Duibhir E, Siebert M, Mayer A, Cramer P, Söding J, Holstege FC, Sträßer K (2013). Recruitment of TREX to the Transcription Machinery by Its Direct Binding to the Phospho-CTD of RNA Polymerase II. *PLoS Genet,* 9(11):e1003914.

Metzger MB, Hristova VA, Weissman AM (2012). HECT and RING finger families of E3 ubiquitin ligases at a glance. *J Cell Sci,* 125(Pt 3):531-7.

Millevoi S, Vagner S (2010). Molecular mechanisms of eukaryotic pre-mRNA 3' end processing regulation. *Nucleic Acids Res,* 38(9):2757-74.

Mischo HE, Proudfoot NJ (2013). Disengaging polymerase: terminating RNA polymerase II transcription in budding yeast. *Biochim Biophys Acta,* 1829(1):174-85.

Mitsui A, Sharp PA (1999). Ubiquitination of RNA polymerase II large subunit signaled by phosphorylation of carboxyl-terminal domain. *Proc Natl Acad Sci U S A,* 96(11):6054-9.

Mocciaro A, Rape M (2012). Emerging regulatory mechanisms in ubiquitin-dependent cell cycle control. *J Cell Sci,* 125(Pt 2):255-63.

Montes M, Becerra S, Sánchez-Álvarez M, Suñé C (2012). Functional coupling of transcription and splicing. *Gene,* 501(2):104-17.

Morris DP, Greenleaf AL (2000). The splicing factor, Prp40, binds the phosphorylated carboxyl-terminal domain of RNA polymerase II. *J Biol Chem,* 275(51):39935-43.

Mosley AL, Pattenden SG, Carey M, Venkatesh S, Gilmore JM, Florens L, Workman JL, Washburn MP (2009). Rtr1 is a CTD phosphatase that regulates RNA polymerase II during the transition from serine 5 to serine 2 phosphorylation. *Mol Cell,* 34(2):168-78.

Nechaev S, Adelman K (2011). Pol II waiting in the starting gates: Regulating the transition from transcription initiation into productive elongation. *Biochim Biophys Acta,* 1809(1):34-45.

Nguyen VT, Giannoni F, Dubois MF, Seo SJ, Vigneron M, Kédinger C, Bensaude O (1996). In vivo degradation of RNA polymerase II largest subunit triggered by alpha-amanitin. *Nucleic Acids Res,* 24(15):2924-9.

Ozkaynak E, Finley D, Varshavsky A (1984). The yeast ubiquitin gene: head-to-tail repeats encoding a polyubiquitin precursor protein. *Nature,* 312(5995):663-6.

Parenteau J, Durand M, Véronneau S, Lacombe AA, Morin G, Guérin V, Cecez B, Gervais-Bird J, Koh CS, Brunelle D, Wellinger RJ, Chabot B, Abou Elela S (2008). Deletion of many yeast introns reveals a minority of genes that require splicing for function. *Mol Biol Cell,* 19(5):1932-41.

Peña A, Gewartowski K, Mroczek S, Cuéllar J, Szykowska A, Prokop A, Czarnocki-Cieciura M, Piwowarski J, Tous C, Aguilera A, Carrascosa JL, Valpuesta JM, Dziembowski A (2012). Architecture and nucleic acids recognition mechanism of the THO complex, an mRNP assembly factor. *EMBO J,* 31(6):1605-16.

Peng J, Schwartz D, Elias JE, Thoreen CC, Cheng D, Marsischky G, Roelofs J, Finley D, Gygi SP (2003). A proteomics approach to understanding protein ubiquitination. *Nat Biotechnol,* 21(8):921-6.

Perales R, Bentley D (2009). "Cotranscriptionality": the transcription elongation complex as a nexus for nuclear transactions. *Mol Cell,* 36(2):178-91.

Petesch SJ, Lis JT (2012). Overcoming the nucleosome barrier during transcript elongation. *Trends Genet,* 28(6):285-94.

Petroski MD, Deshaies RJ (2005). Mechanism of lysine 48-linked ubiquitin-chain synthesis by the cullin-RING ubiquitin-ligase complex SCF-Cdc34. *Cell,* 123(6):1107-20.

Pickart CM (1997). Targeting of substrates to the 26S proteasome. *FASEB J,* 11(13):1055-66.

Piruat JI, Aguilera A (1998). A novel yeast gene, THO2, is involved in RNA pol II transcription and provides new evidence for transcriptional elongation-associated recombination. *EMBO J,* 17(16):4859-72.

Portman DS, O'Connor JP, Dreyfuss G (1997). YRA1, an essential Saccharomyces cerevisiae gene, encodes a novel nuclear protein with RNA annealing activity. *RNA,* 3(5):527-37.

Prakash S, Tian L, Ratliff KS, Lehotzky RE, Matouschek A (2004). An unstructured initiation site is required for efficient proteasome-mediated degradation. *Nat Struct Mol Biol,* 11(9):830-7.

Preker PJ, Kim KS, Guthrie C (2002). Expression of the essential mRNA export factor Yra1p is autoregulated by a splicing-dependent mechanism. *RNA,* 8(8):969-80.

Preker PJ, Guthrie C (2006). Autoregulation of the mRNA export factor Yra1p requires inefficient splicing of its pre-mRNA. *RNA,* 12(6):994-1006.

Puig O, Caspary F, Rigaut G, Rutz B, Bouveret E, Bragado-Nilsson E, Wilm M, Séraphin B (2001). The tandem affinity purification (TAP) method: a general procedure of protein complex purification. *Methods,* 24(3):218-29.

Putnam AA, Jankowsky E (2013). DEAD-box helicases as integrators of RNA, nucleotide and protein binding. Biochim Biophys Acta, 1829(8):884-93.

Qiu H, Hu C, Hinnebusch AG (2009). Phosphorylation of the Pol II CTD by KIN28 enhances BUR1/BUR2 recruitment and Ser2 CTD phosphorylation near promoters. *Mol Cell,* 33(6):752-62.

Qu X, Lykke-Andersen S, Nasser T, Saguez C, Bertrand E, Jensen TH, Moore C (2009). Assembly of an export-competent mRNP is needed for efficient release of the 3'-end processing complex after polyadenylation. *Mol Cell Biol,* 29(19):5327-38.

Raha D, Wang Z, Moqtaderi Z, Wu L, Zhong G, Gerstein M, Struhl K, Snyder M (2010). Close association of RNA polymerase II and many transcription factors with Pol III genes. *Proc Natl Acad Sci U S A,* 107(8):3639-44.

Rando OJ (2012). Combinatorial complexity in chromatin structure and function: revisiting the histone code. *Curr Opin Genet Dev,* 22(2):148-55.

Ratner JN, Balasubramanian B, Corden J, Warren SL, Bregman DB (1998). Ultraviolet radiation-induced ubiquitination and proteasomal degradation of the large subunit of RNA polymerase II. Implications for transcription-coupled DNA repair. *J Biol Chem,* 273(9):5184-9.

Reid J, Svejstrup JQ (2004). DNA damage-induced Def1-RNA polymerase II interaction and Def1 requirement for polymerase ubiquitylation in vitro. *J Biol Chem,* 279(29):29875-8.

Ribar B, Prakash L, Prakash S (2006). Requirement of ELC1 for RNA polymerase II polyubiquitylation and degradation in response to DNA damage in Saccharomyces cerevisiae. *Mol Cell Biol,* 26(11):3999-4005.

Ribar B, Prakash L, Prakash S (2007). ELA1 and CUL3 are required along with ELC1 for RNA polymerase II polyubiquitylation and degradation in DNA-damaged yeast cells. *Mol Cell Biol,* 27(8):3211-6.

Richard P, Manley JL (2009). Transcription termination by nuclear RNA polymerases. *Genes Dev,* 23(11):1247-69.

Richmond TJ, Davey CA (2003). The structure of DNA in the nucleosome core. *Nature,* 423(6936):145-50.

Rodrigo-Brenni MC, Morgan DO (2007). Sequential E2s drive polyubiquitin chain assembly on APC targets. *Cell,* 130(1):127-39.

Rodríguez-Navarro S, Strässer K, Hurt E (2002). An intron in the YRA1 gene is required to control Yra1 protein expression and mRNA export in yeast. *EMBO Rep,* 3(5):438-42.

Rondón AG, Jimeno S, García-Rubio M, Aguilera A (2003). Molecular evidence that the eukaryotic THO/TREX complex is required for efficient transcription elongation. *J Biol Chem*, 278(40):39037-43.

Rondón AG, Jimeno S, Aguilera A (2010). The interface between transcription and mRNP export: from THO to THSC/TREX-2. *Biochim Biophys Acta,* 1799(8):533-8.

Röther S, Clausing E, Kieser A, Strässer K (2006). Swt1, a novel yeast protein, functions in transcription. *J Biol Chem,* 281(48):36518-25.

Rougemaille M, Gudipati RK, Olesen JR, Thomsen R, Seraphin B, Libri D, Jensen TH (2007). Dissecting mechanisms of nuclear mRNA surveillance in THO/sub2 complex mutants. *EMBO J,* 26(9):2317-26.

Rougemaille M, Dieppois G, Kisseleva-Romanova E, Gudipati RK, Lemoine S, Blugeon C, Boulay J, Jensen TH, Stutz F, Devaux F, Libri D (2008). THO/Sub2p functions to coordinate 3'-end processing with gene-nuclear pore association. *Cell,* 135(2):308-21.

Saeki Y, Kudo T, Sone T, Kikuchi Y, Yokosawa H, Toh-e A, Tanaka K (2009). Lysine 63-linked polyubiquitin chain may serve as a targeting signal for the 26S proteasome. *EMBO J,* 28(4):359-71.

Saguez C, Schmid M, Olesen JR, Ghazy MA, Qu X, Poulsen MB, Nasser T, Moore C, Jensen TH (2008). Nuclear mRNA surveillance in THO/sub2 mutants is triggered by inefficient polyadenylation. *Mol Cell,* 31(1):91-103.

Saguez C, Gonzales FA, Schmid M, Bøggild A, Latrick CM, Malagon F, Putnam A, Sanderson L, Jankowsky E, Brodersen DE, Jensen TH (2013). Mutational analysis of the yeast RNA helicase Sub2p reveals conserved domains required for growth, mRNA export, and genomic stability. *RNA,* 19(10):1363-71.

Sakata E, Bohn S, Mihalache O, Kiss P, Beck F, Nagy I, Nickell S, Tanaka K, Saeki Y, Förster F, Baumeister W (2012). Localization of the proteasomal ubiquitin receptors Rpn10 and Rpn13 by electron cryomicroscopy. *Proc Natl Acad Sci U S A,* 109(5):1479-84.

Sampath V, Sadhale P (2005). Rpb4 and Rpb7: a sub-complex integral to multi-subunit RNA polymerases performs a multitude of functions. *IUBMB Life,* 57(2):93-102.

Schmid M, Jensen TH (2008). Quality control of mRNP in the nucleus. *Chromosoma,* 117(5):419-29.

Schmid M, Poulsen MB, Olszewski P, Pelechano V, Saguez C, Gupta I, Steinmetz LM, Moore C, Jensen TH (2012). Rrp6p controls mRNA poly(A) tail length and its decoration with poly(A) binding proteins. *Mol Cell,* 47(2):267-80.

Schmid Schmid M, Jensen TH (2013). Transcription-associated quality control of mRNP. *Biochim Biophys Acta,* 1829(1):158-68.

Schneider-Poetsch T, Ju J, Eyler DE, Dang Y, Bhat S, Merrick WC, Green R, Shen B, Liu JO (2010). Inhibition of eukaryotic translation elongation by cycloheximide and lactimidomycin. *Nat Chem Biol,* 6(3):209-217.

Schroeder SC, Schwer B, Shuman S, Bentley D (2000). Dynamic association of capping enzymes with transcribing RNA polymerase II. *Genes Dev,* 14(19):2435-40.

Segref A, Sharma K, Doye V, Hellwig A, Huber J, Lührmann R, Hurt E (1997). Mex67p, a novel factor for nuclear mRNA export, binds to both poly(A)+ RNA and nuclear pores. *EMBO J,* 16(11):3256-71.

Shandilya J, Roberts SG (2012). The transcription cycle in eukaryotes: from productive initiation to RNA polymerase II recycling. *Biochim Biophys Acta,* 1819(5):391-400.

Sikder D, Johnston SA, Kodadek T (2006). Widespread, but non-identical, association of proteasomal 19 and 20 S proteins with yeast chromatin. *J Biol Chem,* 281(37):27346-55.

Sikorski RS, Hieter P (1989). A system of shuttle vectors and yeast host strains designed for efficient manipulation of DNA in Saccharomyces cerevisiae. *Genetics,* 122(1):19-27.

Singh BN, Hampsey M (2007). A transcription-independent role for TFIIB in gene looping. *Mol Cell,* 27(5):806-16.

Skruzný M, Schneider C, Rácz A, Weng J, Tollervey D, Hurt E (2009). An endoribonuclease functionally linked to perinuclear mRNP quality control associates with the nuclear pore complexes. *PLoS Biol,* 7(1):e8.

Somesh BP, Reid J, Liu WF, Søgaard TM, Erdjument-Bromage H, Tempst P, Svejstrup JQ (2005). Multiple mechanisms confining RNA polymerase II ubiquitylation to polymerases undergoing transcriptional arrest. *Cell,* 121(6):913-23.

Spence J, Sadis S, Haas AL, Finley D (1995). A ubiquitin mutant with specific defects in DNA repair and multiubiquitination. *Mol Cell Biol,* 15(3):1265-73.

Spingola M, Grate L, Haussler D, Ares M Jr (1999). Genome-wide bioinformatic and molecular analysis of introns in Saccharomyces cerevisiae. *RNA,* 5(2):221-34.

Stark H, Lührmann R (2006). Cryo-electron microscopy of spliceosomal components. *Annu Rev Biophys Biomol Struct,* 35:435-57.

Stiller JW, Cook MS (2004). Functional unit of the RNA polymerase II C-terminal domain lies within heptapeptide pairs. *Eukaryot Cell,* 3(3):735-40.

Strässer K, Hurt E (2000). Yra1p, a conserved nuclear RNA-binding protein, interacts directly with Mex67p and is required for mRNA export. *EMBO J,* 19(3):410-20.

Strässer K, Bassler J, Hurt E (2000). Binding of the Mex67p/Mtr2p heterodimer to FXFG, GLFG, and FG repeat nucleoporins is essential for nuclear mRNA export. *J Cell Biol,* 150(4):695-706.

Strässer K, Hurt E (2001). Splicing factor Sub2p is required for nuclear mRNA export through its interaction with Yra1p. *Nature,* 413(6856):648-52.

Strässer K, Masuda S, Mason P, Pfannstiel J, Oppizzi M, Rodriguez-Navarro S, Rondón AG, Aguilera A, Struhl K, Reed R, Hurt E (2002). TREX is a conserved complex coupling transcription with messenger RNA export. *Nature,* 417(6886):304-8.

Struhl K, Segal El (2013). Determinants of nucleosome positioning. *Nat Struct Mol Biol,* 20(3):267-73.

Tan-Wong SM, Zaugg JB, Camblong J, Xu Z, Zhang DW, Mischo HE, Ansari AZ, Luscombe NM, Steinmetz LM, Proudfoot NJ (2012). Gene loops enhance transcriptional directionality. *Science,* 338(6107):671-5.

Tenno T, Fujiwara K, Tochio H, Iwai K, Morita EH, Hayashi H, Murata S, Hiroaki H, Sato M, Tanaka K, Shirakawa M (2004). Structural basis for distinct roles of Lys63- and Lys48-linked polyubiquitin chains. *Genes Cells,* 9(10):865-75.

Thrower JS, Hoffman L, Rechsteiner M, Pickart CM (2000). Recognition of the polyubiquitin proteolytic signal. *EMBO J,* 19(1):94-102.

Tian B, Graber JH (2012). Signals for pre-mRNA cleavage and polyadenylation. *Wiley Interdiscip Rev RNA,* 3(3):385-96.

Tietjen JR, Zhang DW, Rodríguez-Molina JB, White BE, Akhtar MS, Heidemann M, Li X, Chapman RD, Shokat K, Keles S, Eick D, Ansari AZ (2010). Chemical-genomic dissection of the CTD code. *Nat Struct Mol Biol,* 17(9):1154-61.

Tomko RJ Jr, Hochstrasser M (2013). Molecular architecture and assembly of the eukaryotic proteasome. *Annu Rev Biochem,* 82:415-45.

Topisirovic I, Svitkin YV, Sonenberg N, Shatkin AJ (2011). Cap and cap-binding proteins in the control of gene expression. *Wiley Interdiscip Rev RNA,* 2(2):277-98.

Tous C, Aguilera A (2007). Impairment of transcription elongation by R-loops in vitro. *Biochem Biophys Res Commun,* 360(2):428-32.

Tran EJ, Zhou Y, Corbett AH, Wente SR (2007). The DEAD-box protein Dbp5 controls mRNA export by triggering specific RNA:protein remodeling events. *Mol Cell,* 28(5):850-9.

Trempe JF (2011). Reading the ubiquitin postal code. *Curr Opin Struct Biol,* 21(6):792-801.

Ulrich HD (2011). Timing and spacing of ubiquitin-dependent DNA damage bypass. *FEBS Lett,* 585(18):2861-7.

Venter JC, Adams MD, Myers EW, Li PW, Mural RJ et al. (2001). The sequence of the human genome. *Science,* 291(5507):1304-51.

Verma R, Oania R, Fang R, Smith GT, Deshaies RJ (2011). Cdc48/p97 mediates UV-dependent turnover of RNA Pol II. *Mol Cell,* 41(1):82-92.

Vijay-Kumar S, Bugg CE, Cook WJ (1987). Structure of ubiquitin refined at 1.8 A resolution. *J Mol Biol,* 194(3):531-44.

Vinciguerra P, Iglesias N, Camblong J, Zenklusen D, Stutz F (2005). Perinuclear Mlp proteins downregulate gene expression in response to a defect in mRNA export. *EMBO J,* 24(4):813-23.

Voynov V, Verstrepen KJ, Jansen A, Runner VM, Buratowski S, Fink GR (2006). Genes with internal repeats require the THO complex for transcription. *Proc Natl Acad Sci U S A,* 103(39):14423-8.

Walczak H, Iwai K, Dikic I (2012). Generation and physiological roles of linear ubiquitin chains. *BMC Biol,* 10:23.

Wellinger RE, Prado F, Aguilera A (2006). Replication fork progression is impaired by transcription in hyperrecombinant yeast cells lacking a functional THO complex. *Mol Cell Biol,* 26(8):3327-34.

White RJ (2011). Transcription by RNA polymerase III: more complex than we thought. *Nat Rev Genet*, 12(7):459-63.

Wilson MD, Harreman M, Svejstrup JQ (2013). Ubiquitylation and degradation of elongating RNA polymerase II: the last resort. *Biochim Biophys Acta,* 1829(1):151-7.

Wilson MD, Harreman M, Taschner M, Reid J, Walker J, Erdjument-Bromage H, Tempst P, Svejstrup JQ (2013). Proteasome-mediated processing of Def1, a critical step in the cellular response to transcription stress. *Cell,* 154(5):983-95.

Windgassen M, Sturm D, Cajigas IJ, González CI, Seedorf M, Bastians H, Krebber H (2004). Yeast shuttling SR proteins Npl3p, Gbp2p, and Hrb1p are part of the translating mRNPs, and Npl3p can function as a translational repressor. *Mol Cell Biol,* 24(23):10479-91.

Winget JM, Mayor T (2010). The diversity of ubiquitin recognition: hot spots and varied specificity. *Mol Cell,* 38(5):627-35.

Woudstra EC, Gilbert C, Fellows J, Jansen L, Brouwer J, Erdjument-Bromage H, Tempst P, Svejstrup JQ (2002). A Rad26-Def1 complex coordinates repair and RNA pol II proteolysis in response to DNA damage. *Nature,* 415(6874):929-33.

Xiang S, Cooper-Morgan A, Jiao X, Kiledjian M, Manley JL, Tong L (2009). Structure and function of the 5'-->3' exoribonuclease Rat1 and its activating partner Rai1. *Nature,* 458(7239):784-8.

Xu P, Duong DM, Seyfried NT, Cheng D, Xie Y, Robert J, Rush J, Hochstrasser M, Finley D, Peng J (2009). Quantitative proteomics reveals the function of unconventional ubiquitin chains in proteasomal degradation. *Cell,* 137(1):133-45.

Yu MC, Bachand F, McBride AE, Komili S, Casolari JM, Silver PA (2004). Arginine methyltransferase affects interactions and recruitment of mRNA processing and export factors. *Genes Dev,* 18(16):2024-35.

Zenklusen D, Vinciguerra P, Strahm Y, Stutz F (2001). The yeast hnRNP-Like proteins Yra1p and Yra2p participate in mRNA export through interaction with Mex67p. *Mol Cell Biol,* 21(13):4219-32.

Zenklusen D, Vinciguerra P, Wyss JC, Stutz F (2002). Stable mRNP formation and export require cotranscriptional recruitment of the mRNA export factors Yra1p and Sub2p by Hpr1p. *Mol Cell Biol,* 22(23):8241-53.

Zhang Y, Sikes ML, Beyer AL, Schneider DA (2009). The Paf1 complex is required for efficient transcription elongation by RNA polymerase I. *Proc Natl Acad Sci U S A,* 106(7):2153-8.

Zhang DW, Rodríguez-Molina JB, Tietjen JR, Nemec CM, Ansari AZ (2012). Emerging Views on the CTD Code. *Genet Res Int,* 2012:347214.

Abbreviations

6-AU	6-azauracil
ATP	adenosine triphosphate
bp	base pairs
°C	degree Celsius
ChIP	chromatin immunoprecipitation
ChIP-chip	chromatin immunoprecipitation with array hybridization
ChIP-qPCR	chromatin immunoprecipitation with single loci qPCR
CHX	cycloheximide
CTD	C-terminal domain of Rpb1, the largest RNAPII subunit
CUT	cryptic unstable transcript
d	day(s)
Da	Dalton
DNA	deoxyribonucleic acid
dNTP	deoxyribonucleoside triphosphate
DUB	deubiquitylase
E. coli	*Escherichia coli*
ECL	enhanced chemiluminescence (detection solution)
et al.	et alii (Latin for "and others")
5'-FOA	5'-Fluoroorotic acid
fw	forward (PCR primer)
g	gram
G	one letter code for the amino acid glycine
GG-NER	Global Genome Nucleotide Excision Repair
h	hour(s)
INP	input
IP	immunoprecipitation
K	one letter code for the amino acid lysine
kDa	kilo Dalton
l	litre
LB	Luria Bertani medium (for *E. coli*)
LB	Lysis Buffer
M	molar
M	one letter code for the amino acid methionine
min.	minute(s)
mDa	mega Dalton
miRNA	microRNA
mRNA	messenger RNA
mRNP	messenger ribonucleoprotein particle
NER	nucleotide excision repair
nm	nanometer
OD	optical density
ORF	open reading frame
PABP	pola(A) binding protein

PAGE	polyacrylamide gel electrophoresis
PBS	phosphate-buffered saline
PBST	PBS plus Tween-20 (0.1 %)
PCR	polymerase chain reaction
pH	potential of hydrogen
qPCR	quantitative polymerase chain reaction
qWB	quantitative Western Blot
RNA	ribonucleic acid
RNAP	RNA Polymerase
rRNA	ribosomal rRNA
R	one letter code for the amino acid arginine
rev	reverse (PCR primer)
rpm	rotations per minute
RT	room temperature
S	Svedberg coefficient
S	one letter code for the amino acid serine
S. c.	*Saccharomyces cerevisiae*
SB	sample buffer
SDC	synthetic complete medium (for *S.c.*)
SDS	sodium dodecyl sulfate
SL	synthetic lethal(ity)
sn(o) RNA	small nuclear (nucleolar) RNA
SR	serine-arginine (-rich proteins)
SUT	stable unannotated transcript
T	one letter code for the amino acid threonine
TAP	tandem affinity purification
TBS	TRIS-buffered saline
TBST	TBS plus Tween-20 (0.1 %)
TCA	trichloroacetic acid
TCR	transcription-coupled repair
TEV	*Tobacco etch virus* protease
TREX	transcription and export complex
tRNA	transfer RNA
ts	temperature-sensitive
UPS	ubiquitin proteasome system
UV	ultraviolet radiation
WB	Western Blot
WGA	whole genome amplification
Y	one letter code for the amino acid tyrosine
YPD	yeast extract - peptone - glucose (full medium for *S.c.*)

Acknowledgements

I would like to thank…

… my supervisor Dr. Katja Sträßer for giving me the opportunity to work on many different and interesting projects during my PhD, for scientific exchange and letting me work independently, and for providing many opportunities for me to learn and grow.

… Prof. Dr. Klaus Förstemann for being the second examiner of my thesis. I'd like to thank him and PD Dr. Dietmar Martin for helpful scientific discussions and for their support over the last years, and all members of my thesis evaluation committee for their time.

… the EMBO Young Investigator Program for organizing and sponsoring an interesting and highly stimulating PhD course. I enjoyed participating very much!

… CIPSMwomen for funding part of my research and my participation at the 2012 EMBO conference "Transcription and Chromatin".

… all past and present members of the Sträßer lab. To Lina I'm especially grateful for introducing me to the lab and teaching me the ChIP technique. Dominik, I enjoyed working together with you on T-REX! Anja, thank you very much for your support, technical and otherwise ;-), and for being such a nice bench neighbor. Juliane, I enjoyed your calm and friendly presence. And thanks for your constant efforts to remind everyone of their responsibilities to keep the lab clean! Rashmi, thanks for your compassionate personality and for giving me a glimpse of a different and interesting culture. Katharina, thanks a lot for our early-morning discussions, especially during the last year. In addition, I'm very grateful to all members of the Sträßer lab for their readiness to help, for discussions, and for the nice working atmosphere in the lab. Also, a big thank you to my students Mika and Elisabeth. I enjoyed supervising your Master's and Bachelor's theses, and it was a very rewarding experience to see you work so well and independently on your projects.

… my father for his constant and encouraging support. Thank you for believing in me! And thank you for appreciating and accepting my wish to study something of which you don't really understand what it's all about ;-)

… Peter for his support and being my companion for more than eight years now. I very much value the different perspective you bring to our conversations. Thank you for tolerating all the long workdays and the weekends spent in the lab and for being there for me during the good and the difficult times!

Curriculum Vitae

Personal information

name	Cornelia Burkert-Kautzsch (née Burkert)
date of birth	21. 09. 1982
place of birth	Kulmbach, Germany
nationality	German

Education

10/2008 - present **PhD studies in Biochemistry**

Thesis advisor: Dr. Katja Sträßer (Ludwig-Maximilians-Universität München)

10/2006 - 07/2008 **Master of Science Program in Biomedicine**

Thesis advisor: Prof. Dr. Dr. Peter Friedl (Julius-Maximilians-Universität Würzburg and Rudolf-Virchow Center - DFG Research Center for Experimental Biomedicine)

10/2003 - 09/2006 **Bachelor of Science Program in Biomedicine**

Thesis advisor: Prof. Dr. Dr. Stefan Engelhardt (Julius-Maximilians-Universität Würzburg and Rudolf-Virchow Center - DFG Research Center for Experimental Biomedicine)

07/2002 **Abitur**

Caspar-Vischer-Gymnasium, Kulmbach

Publications

Karakasili E*, <u>Burkert-Kautzsch C</u>*, Kieser A, Strässer K (2013). Degradation of DNA damage-independently stalled RNA polymerase II is independent of the E3 ligase Elc1. *Nucl Acids Res* (under revision) *these authors contributed equally*

Meinel DM, Burkert-Kautzsch C, Kieser A, O'Duibhir E, Siebert M, Mayer A, Cramer P, Söding J, Holstege FC, Sträßer K (2013). Recruitment of TREX to the Transcription Machinery by Its Direct Binding to the Phospho-CTD of RNA Polymerase II. *PLoS Genet,* 9(11):e1003914.

Chanarat S, Burkert-Kautzsch C, Meinel DM, Sträßer K (2012). Prp19C and TREX: interacting to promote transcription elongation and mRNA export. *Transcription,* 3(1):8-12.

Röther S*, <u>Burkert C</u>*, Brünger KM*, Mayer A*, Kieser A, Strässer K (2010). Nucleocytoplasmic shuttling of the La motif-containing protein Sro9 might link its nuclear and cytoplasmic functions. *RNA,* 16(7):1393-401. *these authors contributed equally*

Wu HH, Bellmunt E, Scheib JL, Venegas V, <u>Burkert C</u>, Reichardt LF, Zhou Z, Fariñas I, Carter BD (2009). Glial precursors clear sensory neuron corpses during development via Jedi-1, an engulfment receptor. *Nat Neurosci,* 12(12):1534-41